Chinese Chemical Letters 37 (2026) 111886

Contents lists available at ScienceDirect

Chinese Chemical Letters

journal homepage: www.elsevier.com/locate/cclet

Recent development in radical cycloaddition reactions for the synthesis of carbo- and heterocycles

Saima Perveen[a,1,*], Lulu Qin[b,1], Min Zhao[b], Zhengwei Ding[c], Yingying Wang[b], Zaicheng Nie[b], Pengfei Li[a,b,*]

[a] School of Chemistry, Xi'an Jiaotong University, Xi'an 710049, China
[b] Frontier Institute of Science and Technology and Interdisciplinary Research Centre of Frontier Science and Technology, Xi'an Jiaotong University, Xi'an 710049, China
[c] School of Pharmacy, Xi'an Jiaotong University, Xi'an 710049, China

ARTICLE INFO

Article history:
Received 19 June 2025
Revised 23 August 2025
Accepted 23 September 2025
Available online 25 September 2025

Keywords:
Radical cycloaddition
Carbo- and heterocycle
Visible-light photoaddition
Transition metal catalysis
Organic small molecule

ABSTRACT

Radical cycloaddition reactions (RCRs) are highly effective methods for constructing complex carbo- and heterocycles, which are frequently encountered in natural products that exhibit intriguing biological properties and hold significant potential for applications in medicinal chemistry. Radical-mediated cycloaddition strategies, which recycle radical character, are particularly appealing because they require only a catalytic amount of reagent and promise reactions with theoretically high atom economy. This review focuses on recent developments and synthetic applications in RCRs, with an emphasis on visible light-induced radical photocycloaddition reactions (RPCRs), transition metal-catalyzed approaches, and small molecule-catalyzed methods. By highlighting some outstanding innovations and addressing current challenges, this review aims to identify potential areas for improvement. These advancements will provide more efficient pathways for the synthesis of natural product molecules and offer valuable insights for the development of new synthetic methodologies.

© 2025 Published by Elsevier B.V. on behalf of Chinese Chemical Society and Institute of Materia Medica, Chinese Academy of Medical Sciences.

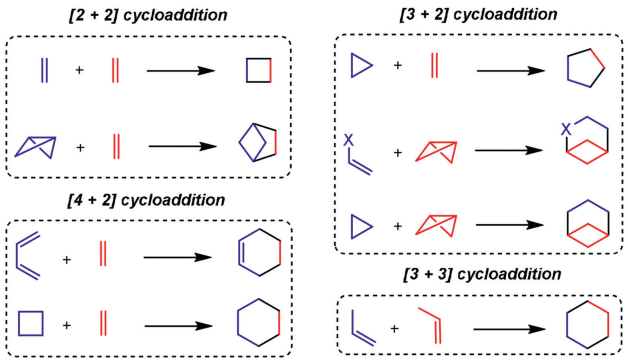
1. Introduction

Carbo- and heterocycles are fundamental structures in numerous natural products and bioactive compounds, particularly in medicinal chemistry [1,2]. Over 85% of biologically active molecules contain heterocycles, underscoring their significance in synthetic research [3,4]. Radical cycloaddition reactions have emerged as particularly valuable tools in this context. The discovery of the triphenylmethyl radical by Gomberg in 1900 marked the beginning of free radical chemistry [5]. Since then, radical reactions have garnered significant attention due to their high tolerance for functional groups, mild reaction conditions, and the presence of non-charged intermediates [6]. These features make radical reactions highly attractive for synthetic chemists. Compared to traditional methods, radical reactions offer several advantages, including broader functional group compatibility, gentler reaction conditions, and simpler pathways with fewer byproducts [7–22].

Cycloaddition reactions represent a crucial class of organic chemical reactions, renowned for their efficiency in forming carbon-carbon bonds without the need for nucleophiles or electrophiles [23–34]. The Diels-Alder reaction, a [4+2] cycloaddition, is perhaps the most well-known example. These reactions are not only atom-efficient but also offer high levels of convergence and stereoselectivity, making them highly desirable for preparative chemistry. Their versatility is further demonstrated through applications in developing photoresponsive materials and membranes [35,36]. Cycloaddition reactions are primarily employed to construct carbocycles and heterocycles of various sizes, which are frequently found in natural products with intriguing biological properties and potential medicinal applications. Given these advantages, significant efforts have been dedicated to developing novel synthetic methods using radical cycloaddition strategies. These reactions are increasingly utilized in diversity-oriented synthesis to enhance the structural diversity and complexity of small molecules. Consequently, the collection of chemical reactions for constructing cyclic compounds has become an indispensable toolbox for synthetic chemists [37,38]. Highlighting innovative advancements and identifying areas for improvement are essential to provide more efficient pathways for synthesizing natural prod-

* Corresponding authors.
E-mail addresses: saima.364@mail.xjtu.edu.cn (S. Perveen), lipengfei@xjtu.edu.cn (P. Li).
[1] These authors contributed equally to this work.

https://doi.org/10.1016/j.cclet.2025.111886
1001-8417/© 2025 Published by Elsevier B.V. on behalf of Chinese Chemical Society and Institute of Materia Medica, Chinese Academy of Medical Sciences.



Scheme 1. Types of cycloaddition covering this review.

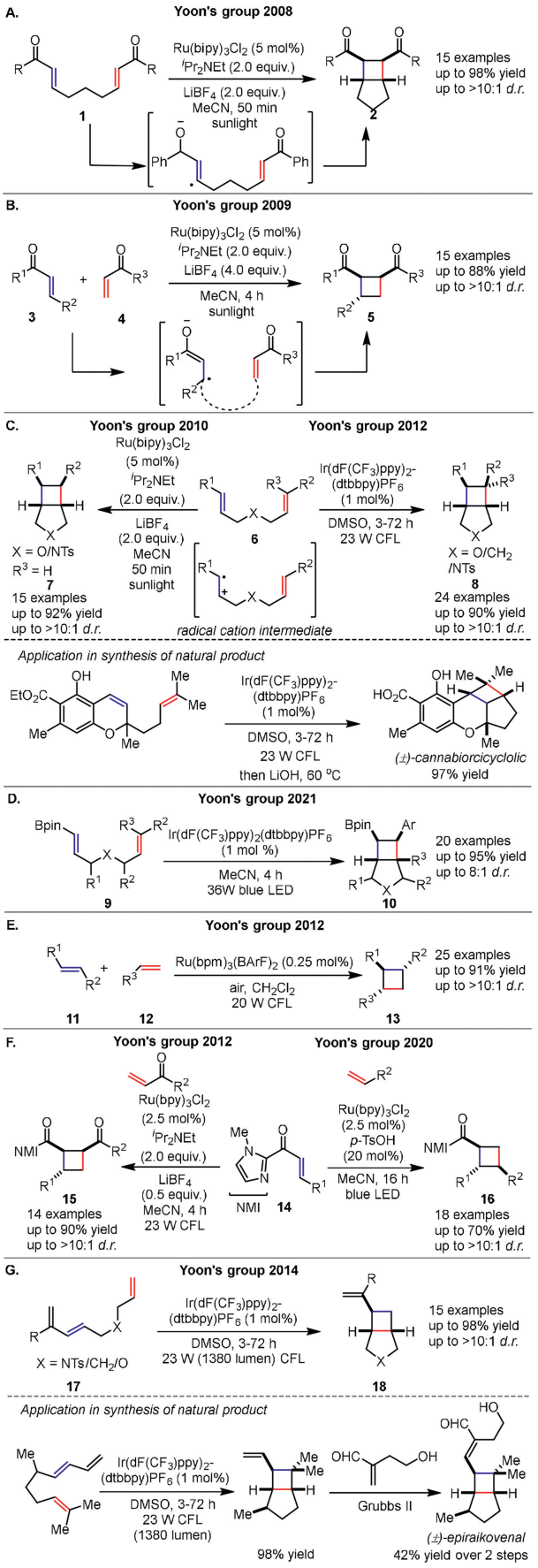
uct molecules and to inspire further research into new synthetic methodologies.

This review examines recent developments and applications of radical cycloaddition reactions (RCRs), including visible light-induced radical photocycloaddition reactions (RPCRs), transition metal-catalyzed approaches, and small molecule-catalyzed methods. As outlined in Scheme 1, this review is sub-organized by the type of cycloaddition reactions, such as [2+2], [3+2], [4+2], and [3+3] cycloadditions, covering the product scope and mechanisms for various methods. It concludes by discussing challenges, future directions, and emerging trends in radical cycloaddition chemistry.

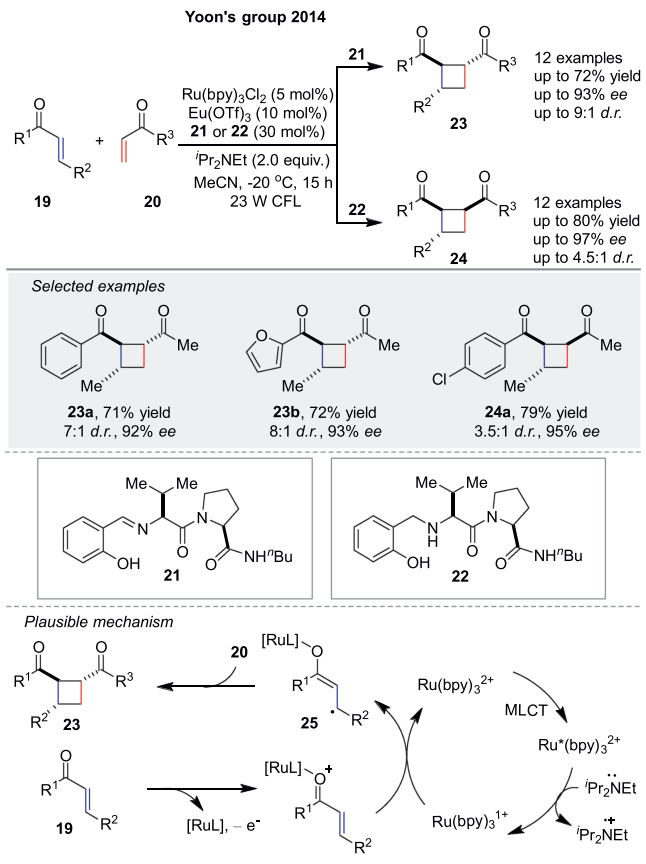
2. Visible light induced RPCRS

2.1. [2+2] cycloaddition

The Yoon group has been at the forefront of radical photocycloaddition reactions, developing several elegant [2+2] cycloaddition methods using visible light photocatalysis, significantly expanding the scope and applicability of this synthetic strategy. In 2008, they demonstrated the efficient visible light photocatalysis of [2+2] cycloadditions of bis(enone) **1** using $Ru(bpy)_3Cl_2$ as a photocatalyst, achieving high yields and stereoselectivity of cyclobutane-containing bicyclic dione **2**. Importantly, the light source used in this procedure was a standard 275 W floodlight, without any specialized high-pressure UV photolysis apparatus (Scheme 2A) [39]. In 2009, they focused on crossed intermolecular [2+2] cycloadditions of acyclic enones **3** and **4**, overcoming the challenge of intermolecular photochemical [2+2] cycloadditions by using a $Ru(bpy)_3Cl_2$-catalyzed system *via* a radical mechanism. Strained four-membered rings **5** were constructed with excellent chemo- and stereoselectivity (Scheme 2B) [40]. In 2010, they introduced a photooxidative approach for intramolecular [2+2] cycloadditions of electron-rich olefins **6** using $Ru(bpy)_3^{2+}$, enabling the synthesis of cyclobutanes **7** from styrenes (Scheme 2C left) [41]. Extending this work, in 2012, they explored energy transfer mechanisms for this intramolecular [2+2] cycloadditions of styrenes **6** using iridium complexes, demonstrating high yields and broad substrate scope (Scheme 2C right) [42]. Following the same mechanism, years later, they also developed intramolecular [2+2] cycloadditions of vinyl boronate esters **9** and found that simple vinyl boronates readily reacted with excited-state triplet alkenes that are generated by visible light triplet sensitization (Scheme 2D) [43]. A crossed [2+2] cycloadditions of styrenes **11** and **12** using visible light photocatalysis with carefully tuned ruthenium photocatalysts was reported by the Yoon group in 2012. A concise synthesis of a complex natural product (cannabiorcicyclolic acid) was also demonstrated (Scheme 2E) [44]. After this, they reported the use of cleavable redox auxiliaries to facilitate [2+2] cycloadditions of enones **14**, expanding the scope of substrates that can be



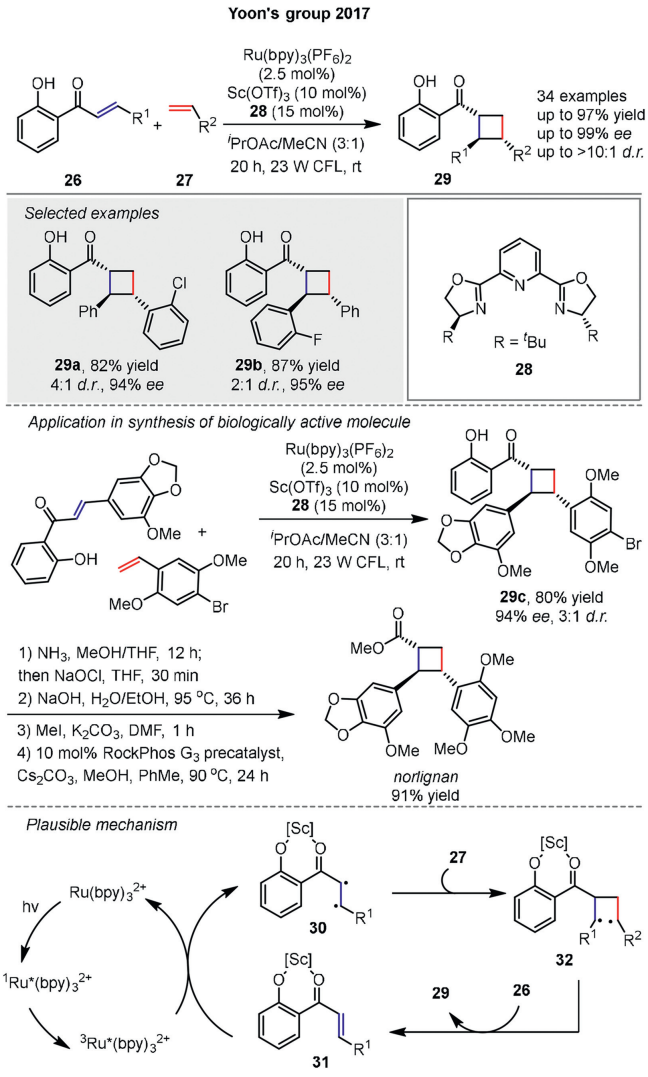
Scheme 2. Visible light-induced intermolecular and intramolecular [2+2] photocycloadditions of olefins.



Scheme 3. Enantioselective [2 + 2] photocycloaddition *via* dual catalysis.

used (Scheme 2F) [45,46]. The [2 + 2] cycloaddition of 1,3-dienes **17** was then demonstrated by the Yoon group, using visible light and transition metal complexes, reflecting the versatility and functional group tolerance of this method. Moreover, highlighting the ability to perform this complex [2 + 2] cycloaddition, they developed a concise and modular synthesis of the cyclobutane-containing natural product (±)-epiraikovenal (Scheme 2G) [47]. Together, these studies showcased the power of visible light photocatalysis in enabling a wide range of [2 + 2] cycloaddition reactions, from enones to styrenes and dienes, and highlight the potential for further development in this field.

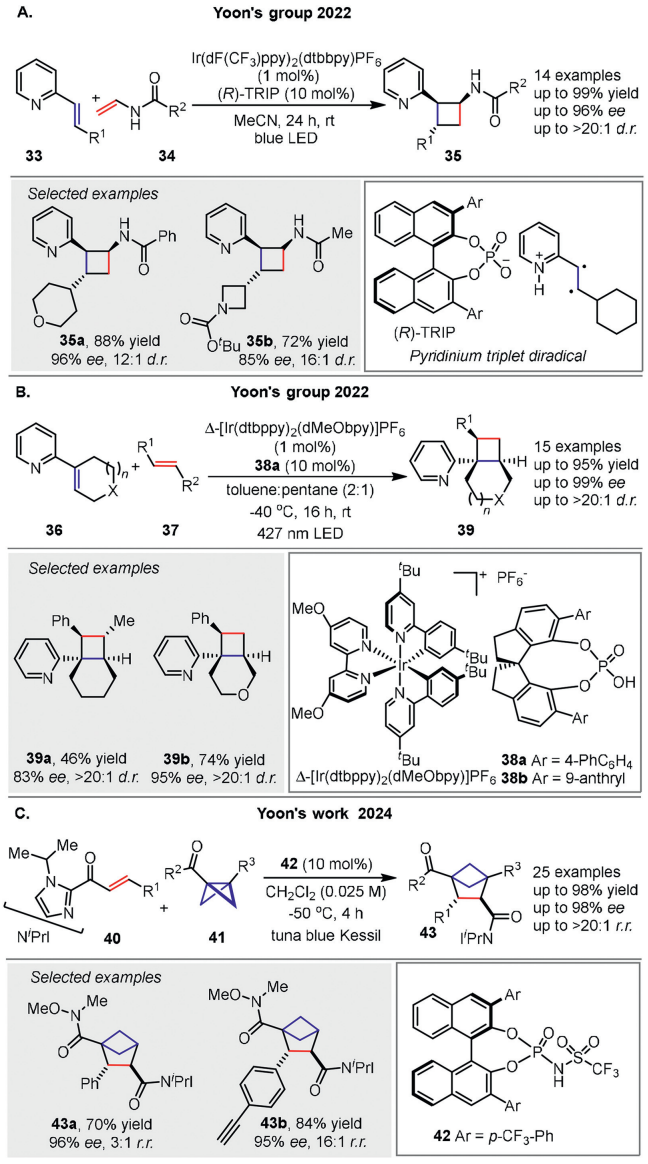
In 2014, the Yoon group presented a dual-catalysis approach to enantioselective [2 + 2] photocycloadditions between **19** and **20** using visible light to produce cyclobutene (**23**, **24**). The authors describe a method that eliminates racemic background reactions, a major challenge in asymmetric photocycloadditions. The strategy involves a combination of a visible light-absorbing transition-metal photocatalyst and a stereocontrolling Lewis acid cocatalyst. This dual-catalyst system *via* radical mechanism enables broader scope, greater stereochemical flexibility, and better efficiency than previously reported methods (Scheme 3). The mechanism of this enantioselective [2 + 2] photocycloaddition reaction involves the activation of $Ru(bpy)_3^{2+}$ by visible light, which then reduces the aryl enone substrate in the presence of a Lewis acid ($Eu(OTf)_3$) and a chiral ligand. The resulting radical anion intermediate **25** reacts with an aliphatic enone **20** to form a cyclobutane radical intermediate, which recombines to produce the desired cyclobutane product. The chiral Lewis acid cocatalyst, composed of $Eu(OTf)_3$ and the chiral ligand, controls the stereochemistry of the reaction, ensuring high enantioselectivity. This dual-catalyst system effectively eliminates racemic background reactions, providing a highly enantioselective method for the synthesis of cyclobutanes [48].



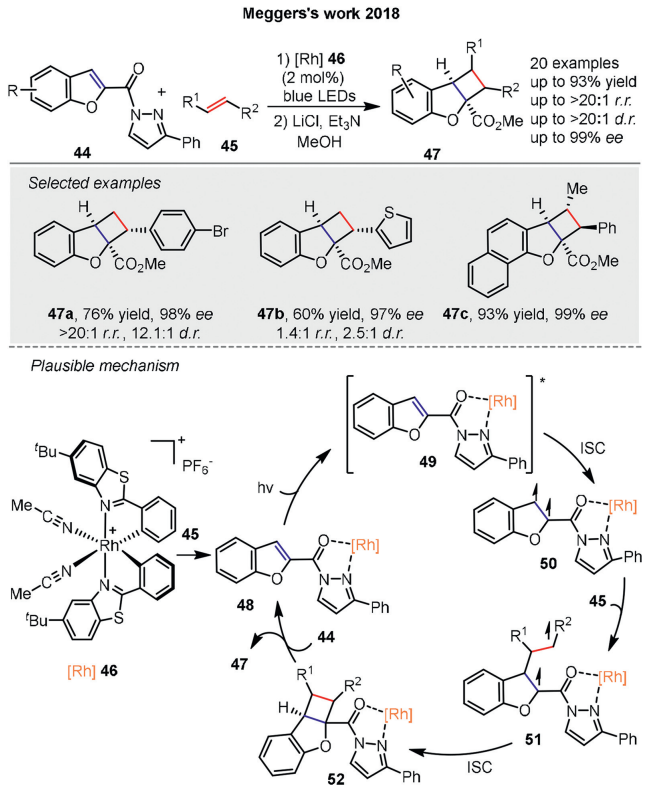
Scheme 4. Enantioselective [2 + 2] crossed photocycloaddition of 2'-hydroxychalcones and olefin.

In 2017, the Yoon group explored enantioselective crossed photocycloadditions of styrenic olefins **27** *via* Lewis acid catalyzed triplet sensitization for synthesizing highly enantioenriched diarylcyclobutanes **29** by photocycloaddition of 2'-hydroxychalcones **26** with various styrene **27** coupling partners. The key mechanistic feature is the dramatic lowering of the singlet-triplet gap of the chalcone upon Lewis acid coordination, enabling efficient triplet energy transfer from a $Ru(bpy)_3^{2+}$ photosensitizer (Scheme 4). The reaction is highly enantioselective and can tolerate a wide range of substituents on both the chalcone and styrene partners. The utility of this reaction is demonstrated through the direct synthesis of a representative norlignan cyclobutane natural product [49].

In 2022, the Yoon group presented a novel strategy for enantioselective [2 + 2] photocycloadditions of acyclic vinylpyridines **33** through ternary complex formation and an uncontrolled sensitization mechanism. The authors describe a method where both a chiral catalyst-associated vinylpyridine and a nonassociated, free vinylpyridine substrate can be sensitized by an Ir^{III} photocatalyst. Despite indiscriminate triplet energy transfer from the excited state photosensitizer to both on- and off-catalyst species, high levels of diastereo- and enantioselectivity are achieved through a preferred, highly organized transition state (Scheme 5A). This mechanistic paradigm is distinct from current approaches, which typi-



Scheme 5. Enantioselective intermolecular [2 + 2] photocycloadditions.

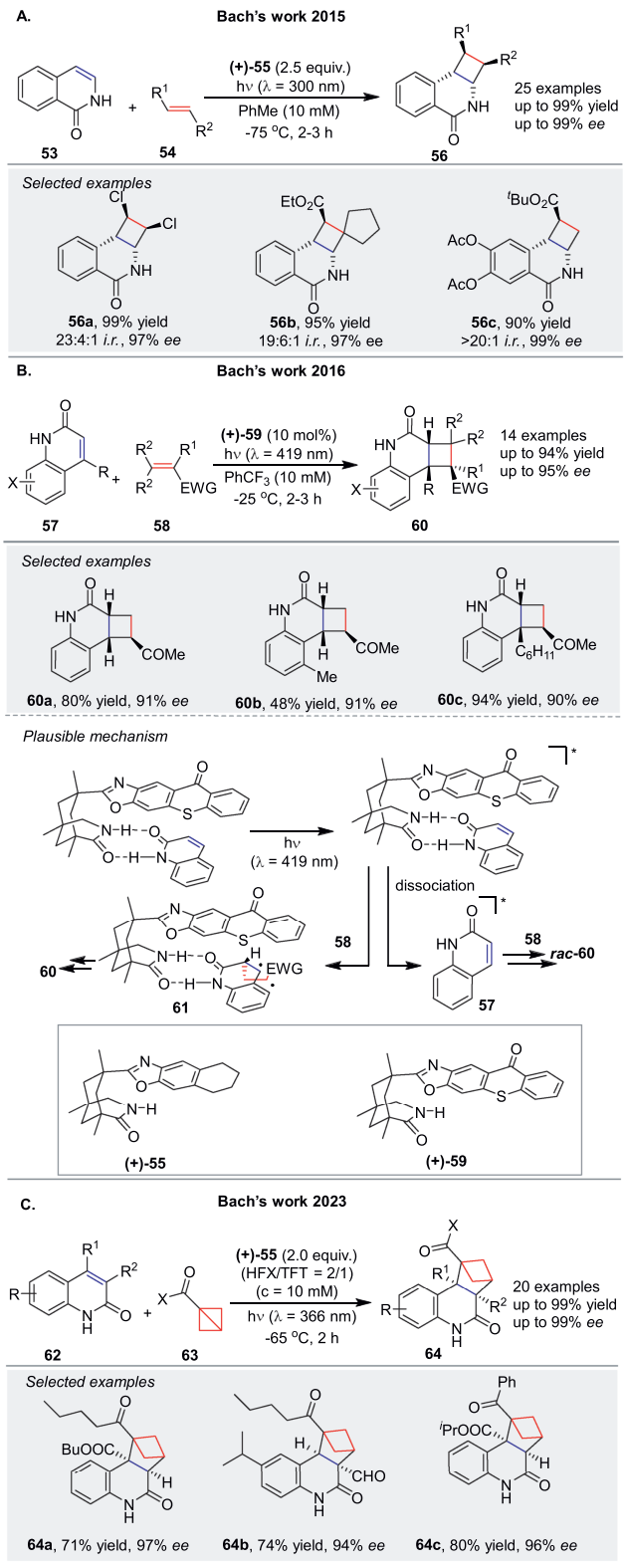


Scheme 6. Rh-catalyzed, asymmetric dearomatization of benzofurane by visible-light activated [2 + 2] photocycloadditions.

cally focus on suppressing off-catalyst pathways. The study demonstrates the successful application of this method to a variety of substrates, including those with dense stereochemical complexity and additional nitrogen-based functionalities, achieving high enantiomeric excess (up to 96% *ee*) and good yields (up to 99%) [50]. In the same year, they reported a cooperative stereoinduction in asymmetric photocatalysis, specifically focusing on the [2 + 2] photocycloaddition of vinylpyridines **36** and alkene **37**. The authors describe a tandem chiral photocatalyst/Brønsted acid strategy that enables highly enantioselective photocycloadditions. A significant finding is the observation of different reaction rates and enantioselectivities between matched and mismatched chiral catalyst pairs, which is attributed to their cooperative behavior in a transient excited-state assembly (Scheme 5B). The study demonstrates that the chirality of the Brønsted acid and the Ir^{III} photocatalyst play a crucial role in determining the enantioselectivity of the reaction. The matched catalyst pair (Δ-[Ir] with (*R*)-CPA) provides higher yields and enantiomeric excess compared to the mismatched pair (Λ-[Ir] with (*R*)-CPA) [51]. Soon after, they introduced an enantioselective [$2\pi + 2\sigma$] photocycloaddition enabled by Brønsted acid catalyzed chromophore activation. The authors demonstrate that Brønsted acid catalysis of C-acyl imidazoles enables highly enantioselective [$2\pi + 2\sigma$] photocycloadditions, which are useful for synthesizing bicyclo[2.1.1]hexanes **43** and other strained small-ring structures relevant to pharmaceuticals and agrochemicals. The study shows that increasing the steric bulk of the imidazole substituent inhibits the formation of undesirable dimers, leading to higher yields of the desired bicyclohexane products (**43**). The imidazole auxiliary can be cleaved to provide useful synthetic handles without erosion of enantiomeric purity (Scheme 5C). This work highlights the versatility of chiral Brønsted acid catalysis in asymmetric photochemical reactions and its potential for practical applications in synthesizing enantiopure libraries of saturated bicyclic motifs [52].

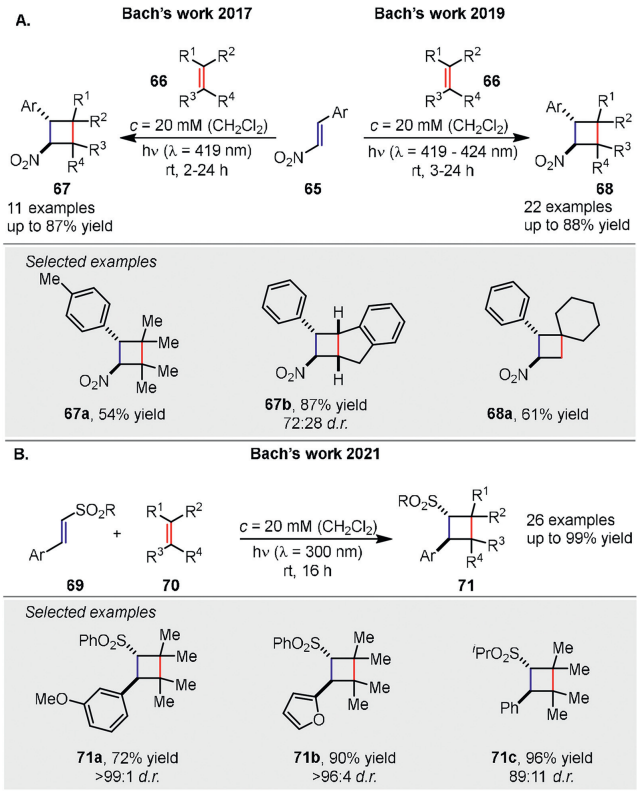
In 2018, Megger and co-workers reported a novel method for catalytic asymmetric dearomatization by visible-light-activated [2 + 2] photocycloaddition using benzofurans **44** yielding chiral tricyclic structures **47** with up to four stereocenters, including quaternary centers. The benzofurans are functionalized at the 2-position with an *N*-acylpyrazole moiety that coordinates with a chiral-*at*-rhodium Lewis acid catalyst **46**. The reaction involves the formation of a reactant complex **48** that absorbs blue light, undergoes intersystem crossing (ISC) to a triplet state **50**, and reacts with an alkene substrate **45** to generate a 1,4-biradical intermediate **51**. This intermediate recombines to form the desired photocycloaddition product **47**. Computational modeling reveals that the regioselectivity is influenced by the stability of the 1,4-biradical intermediate **51**, with the heteroatom in the heterocycle playing a key role in regiocontrol (Scheme 6) [53]. The study demonstrates high enantioselectivity (up to 99% *ee*) and good functional group tolerance, highlighting the potential of this method for synthesizing complex chiral structures.

In 2015, the Bach group introduced an enantioselective [2 + 2] photocycloaddition of isoquinolones **53** with alkenes **54**, utiliz-



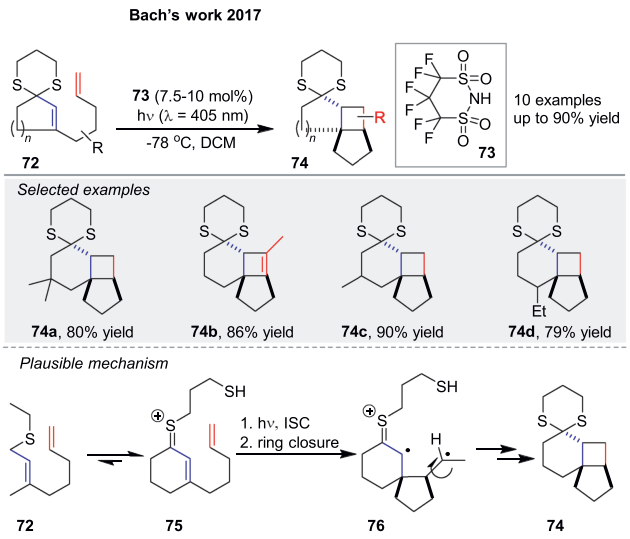
Scheme 7. Enantioselective intermolecular [2+2] photocycloaddition using chiral thioxanthone catalyst.

ing a chiral template **55** to achieve high enantioface differentiation [54]. This method enabled the synthesis of various functionalized cyclobutanes **56** with excellent yields and enantioselectivities (up to 99% *ee*) (Scheme 7A). Subsequently, they described an enantioselective intermolecular [2+2] photocycloaddition of 2(1*H*)-quinolones **57** with electron-deficient alkenes **58**, employing a chiral thioxanthone catalyst **59** (Scheme 7B) [55]. This reaction exhibited high regio- and diastereoselectivity, yielding cyclobutane products **60** with significant enantiomeric excess (up to 95% *ee*). The chiral template enhanced substrate solubility and enantiocontrol through two-point hydrogen bonding between the quinolone and the catalyst, facilitating efficient energy transfer and high enantioface differentiation. The reaction likely proceeds *via* a triplet state of the quinolone, with the alkene **58** reacting at carbon atom C3, leading to a 1,4-diradical intermediate **61** and product formation. Continuing their work, they reported the first enantioselective [2π + 2σ] photocycloaddition reactions of 1-substituted bicyclo[1.1.0]butanes **63** with 2(1*H*)-quinolones **62**, using a chiral complexing agent **55**. This reaction resulted in the formation of chiral bicyclo[2.1.1]hexane skeletons **64** with high enantiomeric excess (up to 99% *ee*) (Scheme 7C) [56].

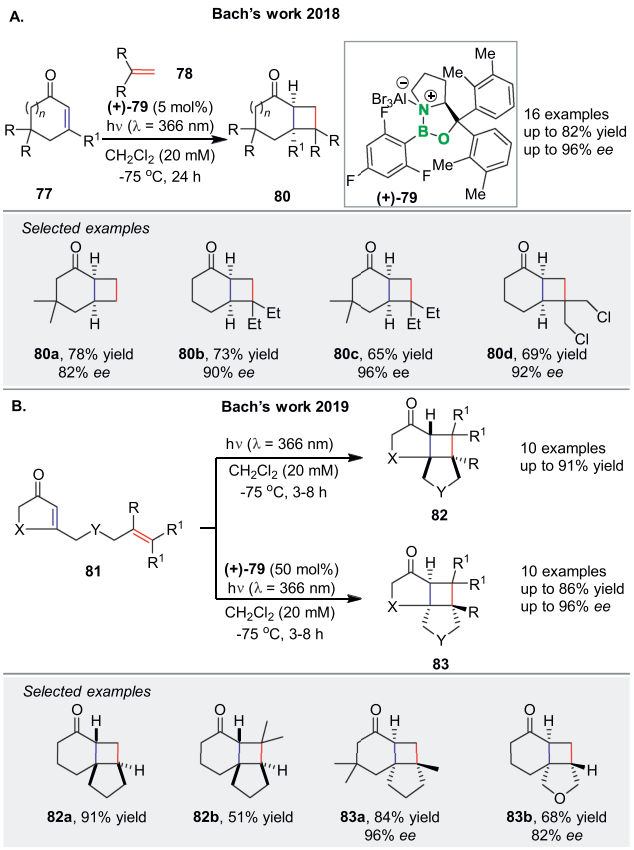


Scheme 8. Visible light-induced intermolecular [2+2] photocycloaddition of *β*-nitrostyrenes and *α*,*β*-unsaturated sulfones with alkenes.

Bach and colleagues have then reported on the visible light-induced [2 + 2] radical photocycloaddition of *β*-nitrostyrenes **65** to various olefins **66**, demonstrating that these reactions can be efficiently conducted at λ = 419 nm in CH_2Cl_2 solvent, yielding cyclobutanes **67** with moderate to good yields (up to 87%) (Scheme 8A left) [57]. This work has been further extended to include **65**, where optimized conditions and a broader range of substrates were explored, achieving yields up to 88% (Scheme 8A right) [58]. In a related study, the intermolecular [2 + 2] photocycloaddition of *α*,*β*-unsaturated sulfones **69** and alkene **70** was achieved at λ = 300 nm, yielding 2-aryl-1-sulfonyl-substituted cyclobutanes **71** with yields up to 99% (Scheme 8B) [59]. These studies collectively highlight the formation of a triplet 1,4-diradical intermediate as a key mechanistic step, supported by the observation of side products and triplet sensitization experiments. The influence of Lewis acids and triplet sensitizers on reaction efficiency and selectivity was also explored, with varying success depending on the substrate and reaction conditions.



Scheme 9. Brønsted acid-catalyzed intramolecular [2 + 2] photocycloaddition.



Scheme 10. Enantioselective intermolecular and intramolecular [2 + 2] cycloaddition of enones.

In 2017, the same group reported a Brønsted acid-catalyzed intramolecular [2 + 2] photocycloaddition of enone dithianes **72** under visible light irradiation (λ = 405 nm). The reaction relies on the formation of colored thionium ions **75**, which are intermediates in the catalytic cycle and can be excited in the visible region. The study demonstrates that the presence of a Brønsted acid **73** is crucial for the success of the reaction, enabling the formation of cyclobutanes **74** in high yields (up to 90%). The mechanism likely involves the formation of a thionium ion **75** upon protonation of the dithiane **72**, which then undergoes intersystem crossing to a triplet state, leading to the formation of a 1,4-diradical intermediate **76** and subsequent ring closure (Scheme 9) [60].

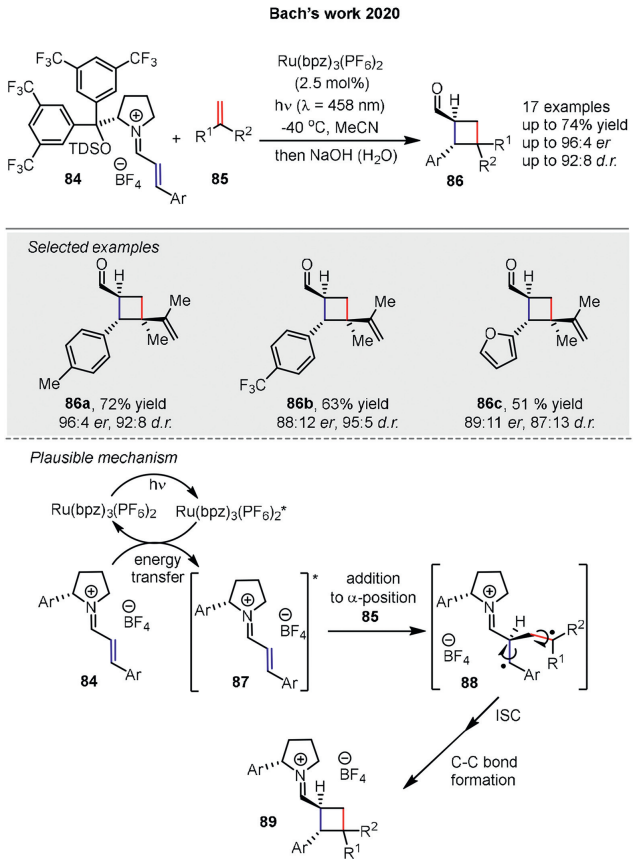
In consecutive years, Bach and colleagues have made significant strides in developing enantioselective intermolecular [2 + 2] photocycloaddition reactions of cyclic enones **77**, exploring the role of Lewis acids in achieving high enantioselectivity and their applications in natural product synthesis. In the intermolecular [2 + 2] photocycloaddition of cyclic enones **77** with olefins **78** using a chiral oxazaborolidine-$AlBr_3$ Lewis acid complex **79** to achieve high enantioselectivity (Scheme 10A) [61].

In the intramolecular [2 + 2] photocycloaddition of alkenyl cycloalkenones **81**, showed that the enantioselectivity is strongly influenced by the aryl group on the oxazaborolidine **79** (Scheme 10B) [62]. DFT calculations suggest that dispersion forces may affect the binding mode and enantioselectivity. Both studies emphasize the utility of Lewis acids in enhancing reaction selectivity and provide valuable insights for the synthesis of complex natural products.

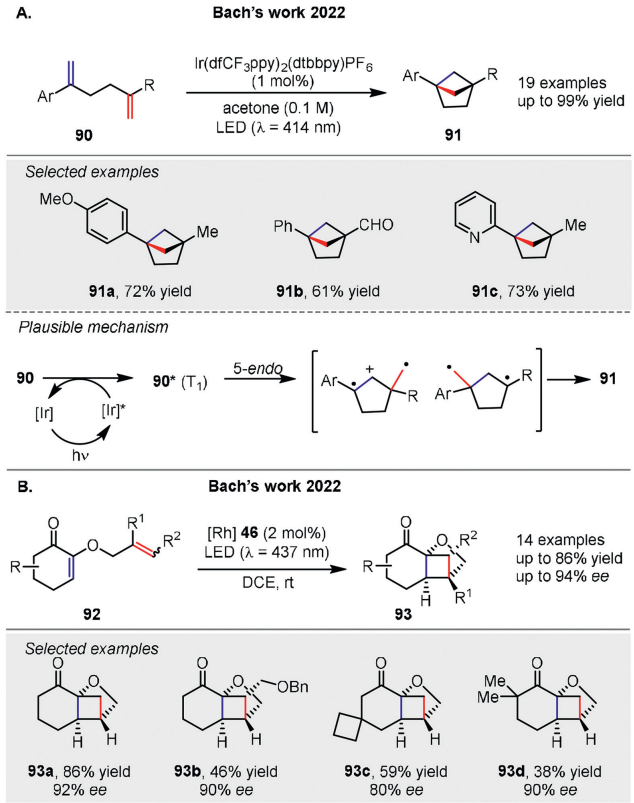
An enantioselective synthesis of chiral cyclobutanecarbaldehydes **86** *via* [2 + 2] photocycloaddition of chiral eniminium ion **84** with alkene **85** using $Ru(bpz)_3(PF_6)_2$ as catalysts was reported by Bach group in 2020. The reaction yields **86** with high selectivity (up to 74% yield, up to 96:4 *er*) (Scheme 11). Mechanistic studies using laser flash photolysis showed that the reaction proceeds *via* triplet-energy transfer from the ruthenium catalyst to the eniminium ion **84**, which is then quenched by the olefin **85** to form the product. Upon visible light irradiation, the ruthenium complex transfers energy to the eniminium ions **84**, exciting them to a reactive triplet state **87**. These excited ions **87** then react with olefins **85** to form cyclobutane intermediates **89**, which upon hydrolysis yield chiral cyclobutanecarbaldehydes **86**. The reaction is highly enantioselective due to the influence of a chiral secondary amine cocatalyst. The study explores catalytic enantioselective reactions using a chiral secondary amine co-catalyst, demonstrating the potential for this method in synthesizing chiral cyclobutanecarbaldehydes **86** [63].

In 2022, Bach group reported a visible light-driven intramolecular crossed [2 + 2] photocycloaddition to synthesize bicyclo[2.1.1]hexanes **91**, a valuable motif in medicinal chemistry. The reaction leverages triplet energy transfer from an iridium photosensitizer to styrene derivatives **90**, leading to the formation of these bridged scaffolds with good to high yields (up to 99%). The mechanism likely involves energy transfer from the excited iridium catalyst to the substrate **90**, forming a triplet intermediate **90*** that cyclizes in a 5-endo mode to produce the desired product **91** (Scheme 12A). This method enables the synthesis of a variety of 1,4-disubstituted bicyclo[2.1.1]hexanes **91**, which can be further functionalized, highlighting its potential for constructing complex and rigid scaffolds [64]. An enantioselective crossed intramolecular [2 + 2] photocycloaddition of 2-(alkenyloxy)cyclohex-2-enones **92** using a chiral rhodium Lewis acid catalyst **46** was presented by Bach group in 2022, achieving high enantioselectivity (80%-94% *ee*) under visible light (Scheme 12B) [65]. The mechanism involves the formation of a 1,4-diradical intermediate that forms the complex cyclobutane bridged skeletons **93**.

Walker group discovered a visible-light organophotocatalytic [2 + 2] cycloaddition reaction involving electron-deficient styrenes **94,** in 2022. They found that an organic cyanoarene photocatalyst (4CzIPN) can efficiently catalyze the formation of cyclobutanes **95** from electron-deficient styrenes with good functional group tolerance. The study explores the scope of the reaction, demonstrating its applicability to a range of electron-deficient substituents and achieving both homodimerizations and intramolecular [2 + 2] cycloadditions. The mechanism likely involves an energy-transfer pathway, supported by experiments showing re-



Scheme 11. Synthesis of chiral cyclobutanecarbaldehydes *via* [2 + 2] photocycloaddition of chiral eniminium ions with alkene.



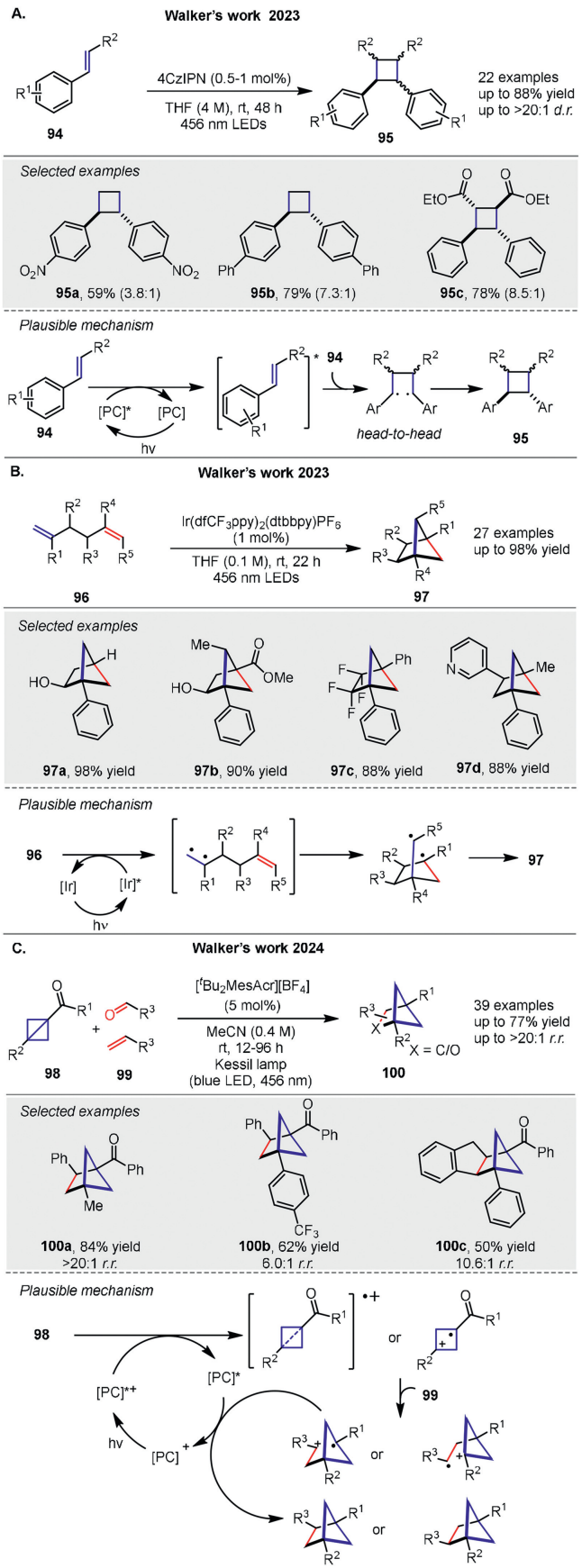
Scheme 12. Ir-catalyzed photochemical intramolecular crossed [2 + 2] photocycloaddition of styrene derivatives.

duced yields in the presence of a triplet quencher (Scheme 13A) [66]. This method offers a sustainable and cost-effective alternative to traditional transition-metal-based catalysts, expanding the toolkit for synthetic chemists working with cyclobutane derivatives. Following this, a visible light-mediated photocatalytic [2 + 2] cycloaddition reaction that provides access to polysubstituted bicyclo[2.1.1]hexanes (BCHs) **98** from **97**. They developed a protocol using [Ir{dF(CF_3)ppy}$_2$(dtbbpy)]PF_6 as a photocatalyst to synthesize BCHs **98** with distinct substitution patterns, including structures that can serve as bioisosteres for *ortho*-, *meta*-, and polysubstituted benzenes. The method is operationally simple and tolerates a broad range of functional groups (Scheme 13B) [67]. Key findings include the preparation of BCHs with various substituents, such as esters, alcohols, and boronate esters, in high yields. The study also demonstrates the potential for these compounds to occupy chemical space inaccessible to aromatic systems, highlighting their utility in drug design. Mechanistic studies suggest an energy-transfer mechanism, with the excited state of the photocatalyst facilitating the cycloaddition. Later they presented a novel photocatalytic oxidative activation of bicyclo[1.1.0]butanes (BCBs) **98** using an acridinium organophotocatalyst, enabling formal [$2\sigma + 2\pi$] cycloadditions with alkenes and aldehydes **99** to form bicyclo[2.1.1]hexanes and oxabicyclo[2.1.1]hexanes **100**. The reaction involves the formation of radical cation intermediates from BCBs, which then react with the alkenes or aldehydes. Mechanistic studies, including electrochemical, photophysical, radical trapping, and computational analyses, support the proposed oxidative pathways. The subtle interplay between the BCB and alkene identity dictates the reaction mechanism, leading to regiodivergent pathways and complementary products with up to >20:1 regioselectivity (Scheme 13C) [68]. This work highlights a rare example of oxidative BCB activation, expanding the synthetic utility of BCBs in organic synthesis.

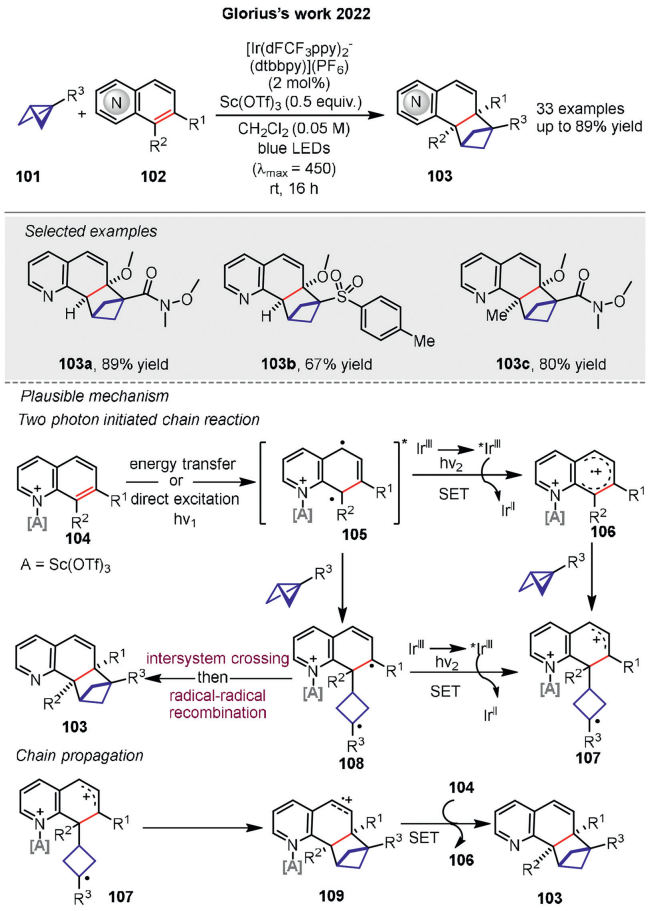
In recent years, several elegant examples have been reported for bicyclo[1.1.0]butanes (BCBs) in radical cycloaddition reactions. Glorius group disclosed a strain-release-enabled *ortho*-selective [$2\pi + 2\sigma$] photocycloaddition of bicyclic aza-arenes **102** with bicyclo[1.1.0]butanes **101** (Scheme 14). In the presence of [Ir($dFCF_3ppy$)$_2$(dtbbpy)](PF_6) (2 mol%) as the photosensitizer under irradiation with blue LEDs ($\lambda max = 450$ nm) in CH_2Cl_2, this reaction strategy not only conserves the typical photolabile *ortho*-cycloaddition product but also provides access to highly decorated bicyclo[2.1.1]hexane frameworks in direct proximity to *N*-heteroarenes. The proposed mechanism is shown in Scheme 14. Photoexcited $^*Ir^{III}$ oxidizes quinoline **105** in its excited state to form the respective radical cation **106**. The selective addition of **101** to **106** yields cyclobutane radical cation **107**. Alternatively, **107** can also be generated by oxidation of diradical **108**, which is formed *via* the addition of **101** to **105**. Cyclization of **107** subsequently forms radical cation **109**. Finally, oxidation of neutral quinoline **104** by **109** propagates the radical chain by liberating the product **103** and regenerating **106** [69].

In the same year, they also presented a visible-light-induced energy transfer strategy to synthesize polysubstituted 2-oxabicyclo[2.1.1]hexanes **112** from benzoylformate esters **110** and bicyclo[1.1.0]butanes **111**. The reaction involves a formal [$2\pi + 2\sigma$] photocycloaddition, followed by backbone C-H abstraction and aryl group migration (Scheme 15). The mechanism begins with energy transfer from the excited-state photocatalyst to the benzoylformate ester **110**, generating an excited triplet state **113**. This intermediate undergoes a stepwise radical process, including radical-radical coupling and aryl group migration, leading to the formation of the final product **112**. The reaction is highly regioselective, driven by the formation of the most stable radical intermediate **114** [70].

Following this, Glorius's group reported an intermolecular [2 + 2] photocycloaddition enabled by triplet energy transfer, offering a simple, modular, and diastereoselective route to bi-



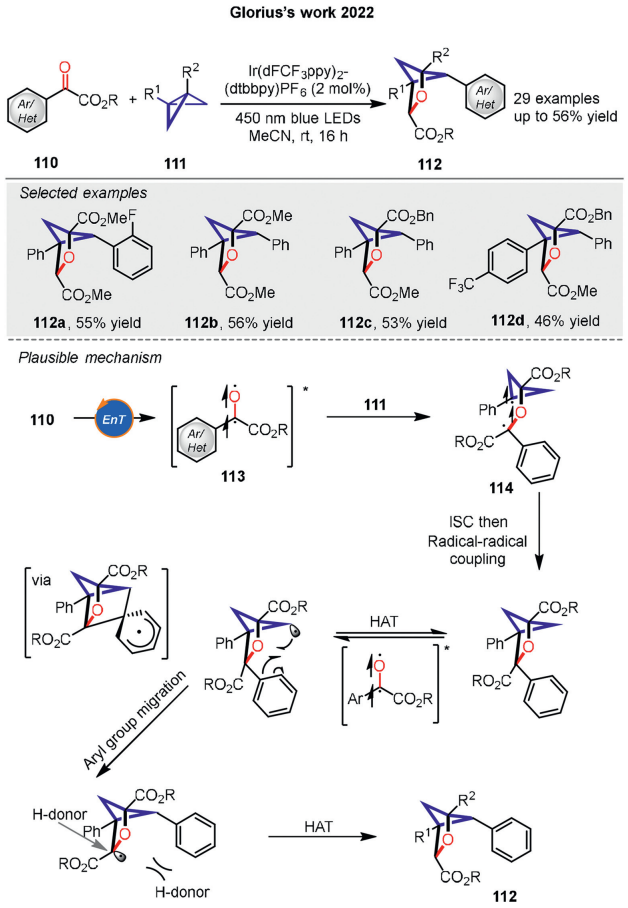
Scheme 13. Ir-catalyzed photochemical intramolecular crossed [2+2] photocycloaddition of styrene derivatives.



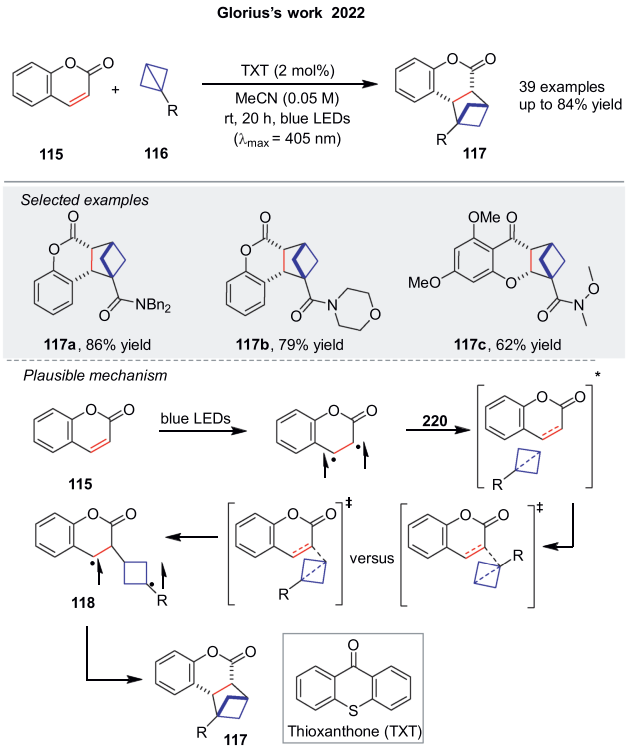
Scheme 14. Ir-catalyzed *ortho*-selective dearomative [2+2] photocycloadditions of bicyclic aza-arenes with bicyclo[1.1.0]butanes.

cyclo[2.1.1]hexanes **117** from heterocyclic olefins **115**, such as coumarins, flavones, and indoles (Scheme 16) [71]. This strategy, utilizing thioxanthone (TXT), extends intermolecular [2+2] photocycloadditions to σ-bonds and accesses previously inaccessible structural motifs. The proposed stepwise mechanism through diradical intermediate **118** is outlined in Scheme 16.

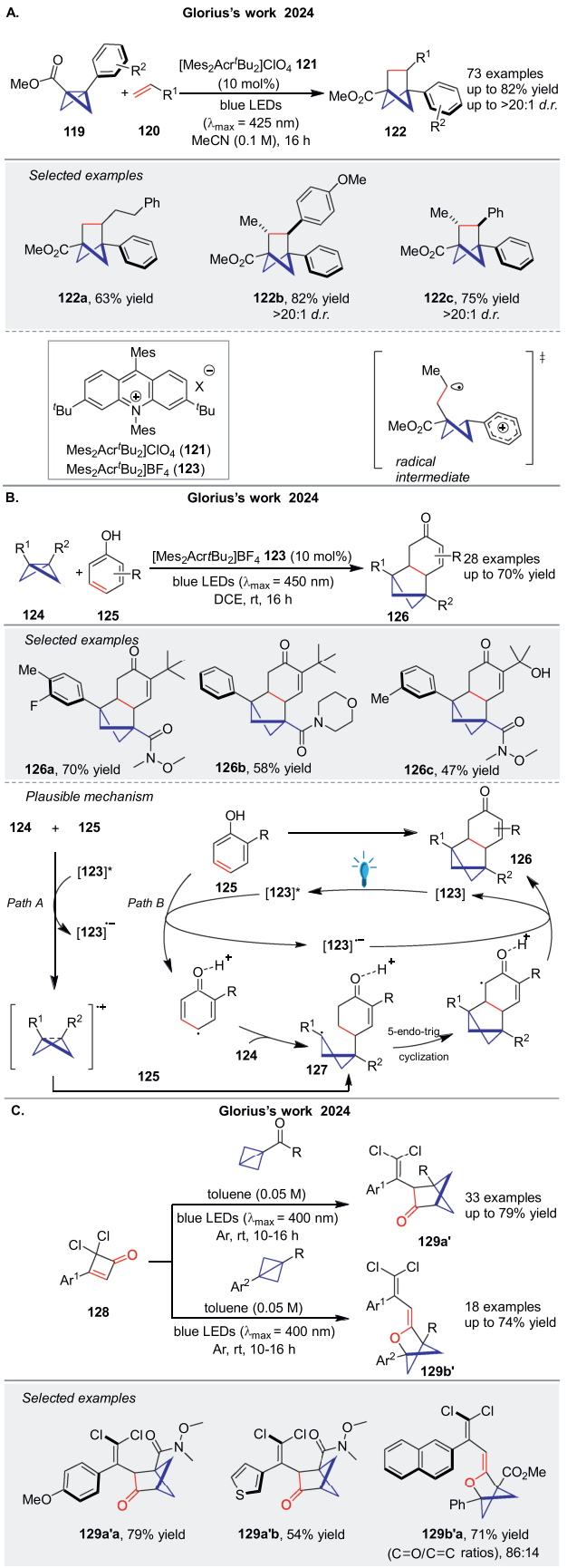
In 2024, Glorius group reported the use of photoredox catalysis to generate bicyclo[1.1.0]butyl radical cations, which undergo highly regio- and diastereoselective [2+2] cycloaddition reactions with a broad range of alkenes to afford bicyclohexanes **122** (Scheme 17A) [72]. The mechanism involves single-electron oxidation of bicyclo[1.1.0]butanes **119** to form radical cations, which then react with alkenes. DFT computations and experimental studies suggest that the initial interaction between the radical cation and the alkene leads to a radical addition, followed by intramolecular ring closure. In the same year, they described a photoredox-catalyzed method for the dearomative [2+2] cycloaddition of phenols **125** with bicyclo[1.1.0]butanes **124**. This reaction produces bicyclo[2.1.1]hexane **126** units fused to cyclic enones (Scheme 17B) [73]. The mechanism likely involves the oxidation of either the phenol or the BCB by the excited photocatalyst, leading to a common intermediate **127** that undergoes cyclization. The study includes experimental evidence supporting the involvement of radical species. Following this, the same group presented a novel double strain-release [$2\pi+2\sigma$] photocycloaddition reaction that synthesizes heterobicyclo[2.1.1]hexane units **129a**, **129b** using cyclobutenone **128** and bicyclo[1.1.0]butane (BCB) under visible light irradiation without a catalyst (Scheme 17C) [74]. The study demonstrates broad substrate scope, yielding diverse products with good



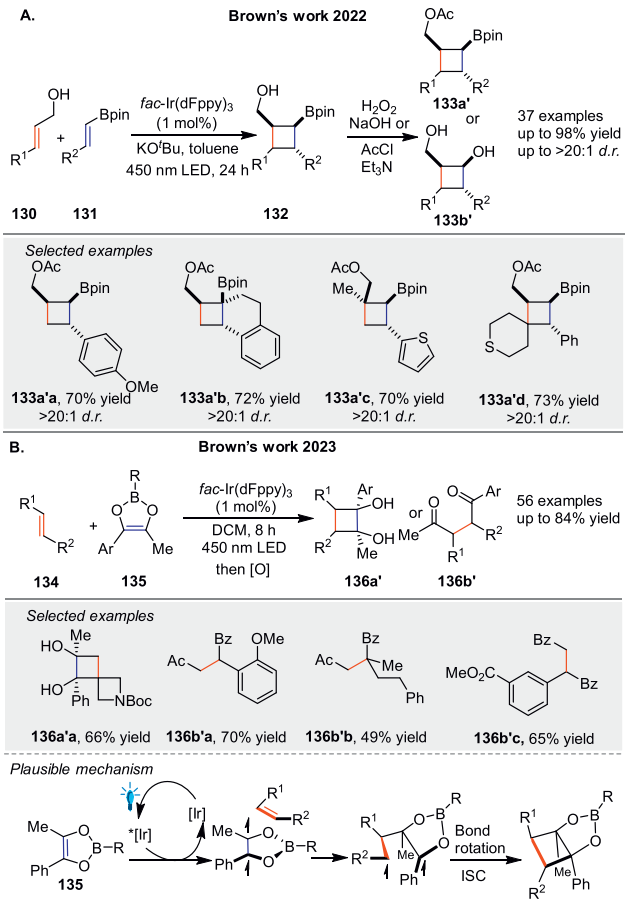
Scheme 15. Ir-catalyzed [2 + 2] photocycloaddition of benzoylformate esters and bicyclo[1.1.0]butanes.



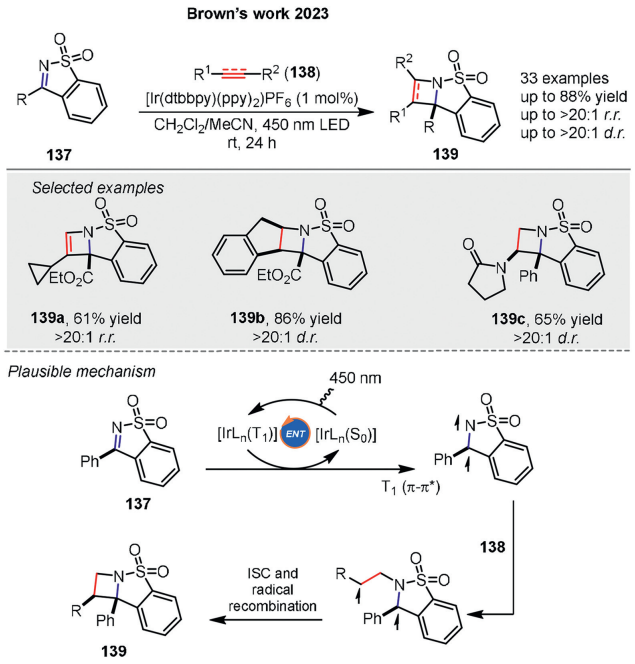
Scheme 16. Intermolecular [2 + 2]-photocycloaddition enabled by triplet energy transfer.



Scheme 17. Photosensitized [2 + 2] cycloadditions of bicyclobutanes.



Scheme 18. Ir-catalyzed [2+2] photocycloaddition reactions of alkenylboronates and dioxaboroles.



Scheme 19. Ir-catalyzed [2+2] cycloaddition reactions of *N*-sulfonylimines with alkenes and alkynes.

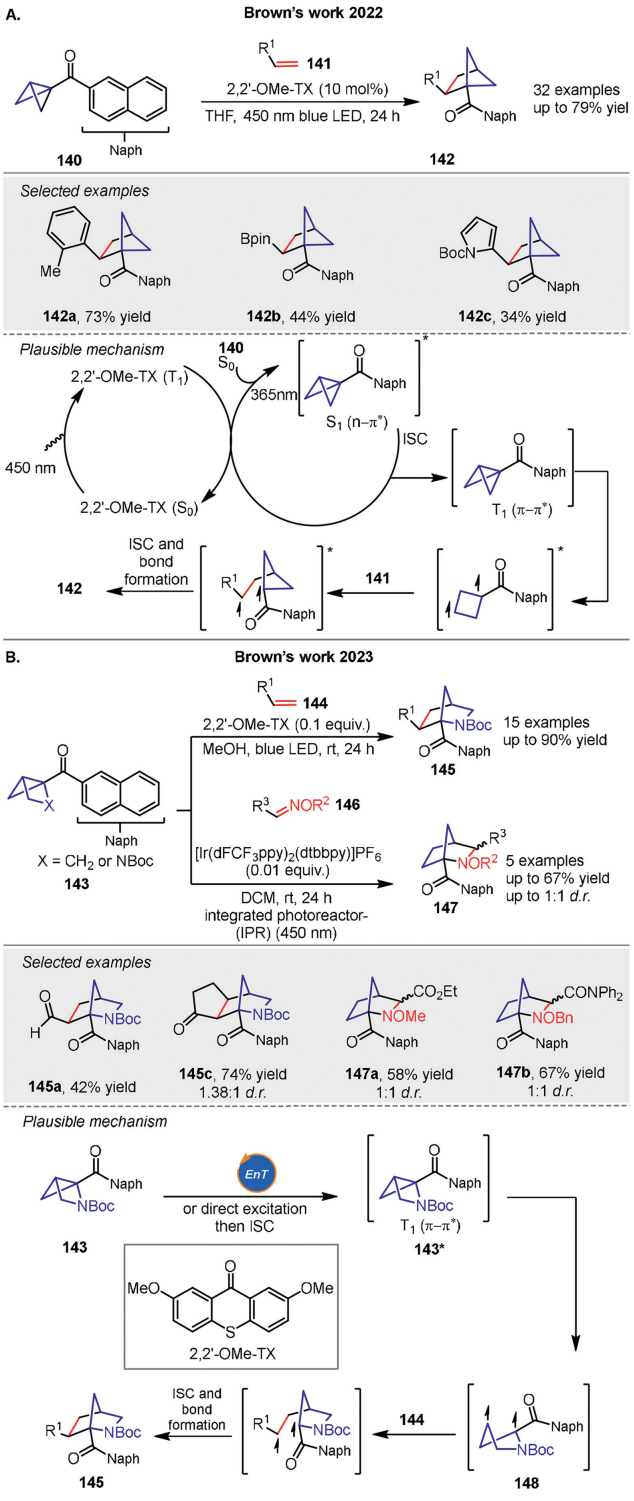
functional group tolerance. Mechanistic studies, including UV-visible spectroscopy and DFT calculations, suggest a triplet state process involving a two-photon excitation of cyclobutenone to form a ketene intermediate, which then reacts with BCB. This work highlights a sustainable and efficient method for synthesis of complex sp^3-rich molecules with potential applications in pharmaceuticals.

In 2022, the Brown group introduced a strategy for the photosensitized cycloaddition of alkenylboronates **131** and allylic alcohols **130** through temporary coordination. This approach allows for the synthesis of a diverse range of cyclobutylboronates **133a** and cyclobutylalcohols **133b** with high levels of stereo- and regiocontrol (Scheme 18A) [75]. The key to this method is the temporary coordination of the allylic alcohol **132** to the Bpin unit, which facilitates intramolecular cyclization. Following this, Brown group introduced another novel strategy for photosensitized [2+2] cycloadditions using dioxaboroles **135**, leveraging boron ring constraint to enable efficient reactions with a broad range of alkenes **134**. This method overcomes limitations of acyclic substrates by stabilizing dioxaborole intermediates, facilitating the synthesis of cyclobutyl diols **136a** and 1,4-dicarbonyl compounds **136b**. Demonstrated through the creation of valuable heterocycles and biatriosporin D, this approach offers high functional group tolerance and regioselectivity. Mechanistic studies suggest a photosensitization pathway involving triplet excited states and radical intermediates (Scheme 18B) [76].

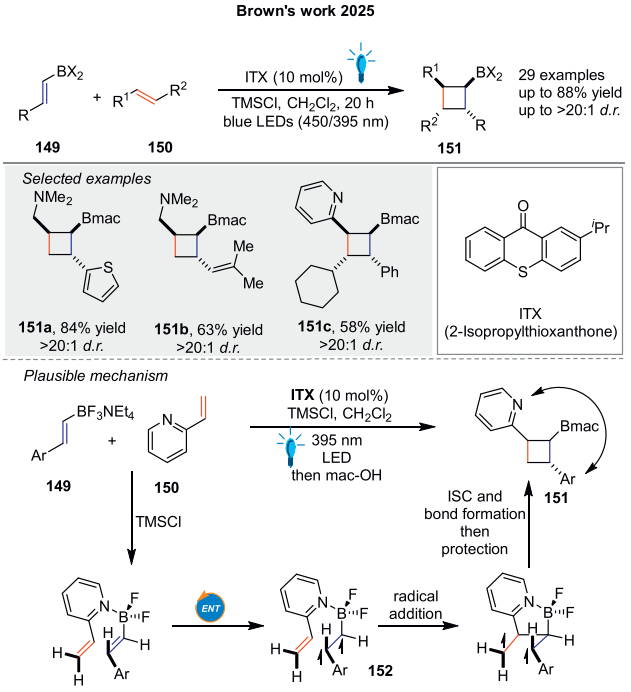
Photosensitized [2+2] cycloaddition reactions of *N*-sulfonylimines **137** was presented by Brown group in 2023, a method for the stereoselective construction of azetidine derivatives **139**. Mechanistic studies suggested that the reactions proceed *via* Dexter energy transfer, where the excited triplet state of the photosensitizer transfers energy to the substrate, leading to the formation of a diradical intermediate that subsequently reacts to form the cycloaddition products (Scheme 19) [77].

A new strategy for synthesizing bicyclo[2.1.1]hexanes **142** *via* strain-release $[2\pi+2\sigma]$ cycloadditions initiated by energy transfer was presented by Brown group in 2022. The reaction involves sensitizing a BCB **140** with a sensitizer, such as 2,2'-OMeTX, followed by cycloaddition with an alkene **141**. The mechanism of this strain-release $[2\pi+2\sigma]$ cycloaddition for synthesizing bicyclo[2.1.1]hexanes involves energy transfer from a sensitizer to a naphthyl ketone-substituted BCB **140**. Upon excitation, the BCB generates a triplet diradical intermediate through strain-release-induced bond cleavage. This intermediate reacts with an alkene **141**, leading to the formation of the desired cyclobutanecarbaldehyde product **142** *via* intersystem crossing and bond formation. The process is facilitated by the use of a thioxanthone-based sensitizer, which enables selective energy transfer to the BCB, driving the reaction forward efficiently. This method allows for the synthesis of a diverse range of bicyclo[2.1.1]hexanes with various substitution patterns (Scheme 20A) [78]. In 2023, the same group introduced the synthesis of 2-azanorbornanes **145** and **147** using strain-release formal cycloadditions initiated by energy transfer. They described two approaches: the formal cycloaddition of azahousanes with alkenes **144** and the formal cycloaddition of housanes with imines **146** [79]. The azahousane reagent was synthesized from Boc-Hyp-OMe through an Appel reaction and intramolecular nucleophilic substitution. The reaction with alkenes likely proceeds *via* Dexter energy transfer or direct excitation to **143**, followed by intersystem crossing and homolysis of the strained C-C bond to generate a diradical intermediate **148**, which then undergoes stepwise radical addition to form the product **145**. Both methods are mild, scalable, and valuable for accessing new chemical spaces in the pharmaceutical industry (Scheme 20B).

In the recent work, Brown group presented a novel strategy for photosensitized [2+2] cycloadditions between styrenyl dihaloboranes **149** and unactivated allylamines **150** (Scheme 21) [80]. The



Scheme 20. Visible light mediated cycloaddition of housane and azahousanes with alkenes and imines.



Scheme 21. Photosensitized [2 + 2] cycloadditions between styrenyl dihaloboranes and unactivated allylamines.

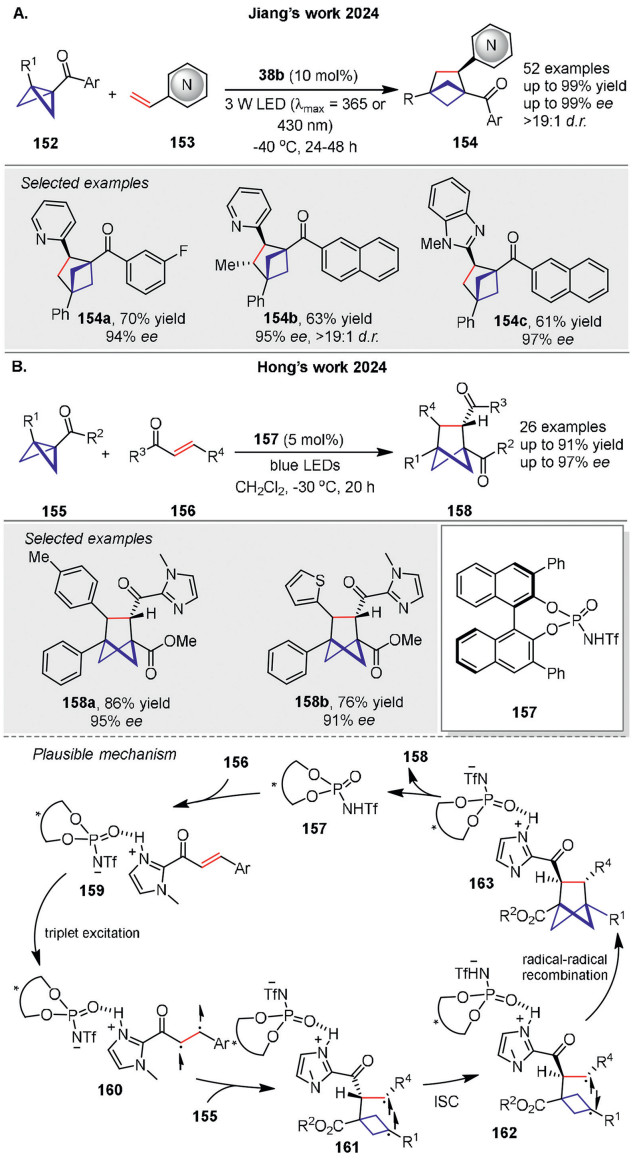
success of the reaction hinges on the use of dihaloboranes, which provide increased Lewis acidity necessary for amine coordination. Mechanistically, this [2 + 2] cycloaddition likely proceeds *via* energy transfer from the photosensitizer to the dihaloborane **149**, followed by coordination and cycloaddition with the allylamine **150**.

An enantioselective [$2\pi + 2\sigma$] photocycloaddition of BCBs **152** with vinylazaarenes **153**, catalyzed by a chiral phosphoric acid **38b** was described by Jiang group in 2024. This method yields high enantioselectivity and diastereoselectivity in producing bicyclo[2.1.1]hexane (BCH) derivatives **154** (Scheme 22A) [81].

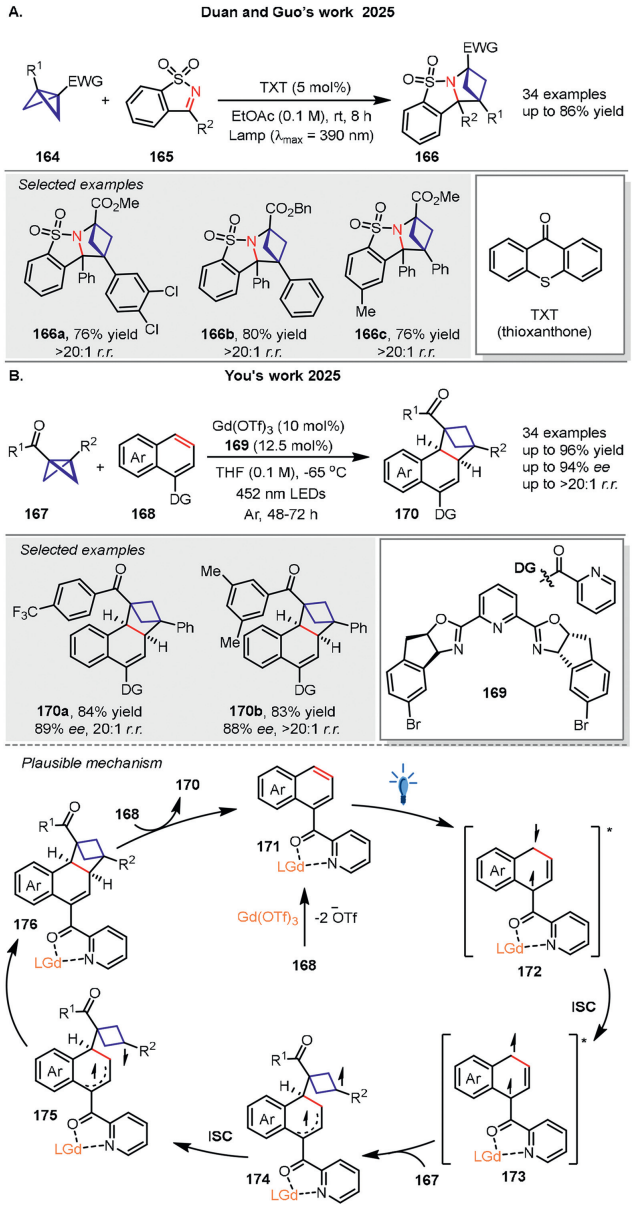
Hong group also developed the photoinduced asymmetric cycloaddition of BCBs **155** and α,β-unsaturated ketones **156** using a chiral Brønsted acid catalyst **157**. **156** is protonated by the catalyst and excited to a triplet state upon light irradiation **160**. This triplet excited state undergoes a stepwise cycloaddition with the BCB (**155**), leading to the insertion of the α-carbon of the ketone into the BCB framework (**161**). The mechanism involves the formation of a diradical intermediate **162**, which then cyclizes to form the desired chiral BCH product **158** (Scheme 22B) [82].

Very recently, Duan and Guo group presented a substrate-regulated divergent addition of *N*-sulfonyl ketimines **165** to BCBs **164** using photoinduced energy transfer resulting in benzosultam-fused aza-BCHs **166**. The mechanism involves triplet energy transfer from a photosensitizer to the BCB **164**, leading to cycloaddition with cyclic ketimines **165** (Scheme 23A) [83]. A highly regio- and enantioselective dearomative [2 + 2] photocycloaddition reaction between naphthalene derivatives **168** and BCBs **167** using Gd(III) catalysis was presented by You and colleagues (Scheme 23B). This method, enabled by photoexcited Gd(III) catalysis, allows for the synthesis of enantioenriched bicyclo[2.1.1]hexanes **170** with a variety of functional groups, achieving yields and enantioselectivities [84]. Mechanistic studies, including UV-vis absorption spectroscopy and triplet quenching experiments, suggest that the reaction involves the excitation of naphthalene to its triplet state **173**, followed by radical addition to the BCB **167**, leading to the formation of a 1,4-diradical intermediate **174** and subsequent product formation. The use of a chiral ligand **169** enhances substrate solubility and enantiocontrol through hydrogen bonding, facilitating efficient energy transfer. This work by You and colleagues represents a significant advancement in the field of photocatalysis and asymmetric synthesis.

Very recently, Davies group presented a method for synthesizing highly functionalized bicyclo[2.1.0]pentanes (housanes) **179** through a two-step sequence involving a silver- or gold-catalyzed cyclopropenation of alkynes to form **177** followed by an in-



Scheme 22. Enantoselective photosensitized [2 + 2] cycloadditions of BCBs.

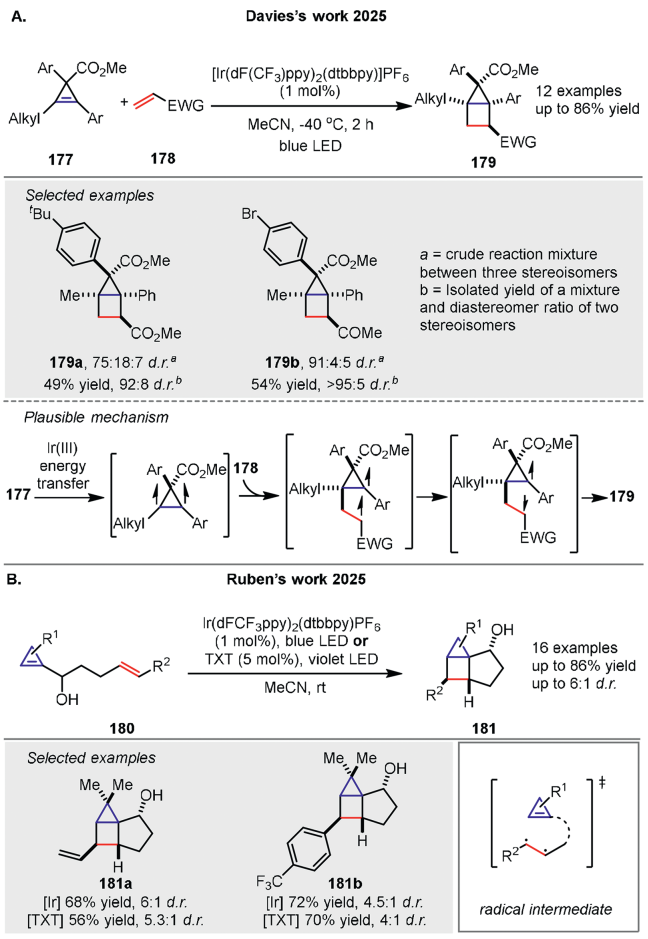


Scheme 23. Visible-light photocatalyzed [2 + 2] cycloaddition of BCBs.

termolecular [2 + 2] photocycloaddition reaction with electron-deficient alkenes **178**. The cyclopropenation step utilizes aryldiazoacetates, while the [2 + 2] cycloaddition is achieved using blue LED irradiation and a commercially available photocatalyst as a triplet sensitizer at low temperatures (-40 °C). The process is highly diastereoselective and proceeds with enantioretention when enantioenriched cyclopropenes are used (Scheme 24A) [85]. The method also allows for the generation of enantioenriched housanes and provides a streamlined approach to accessing complex, strained aliphatic rings with potential applications in medicinal chemistry. A [2 + 2] photocycloaddition of cyclopropenes bearing a styryl group **180** to create housane derivatives **181** was reported by Rubén's group. The reaction is driven by selective excitation of the styrene fragment, leading to a stereoselective cycloaddition [86]. The mechanism involves generating an excited triplet state from the styrene fragment, which then undergoes a stepwise radical cycloaddition. The process is efficient and yields derivatives with high diastereoselectivity, using either an iridium complex or thioxanthone as a sensitizer (Scheme 24B).

2.2. [3 + 2] cycloaddition

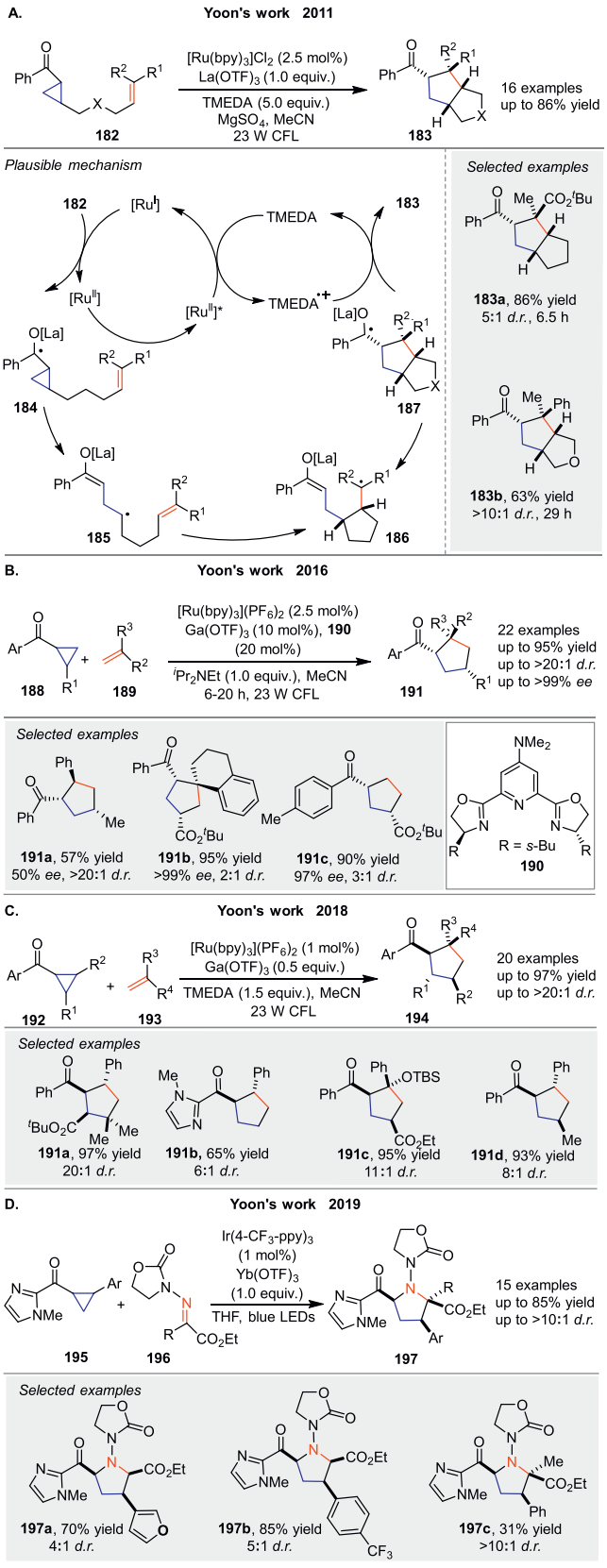
Highly substituted cyclopentane ring systems **183** were generated by the formal intramolecular [3 + 2] cycloaddition of aryl cyclopropyl ketones with olefins **182** in 2011, as reported by Yoon and co-workers. This method utilized a photocatalytic system comprising a ruthenium photocatalyst $[Ru(bpy)_3]Cl_2$, the Lewis acid $La(OTf)_3$, and TMEDA (Scheme 25A) [87]. The key initiation step involves the one-electron reduction of the ketone to the corresponding radical anion **184**, which subsequently undergoes ring opening to generate the distonic radical anion **185**. Sequential radical cyclizations then lead to the formation of the cyclized ketyl radical **183**, promoting cycloaddition to form **187**. The final product obtained through the loss of an electron, completing the formal intramolecular [3 + 2] cycloaddition of **182**. In 2016, the same group reported the enantioselective photocatalytic intermolecular [3 + 2] cycloaddition of aryl cyclopropyl ketones **188** and alkenes **189**. This method provides an asymmetric [3 + 2] photocycloaddition approach using ligand **190** to assemble structurally complex



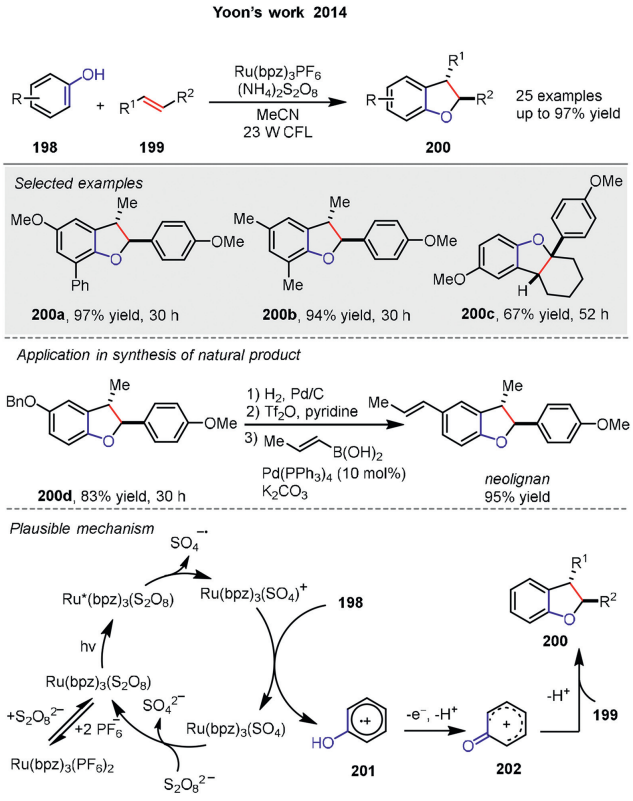
Scheme 24. Ir-catalyzed intermolecular and intramolecular [2 + 2] photocycloaddition reactions to synthesize housanes.

five-membered carbocycles **191**, which are not synthetically accessible using other catalytic strategies (Scheme 25B) [88]. Two years later, the group further developed a general protocol for radical anion [3 + 2] cycloaddition under similar conditions to afford carbocycles **194** (Scheme 25C) [89]. This method offers a valuable complement to existing methodologies in the literature for constructing structurally complex five-membered-ring compounds. In 2019, building on their previous work, Yoon group attempted to replace the olefin reactant with hydrazones **196** and found that a range of structurally diverse pyrrolidine rings **197** could be synthesized using their previously reported photoredox catalysis strategy (Scheme 25D) [90]. The key insight that enabled the expansion of the scope of photoredox [3 + 2] cycloadditions to C=N electrophiles was the use of a redox auxiliary strategy. This approach allowed for the photoreductive activation of the cyclopropyl ketone **195** without the need for an exogenous tertiary amine co-reductant.

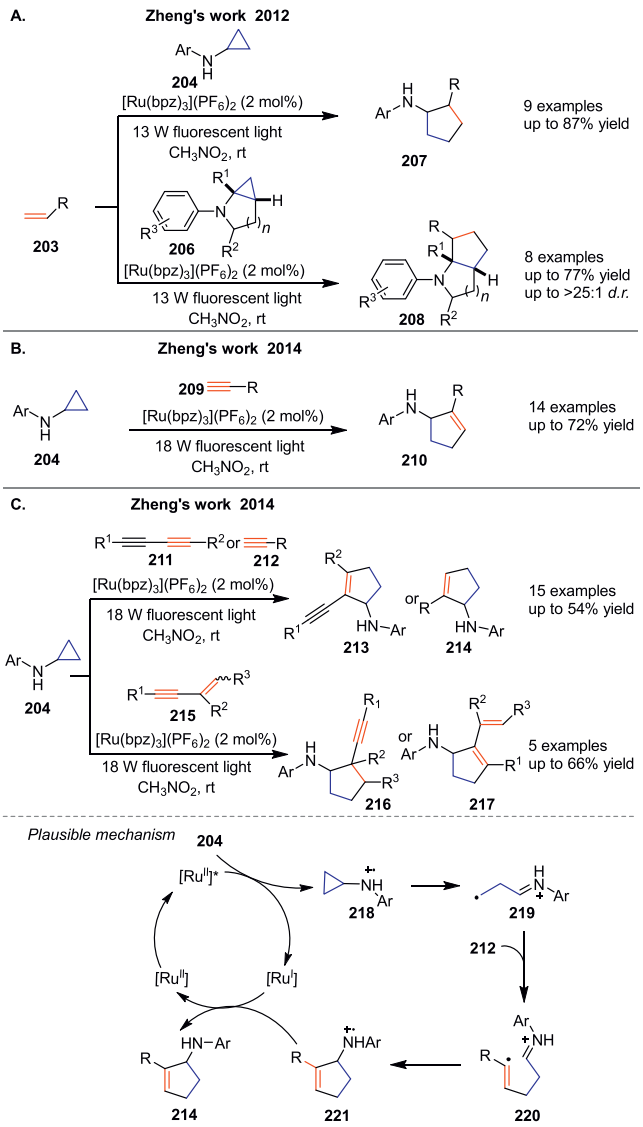
Another [3 + 2] photocatalytic cycloaddition of phenols **198** and alkene **199**, for synthesizing dihydrobenzofuran products **200** developed by Yoon group in 2014. This protocol utilized visible-light-activated transition metal photocatalysis, specifically employing ammonium persulfate as a benign terminal oxidant. This method enables the modular synthesis of a broad range of dihydrobenzofuran products **200** with high yields and selectivity. The study highlights the potential of photoredox catalysis for oxidative transformations, offering a practical and environmentally friendly alternative to traditional synthetic methods. The mechanism of this oxidative [3 + 2] cycloaddition of phenols and alkenes involves a slow salt metathesis process where $Ru(bpz)_3^{2+}$ forms an insoluble



Scheme 25. Ru/Ir-catalyzed [3 + 2] photocycloaddition of aryl cyclopropyl ketones with olefins.



Scheme 26. Ru-catalyzed [3 + 2] photocycloaddition of phenols and alkenes.



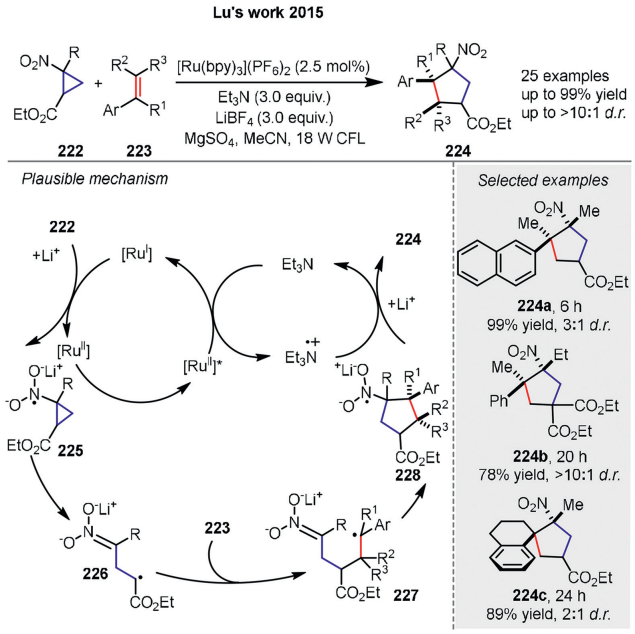
Scheme 27. Ru-catalyzed [3 + 2] photocycloaddition of cyclopropylanilines with alkenes, alkynes, enynes, and diynes.

$Ru(bpz)_3(S_2O_8)$ complex. Upon photoexcitation, this complex generates the active oxidant $Ru(bpz)_3^{3+}$ and a sulfate radical anion. The phenol is oxidized to form a phenoxonium cation **201**, which is then trapped by an electron-rich alkene **199** to form the desired dihydrobenzofuran product **200**. This photocatalytic process requires both light and the $Ru(bpz)_3^{2+}$ catalyst, highlighting the importance of these components in driving the reaction forward. The applicability of this photocatalytic method was also demonstrated by the ability to synthesize the large family of bioactive benzofuranoid natural products (Scheme 26) [91].

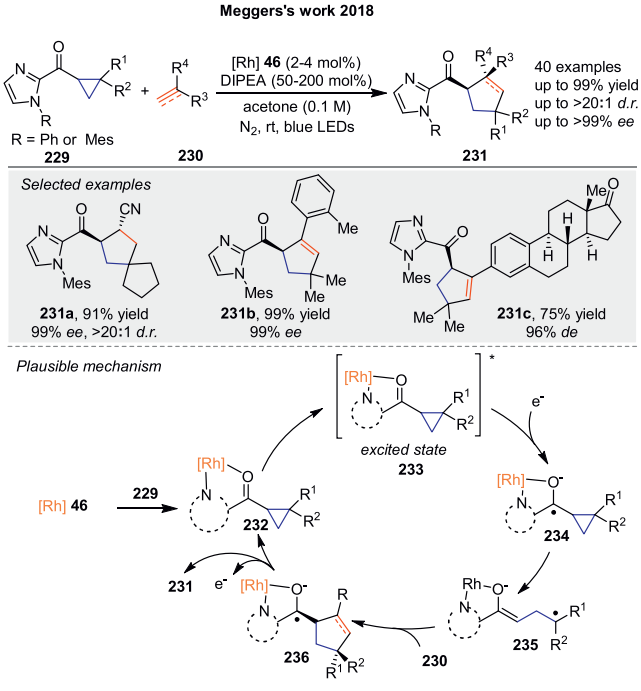
In 2012 and 2014, Zheng group reported intermolecular [3 + 2] cycloaddition reactions of monocyclic cyclopropylanilines **204** with alkenes **203** [92], alkynes **209** [93], diynes **211**, and enynes **212** [94] *via* visible light photoredox catalysis, yielding a variety of methods exhibit significant functional group tolerance, particularly with heterocycles such as fused indolines. Mechanistically, the annulation likely proceeds through the cyclic allylic amine radical cation **221**. Using $[Ru(bpz)_3](PF_6)_2$ as an effective photocatalyst, this pathway shown in Schemes 27A-C. The photoexcited $Ru(bpz)_3^{2+}$ oxidizes **204** to the corresponding amine radical cation **218**, which triggers cyclopropyl ring opening to generate distonic radical cation **219**. The primary carbon radical of **219** adds to the alkynes **212** to afford vinyl radical **220**. Intramolecular addition of the vinyl radical to the iminium ion of distonic radical cation closes the five-membered ring, furnishing amine radical cation **221**. Finally, $Ru(bpz)_3^{+}$ reduces **221** to the annulation product **214** while regenerating $Ru(bpz)_3^{2+}$. In 2017, the same group presented the detection of transient amine radical cations involved in the reaction of **204** and styrene using electrospray ionization mass spectrometry (ESI-MS) in combination with online laser irradiation of the reaction mixture [95]. In particular, the reactive radical cation **218**, the reduced photocatalyst $Ru^{I}(bpz)_3^{+}$, and the product radical cation **221** were all successfully detected and confirmed by high-resolution MS. Thus, this strategy provides a powerful analytical tool to detect transient intermediates and study visible-light photocatalysis mechanistically.

The first nitro-group-initiated redox-neutral [3 + 2] cycloaddition of nitrocyclopropanes **222** with alkenes **223**, using photocatalyst $[Ru(bpy)_3](PF_6)_2$, was reported by Lu group in 2015. Photoexcitation of $Ru(bpy)_3^{2+}$ with visible light results in a photoexcited state $^{*}Ru(bpy)_3^{2+}$, which can undergo reductive quenching by Et_3N to generate the $Ru(bpy)_3^{+}$ species. This powerful reducing agent can transfer an electron to **222**. The distonic radical anion **226**, generated from the nitrocyclopropane radical anion **225**, can be trapped by styrenes **223** and then undergo intramolecular radical cyclization of **227**, followed by the loss of one electron from **228** to afford the products **224** (Scheme 28) [96]. Various functional groups can be tolerated, and multiple quaternary carbon centers are formed with high diastereoselectivity under these reaction conditions.

In 2018, Meggers and co-workers reported a conceptually straightforward and effective protocol for the asymmetric [3 + 2] cycloaddition between cyclopropanes **229** and a wide range of alkenes or alkynes **230** by employing a single Rh-based chiral Lewis acid catalyst. This protocol provides access to chiral cy-



Scheme 28. [3 + 2] redox-neutral cycloaddition of nitrocyclopropanes with styrenes by visible-light photocatalysis.



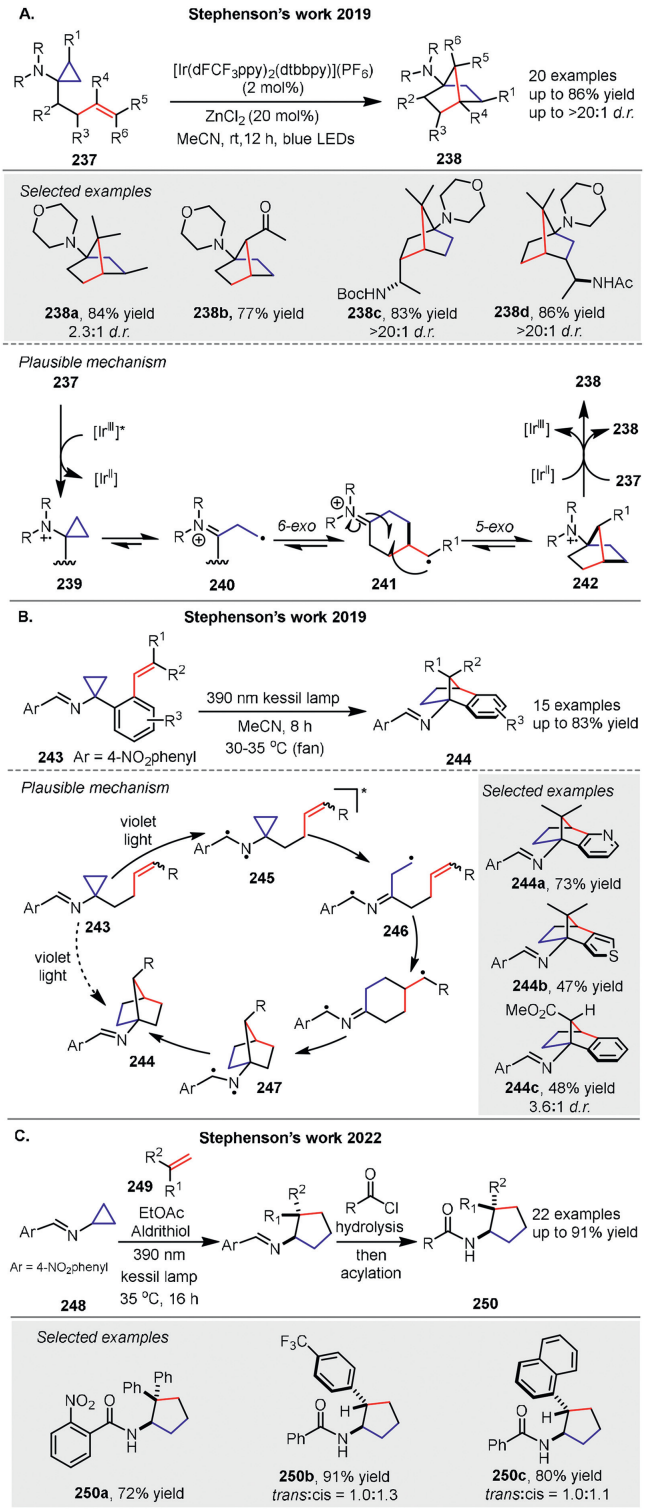
Scheme 29. Rh-catalyzed asymmetric [3 + 2] photocycloadditions of cyclopropanes with alkenes or alkynes.

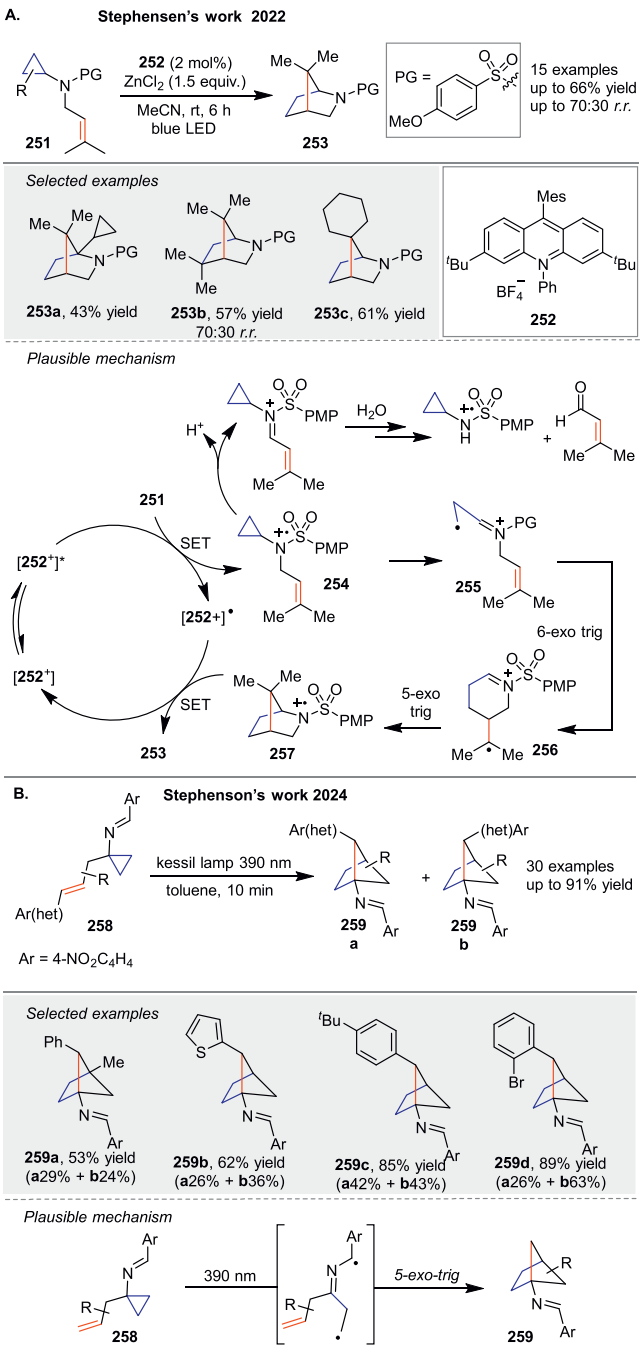
clopentanes and cyclopentenes **231** in up to 99% yields and with excellent enantioselectivities of up to >99% *ee* (Scheme 29) [97]. The proposed mechanism involves the generation of complex **232** upon bidentate coordination of the cyclopropane substrate **229** to the rhodium complex **46**. After photoexcitation, intermediate **233** serves as a strong oxidant and is reduced by a tertiary amine to form intermediate **234**, which subsequently ring-opens to generate the radical intermediate **235**. The subsequent radical addition with **230** affords the corresponding ketyl radical intermediate **236**. Finally, ligand exchange regenerates the catalyst/substrate complex **232**, completing the catalytic cycle and releasing the cycloaddition product **231**.

In 2019, Stephenson group described the photochemical conversion of aminocyclopropanes **237** into 1-aminonorbornanes **238** *via* formal [3 + 2] cycloadditions initiated by homolytic fragmentation of amine radical cation intermediates [98]. Mechanistically, the oxidation of **237** generates amine radical cations that undergo β-scission to form β-iminium radicals **240**. This enables a 6-*exo-trig* radical cyclization to produce distonic radical cations **241**, followed by a 5-*exo-trig* cyclization to forge the norbornane core **242**. Reduction to the product **238** closes the catalytic cycle (or propagates the chain), providing a net redox-neutral transformation (Scheme 30A). In 2019, Stephenson group reported the development of an intramolecular masked *N*-centered radical strategy that harnesses the energy of light to drive the conversion of cyclopropylimines **243** to 1-aminonorbornanes **244** (Scheme 30B) [99]. The proposed mechanism involves an *N*-centered radical **245** initiating the strain-driven homolysis of the cyclopropane ring, generating a formal β-iminyl radical intermediate **246**. Intermediate **246** then engages in an intramolecular addition to the alkene, followed by an intramolecular 5-*exo-trig* cyclization, resulting in the formation of cycloheptane **247**. Notably, both radicals of the excited state imine are terminated *via* recombination to regenerate the C-N bond, yielding the desired 1-aminonorbornanes **244**. In a similar vein, they detailed the development of a photochemical intermolecular formal [3 + 2] cycloaddition between cyclopropylimines **248** and substituted alkenes **249** to generate aminocyclopentane derivatives **250** in 2022 (Scheme 30C) [100]. These new photochemical transformations thus provide new avenues for the modern synthetic photochemist.

After that, Stephenson group presented a photochemical method for synthesizing 2-azanorbornane **253** scaffolds from cyclopropylsulfonamide derivatives **251**. The method employs a Lewis acid additive to promote the formation of amine radical cations, initiating a cascade radical cyclization sequence. This approach allows for the synthesis of substituted 2-azanorbornanes at all possible carbon centers. A plausible catalytic cycle is illustrated in Scheme 31A [101]. The mild and modular nature of this method makes it a valuable tool for accessing saturated aza-heterocycles, which are of significant interest in medicinal chemistry due to their potential as bioactive molecules. Another [3 + 2] photochemical method was presented by Stephensen's group in 2024. For synthesizing bicyclo[2.1.1]hexanes using imine photochemistry, this approach involves an intramolecular formal [3 + 2] cycloaddition of allylated cyclopropanes with a 4-nitrobenzimine substituent **258**, allowing for high functional group tolerance and mild reaction conditions *via* diradical intermediate. The resulting imines **259** can be hydrolyzed to yield primary amine building blocks, demonstrating the versatility of this method in preparing complex bicyclic scaffolds (Scheme 31B) [102].

In 2020, Ooi group strategically utilized urea as a redox-active directing group with anion-binding ability to achieve photoinduced, highly diastereo- and enantioselective [3 + 2] cycloaddition of cyclopropylamine **260** with α-alkylstyrenes **261**, providing access to a series of aminocyclopentanes **264** bearing stereochemically defined, vicinal tertiary and quaternary stereocenters [103]. A preparatory step involves the assembly of the photoactive Ir-chiral borate ion pair **262** and the **260** into the supramolecular ion pair **265**. Upon irradiation with visible light, **265** is excited and undergoes single-electron transfer (SET) to generate intermediate **266**. In this assembly, the radical cation **267** is considered to exist as a formal equilibrium mixture of an N-radical cation and a distonic radical cation, with the latter reacting with the alkene **261**. The intermediary alkyl radical **268** then undergoes stereoselective five-exo cyclization under the guidance of the accompanying **262** to afford



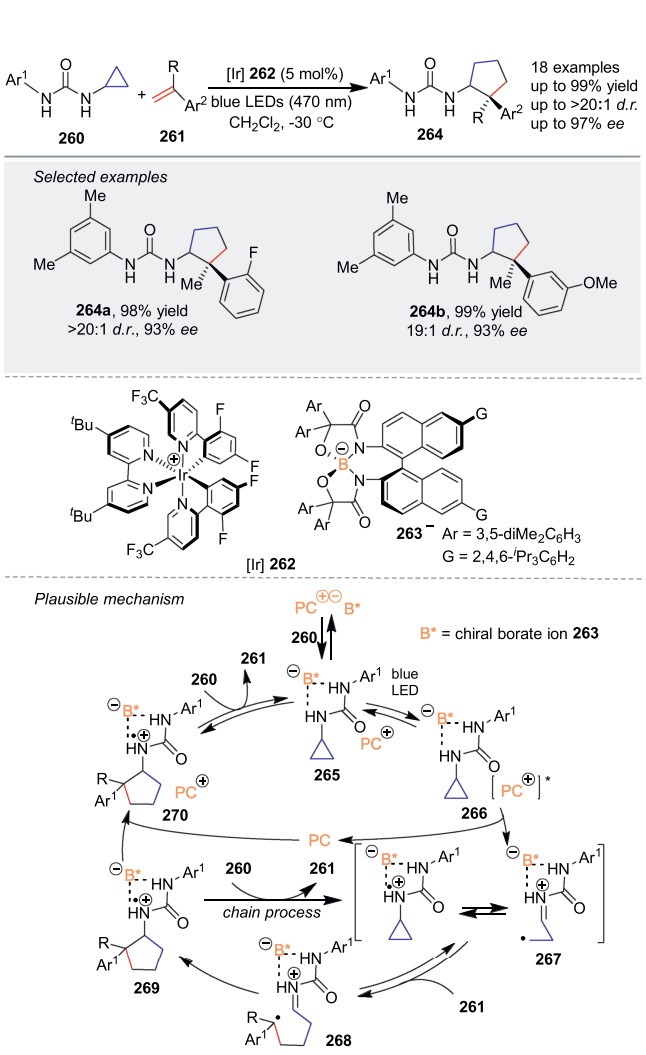


Scheme 30. Intra- and intermolecular [3+2] photocycloadditions of cyclopropanes with alkenes.

Scheme 31. Intramolecular [3+2] photocycloadditions of cyclopropanes with alkenes.

aminocyclopentane **270** in the form of an N-radical cation paired with **262** (Scheme 32).

A radical-based asymmetric olefin difunctionalization strategy for rapidly forging all-carbon quaternary stereocenters to diverse azaarenes **273** was presented by Jiang group in 2020 (Scheme 33A) [104]. Under cooperative photoredox and Brønsted acid catalysis, readily accessible cyclopropylamines **204** and α-branched 2-vinylazaarenes **271** can efficiently undergo a tandem two-step radical addition process, accomplishing a formal [3+2] cycloaddition. In 2022, the same group developed redox-neutral, asymmetric [3+2] photocycloaddition reactions of *N*-aryl cyclopropylanilines **204** with a variety of electron-rich and electron-neutral olefins **271** *via* cooperative visible-light-driven photoredox and chiral H-bond catalysis (Scheme 33B) [105]. Mechanistically, catalyst **38b** and **204** might form a noncovalent complex with a H-bonding interaction between the N-H of **204** and the P=O of **38b**. After photoexcitation, DPZ* serves as an oxidant and is reduced by the amine moiety of **204**, and then the resulting radical cation **276** undergoes ring-opening to form intermediate **277**. With the help of another H-bonding interaction between the OTf of alkene **274** and the P-OH group of **38b**, the subsequent intermolecular radical addition

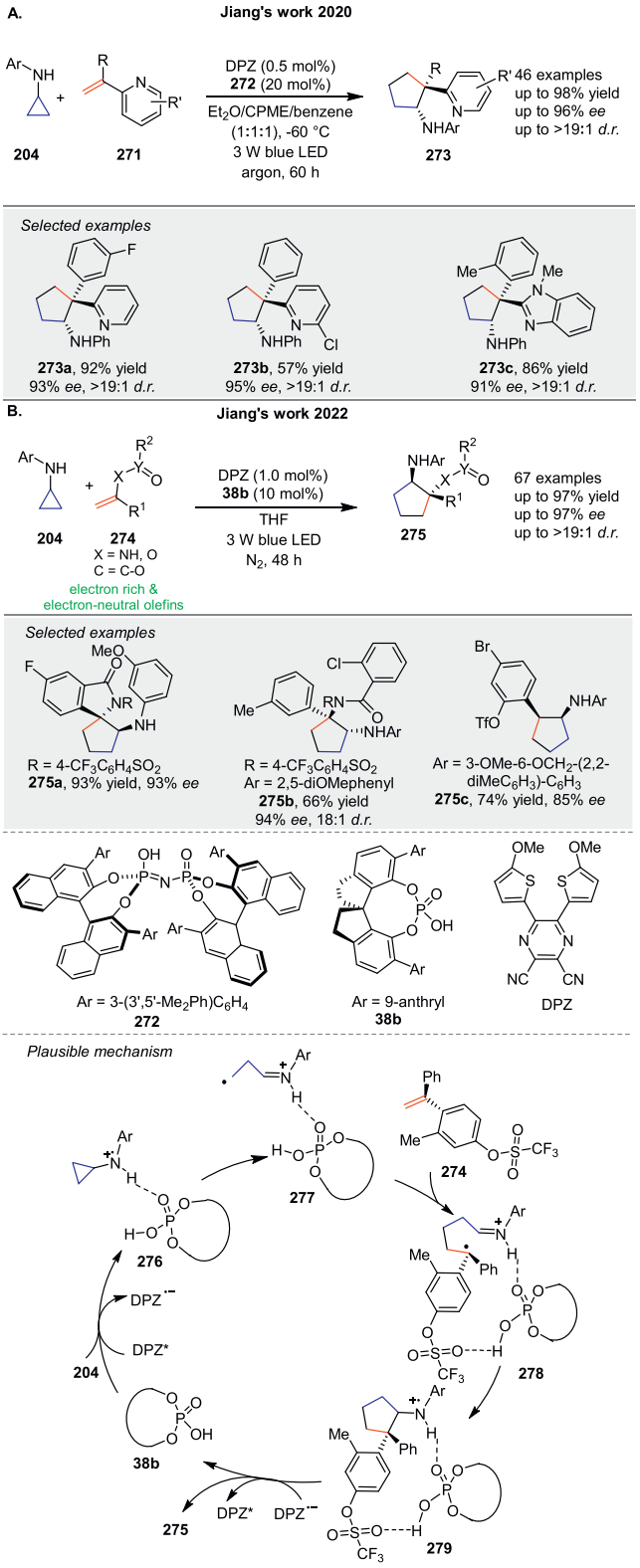


Scheme 32. Iridium-chiral borate ion pairs induced [3 + 2] cycloaddition of *N*-cyclopropylurea with α-alkylstyrenes.

proceeds and leads to radical intermediate **278**. Given the formation of stereogenic centers, the subsequent cyclization *via* radical addition to generate radical cation **279** is responsible for determining enantio- and diastereose-lectivities. Finally, the oxidizing amine radical cation **279** accepts an electron from DPZ$^{\bullet-}$ to give product **275**.

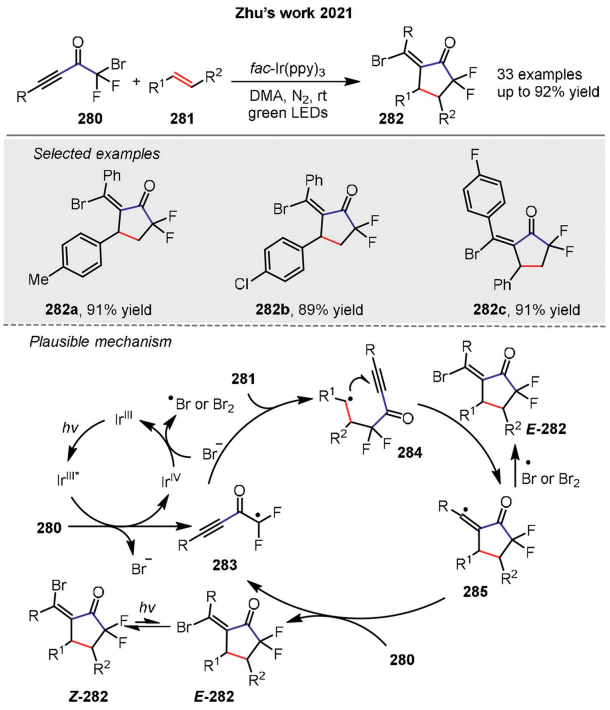
In 2021, Zhu group developed a radical-mediated [3 + 2] cycloaddition to synthesize α,α-difluorocyclopentanones **282** using bromodifluoromethyl alkynyl ketones **280** and alkenes **281** under photochemical conditions with DMA as solvent and fac-Ir(ppy)$_3$ as photosensitizer under green LED irradiation. The reaction showed broad functional group tolerance yielding products with good selectivity and allowing further transformations through cross-coupling reactions (Scheme 34) [106]. The mechanism involves SET from the excited photosensitizer to the ketone **280**, forming a difluoromethyl radical **283** that adds to the alkene **281** and undergoes intramolecular cyclization, intercepted by bromine to form the product **282**.

In 2021, Opatz group presented a metal-free, Hantzsch ester-mediated synthesis of cyclopentenylketones **288** from ketocyclopropanes **286** under eco-friendly conditions (Scheme 35). They explore the mechanism of these transformations, focusing on the role of the Hantzsch ester in facilitating the reactions. The mechanism

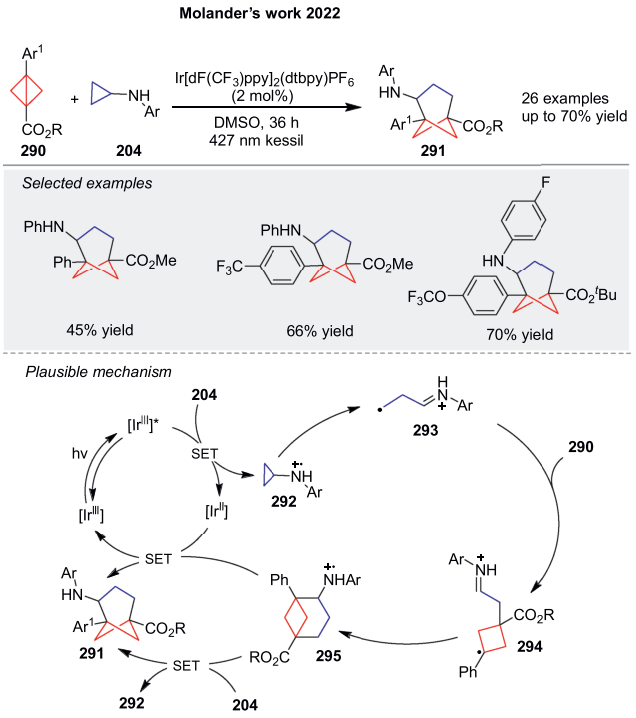


Scheme 33. Photoredox and bronsted acid or chiral H-bond catalyst co-catalyzed [3 + 2] photocycloadditions.

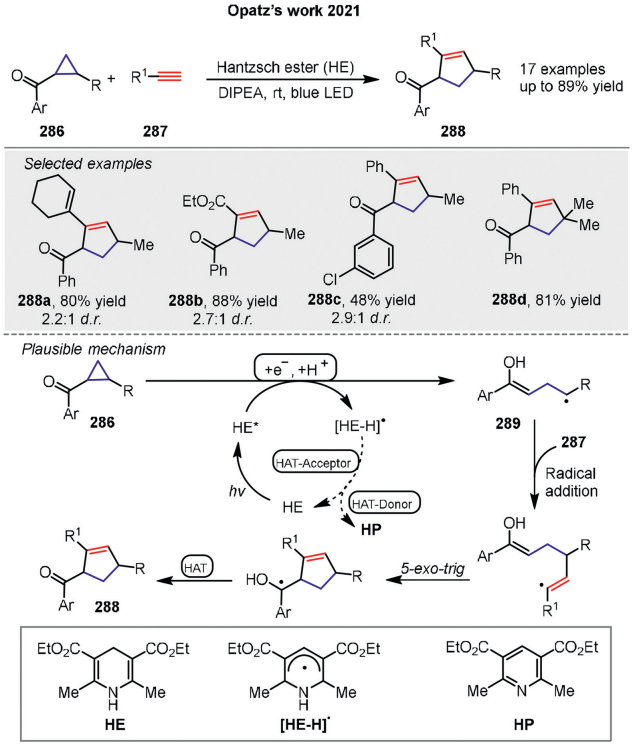
involves the initial photoexcitation of the Hantzsch ester, which generates a highly reducing species capable of inducing SET to the carbonyl group of the cyclopropane **286**. This SET step leads to the formation of a ketyl radical intermediate, which undergoes ring-opening to produce a radical species **289**. This radical then reacts with terminal alkynes **287** through a radical addition and cycliza-



Scheme 34. Visible-light-mediated radical [3 + 2] cycloaddition for synthesis of difluorocyclopentanones.



Scheme 36. Ir-catalyzed photochemical intermolecular [3 + 2] cycloaddition bicyclo[1.1.0]butanes.



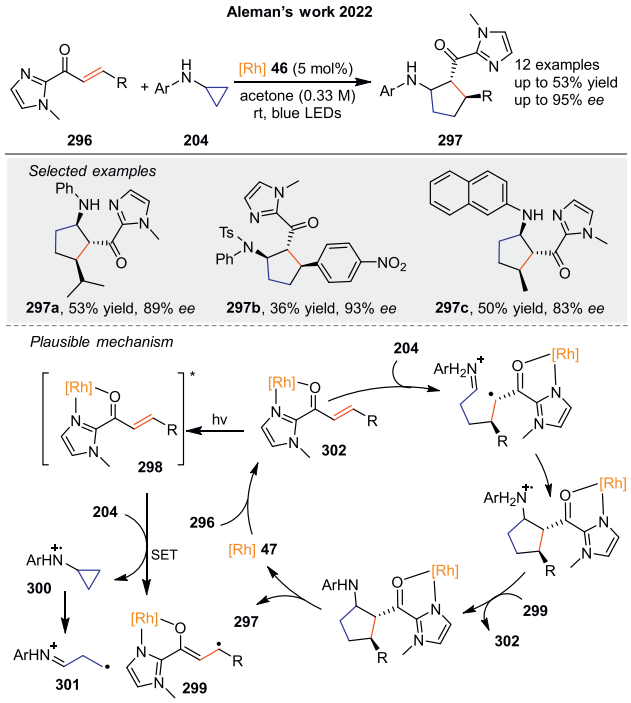
Scheme 35. Visible-light mediated metal-free [3 + 2] cycloaddition of ketocyclopropanes and terminal alkynes.

tion pathway, resulting in the formation of cyclopentenes **288**. This work provides a sustainable and efficient method for the synthesis of complex cyclopentene structures, leveraging the strain release from cyclopropane intermediates [107].

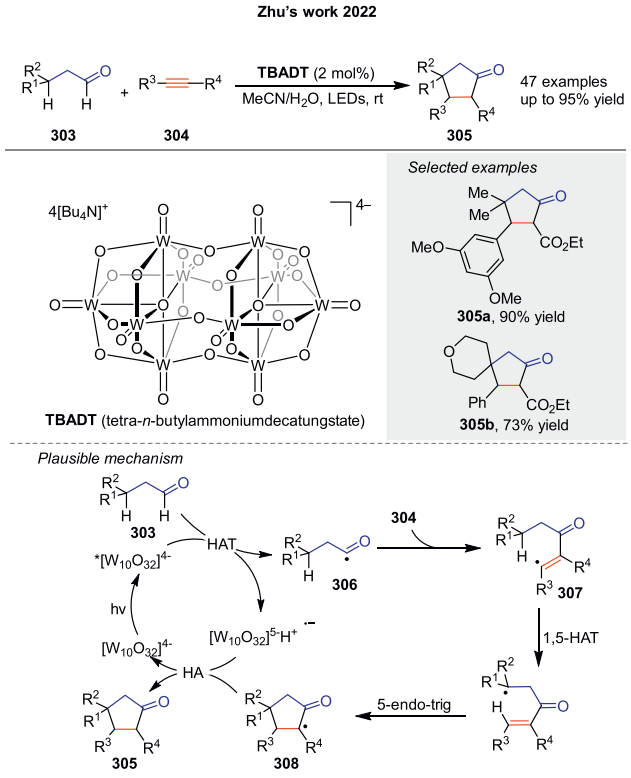
In 2022, Molander group disclosed the first photoinduced [3σ + 2σ] cycloaddition for the synthesis of trisubstituted bicyclo[3.1.1]heptanes **291** using bicyclo[1.1.0]butanes **290** and cyclopropylamines **204** (Scheme 36) [108]. SET to the cyclopropylamine **204** induces the formation of the radical cation species **292**, followed by ring opening *via* β-scission to the distonic radical cation **293**. Subsequent addition of **290** furnishes another relatively stabilized distonic radical cation **294**. The specie **294** then undergoes cyclization, providing access to the radical cation **295**, which can be reduced by the Ir^{II} species generated in the reductive quenching photoredox cycle or by the presence of the cyclopropylamine **204**.

In 2022, Aleman group introduced a visible-light-mediated strategy for the asymmetric synthesis of cyclic β-amino carbonyl derivatives **297** bearing three contiguous stereogenic centers through a formal [3 + 2] photocycloaddition (Scheme 37) [109]. The reaction involves the use of a chiral-at-rhodium catalyst to promote the enantioselective [3 + 2] photocycloaddition between α,β-unsaturated acyl imidazoles **296** and cyclopropylamine **204** derivatives. Mechanically, the authors proposed that it can evolve in two different pathways, in which the one involved in radical cycloaddition strategy is shown in Scheme 37. The mechanism begins with the coordination of the acyl imidazole **296** to the rhodium complex **46**, forming an intermediate that, upon blue LED irradiation, reaches an excited state **298** capable of oxidizing the cyclopropylamine **204**. This generates a radical cation of the amine **301**, which reacts with the rhodium complex **302** to form the final cyclopentane product **297**. The study achieves excellent enantioselectivity (up to 95% *ee*) and demonstrates the utility of the method through various synthetic transformations.

In the same year, a novel method for synthesizing cyclopentanones **305** through a photoinduced [3 + 2] cycloaddition reaction of alkyl aldehydes **303** and alkynes **304** enabled by photoinduced hydrogen atom transfer was presented by Zhu group (Scheme 38). First, the decatungstate anion (TBADT) is photoexcited to form an excited state, which abstracts a hydrogen atom from an aldehyde **303**, generating an acyl radical **306**. This radical then adds to an alkyne **304** to form a vinyl radical **37**, which undergoes 1,5-



Scheme 37. Asymmetric synthesis of cyclic β-amino carbonyl derivatives by a formal [3 + 2] photocycloaddition.



Scheme 38. Photoinduced decatungstate-catalyzed [3 + 2] cycloaddition of various internal alkynes with aliphatic aldehydes.

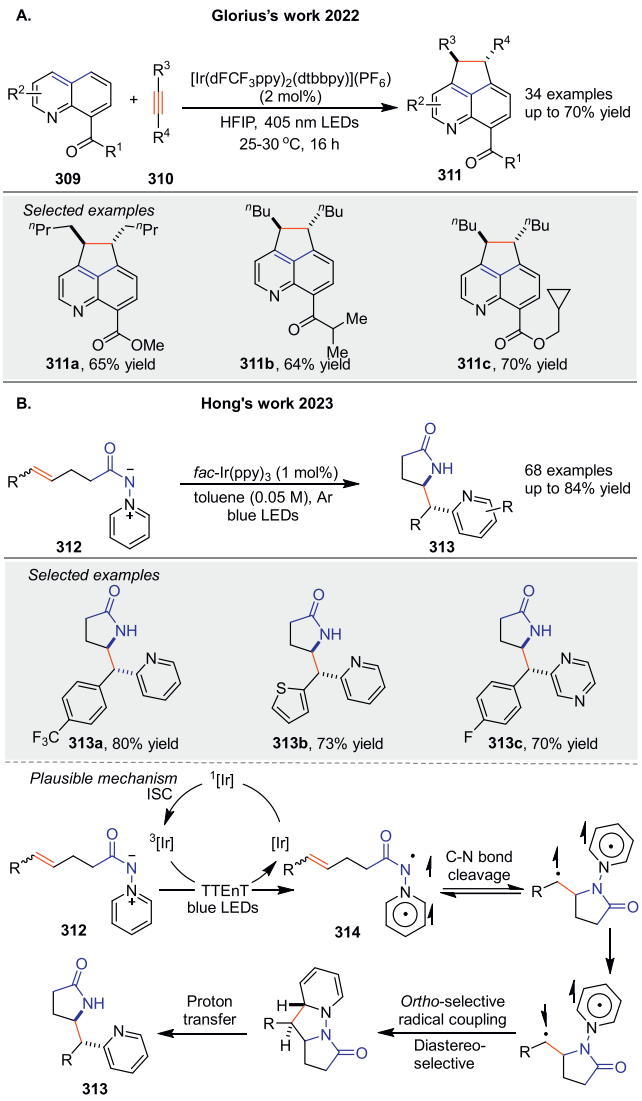
hydrogen atom transfer (HAT) and a rare 5-*endo-trig* cyclization to form a cyclopentanone **308** intermediate. Finally, a back-hydrogen abstraction by the reduced form of the tungstate anion restores the catalyst and completes the cycle. This process is highly selective and atom-economic, producing complex cyclopentanone **305** with excellent site-, regio-, and diastereoselectivity under mild conditions [110].

In 2022, Glorius group described a visible-light photocatalyzed peri-[3 + 2] cycloaddition of quinolines **309** with alkynes **310** to synthesize aza-acenaphthenes **311**. The reaction uses an iridium complex as both a photosensitizer and a photoredox catalyst, driving a cyclization/rearomatization cascade. Initially, energy transfer from the excited photocatalyst to the quinoline generates a triplet state, which reacts with the alkyne to form a cycloadduct. Subsequent redox shuttling, involving reductive quenching and oxidation steps, leads to aromatization of the product [111]. The process is highly regio- and diastereoselective, yielding products with excellent selectivity. Density functional theory calculations support the intertwined energy transfer/single electron transfer nature of the mechanism, highlighting the role of electron-withdrawing groups in facilitating the rearomatization step. Later, Hong group reported a novel approach to synthesize *ortho*-pyridyl γ- and δ-lactam scaffolds **313** through a photoinduced [3 + 2] cycloaddition reaction. The key innovation in this energy-transfer-induced [3 + 2] cycloaddition of N-N pyridinium ylides **312** lies in their unique triplet-state reactivity when activated by a photosensitizer under visible light. The reaction mechanism involves initial EnT from the excited photosensitizer to the N-N pyridinium ylide **312**, generating a triplet diradical intermediate **314**. This intermediate then undergoes radical addition to the alkene, followed by cyclization to form the desired lactam product **313** with high diastereoselectivity (Scheme 39) [112].

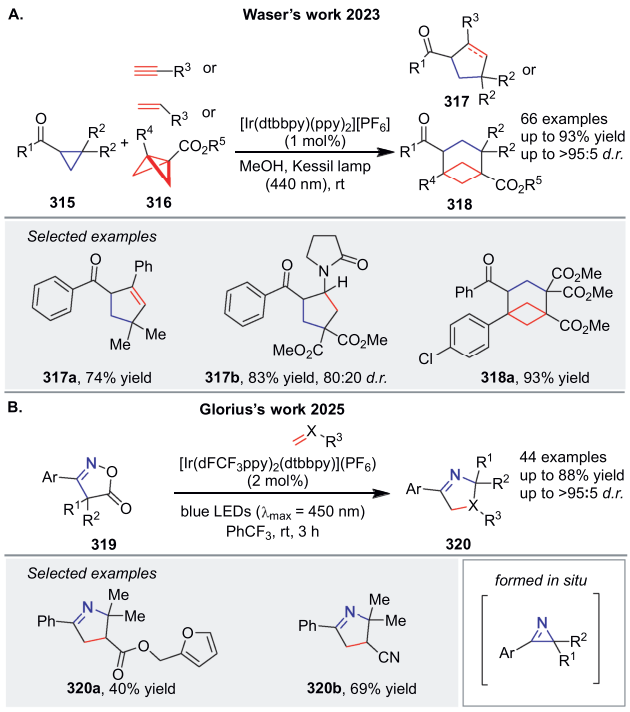
In 2023 Waser's group presented a photocatalytic method for the homolytic ring-opening of carbonyl cyclopropanes **315** to synthesize 5-membered carbocycles **317** and BCHs **318**. The study optimizes conditions using thioxanthone and iridium-based photocatalysts, achieving good yields with various substrates [113]. Mechanistic studies suggest a 1,3-biradical intermediate is key to the transformation (Scheme 40A). Recetly, Glorius group presented an energy transfer (EnT)-catalyzed method to generate strained 2*H*-azirines from isoxazole-5(4*H*)-ones **319**, which then undergo a formal [3 + 2] cycloaddition with various electrophiles [114]. The process involves triplet energy transfer to form a reactive azaallenyl diradical intermediate, leading to cycloaddition products with high selectivity. This mild method enables the rapid synthesis of valuable cyclic imines **320** and their derivatives (Scheme 40B).

2.3. [4 + 2] cycloaddition

A visible light photocatalysis method for radical cation Diels Alder cycloadditions using ruthenium^{II} polypyridyl complexes was developed by Yoon group in 2011. The reaction efficiently forms [4 + 2] cycloadducts between electron-rich dienophiles **321** and dienes **322** under mild conditions. The mechanism involves photoexcitation of the ruthenium complex, followed by oxidative quenching to generate the radical cation intermediate **324**, which then reacts with the diene **322**. This method is highly efficient, yielding high products with short reaction times. They also applied this method for synthesis of natural product heitziamide A (Scheme 41A) [115]. In 2017, they introduced a redox auxiliary strategy for radical cation cycloadditions using arylsulfide moieties **326**. This approach enables the photocatalytic generation of alkene radical cations that undergo cycloadditions with electron-rich partners. The sulfide auxiliary is later cleaved to obtain the desired products. The mechanism involves photooxidation of the vinyl sulfide to form the radical cation, which then reacts with the diene or alkene (Scheme 41B) [116]. This method overcomes the limitations of direct photoredox activation of simple alkenes. In the same year, they described a heterogeneous photocatalytic Diels Alder reaction of indoles **329** using Pt(0.2%)@TiO_2 under visible light. The reaction



Scheme 39. Energy-transfer-induced [3 + 2] cycloadditions of N-N pyridinium ylide synthesis of cyclopentanones.



Scheme 40. Ir-catalyzed intermolecular and intramolecular [3 + 2] photocycloaddition reactions.

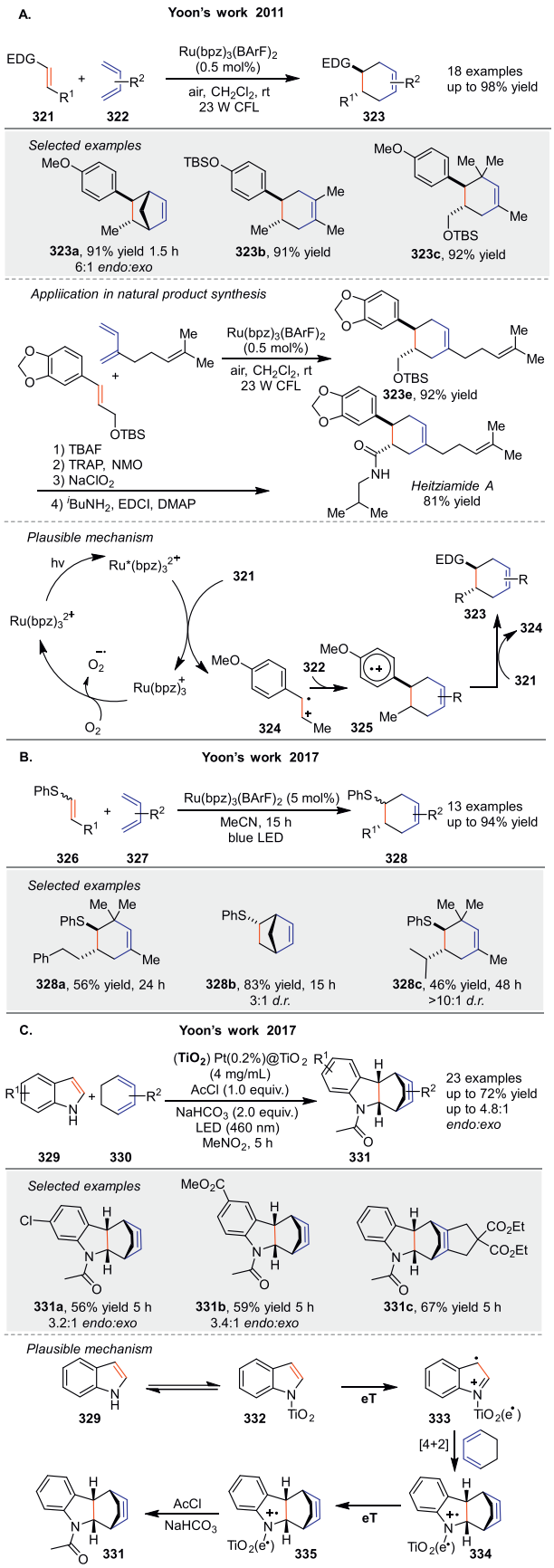
involves the formation of indole radical cations **333** that react with electron-rich dienes **330**. The mechanism includes indole adsorption on TiO_2, visible light excitation, and radical cation formation, followed by cycloaddition and reduction by the catalyst (Scheme 41C) [117]. The reaction is efficient, with broad scope and good catalyst recyclability, offering advantages over homogeneous methods.

In 2015, Zheng group reported the first example of an intermolecular [4 + 2] annulation of cyclobutylanilines **336** with alkynes **337** enabled by visible-light photocatalysis (Scheme 42) [118]. After extensive screening, [Ir(dtbbpy)(ppy)$_2$](PF$_6$) in MeOH under irradiation with two 18 W LEDs was identified as the optimal condition, providing the desired product in 97% yield as determined by gas chromatography. Monocyclic and bicyclic cyclobutylanilines successfully undergo the annulation with terminal and internal alkynes to generate a wide variety of amine-substituted cyclohexenes **338**. This approach can potentially be applied to open rings larger than three- and four-membered rings, provided they have suitable built-in ring strain. The plausible catalytic mechanism of this reaction is similar to Scheme 27.

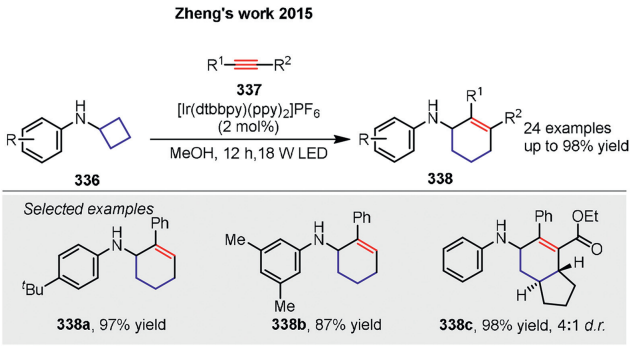
Photochemical intermolecular dearomative cycloaddition of azaarenes **339** with alkenes **340**, enabled by energy transfer (EnT) and Lewis acid mediation was reported by Brown group in 2021. This method allows for the selective formation of *para*-cycloadducts **341** with high diastereo- and regioselectivity. (Scheme 43A) [119]. In 2022, following the same mechanism, another photochemical intermolecular dearomative cycloaddition of quinolines **342** with alkenes **343**, enabled by energy transfer (EnT) and Lewis acid mediation was reported by their group (Scheme 43B) [120]. The reaction involves the formation of a triplet state intermediate **345** through EnT from a photosensitizer to the azaarene **342**, followed by a stepwise radical addition to the alkene **343**. The mechanism includes a reversible radical addition and a selectivity-determining radical recombination. The study also revealed that the stability of the biradical intermediate **346** and the solvent polarity significantly influence the regioselectivity and diastereoselectivity of the reaction. The reaction was shown to be applicable to a wide range of substrates, including sterically congested alkenes and allenes.

The conversion of bicyclo[1.1.1]pentan-1-amines **347** to a wide range of polysubstituted bicyclo[3.1.1]heptan-1-amines **349** was reported by Stephenson group in 2021 through a photochemical formal [4 + 2] cycloaddition of an intermediate imine diradical **351**. The mechanism involves the generation of an excited state imine diradical intermediate **350** upon irradiation with visible light. This excited state facilitates the homolytic cleavage of a bond in the adjacent cyclopropane ring, leading to the formation of a reactive diradical intermediate **351**. This diradical **351** can then add to an alkene **348**, followed by a cyclization step to form the desired bicyclo[3.1.1]heptan-1-amine product **349**. The process is photochemical in nature, requiring light activation to proceed, and results in the conversion of a bicyclo[1.1.1]pentane skeleton **347** to a more complex bicyclo[3.1.1]heptane skeleton **349**, providing a rich source of sp^3-rich primary amine building blocks for medicinal chemistry. This represents the first reported method to convert the bicyclo[1.1.1]pentane skeleton **347** to the bicyclo[3.1.1]heptane skeleton **349** (Scheme 44) [121].

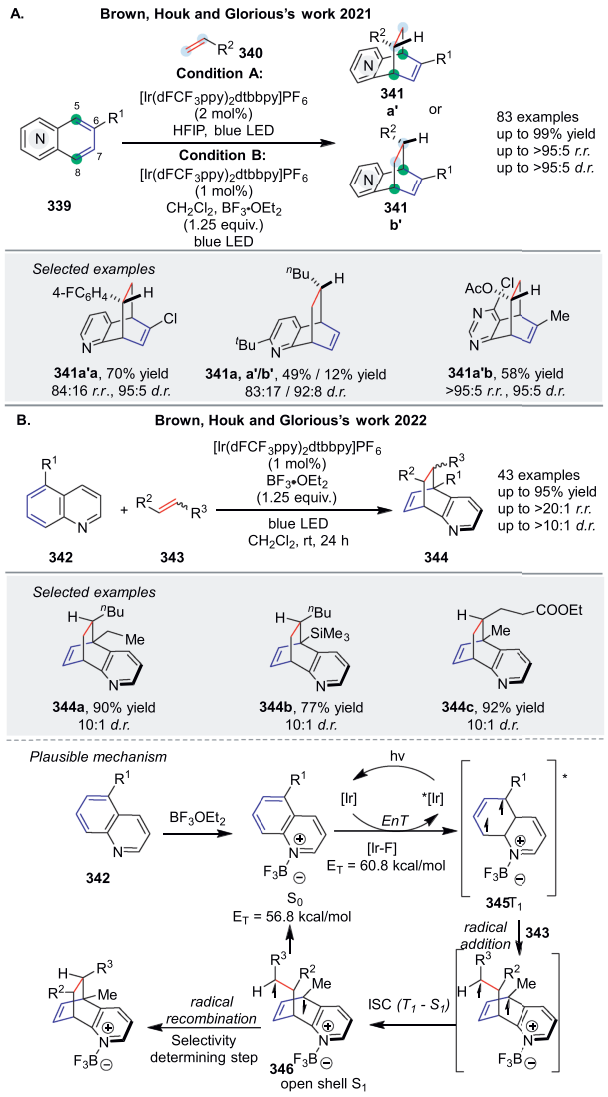
Recently, Wang group developed a visible-light-promoted [4 + 2] cycloaddition of arylcyclobutylamines **352** with olefins **353**



Scheme 41. Ru and Pt catalyzed [4+2] photocycloadditions of diene and dienophile.

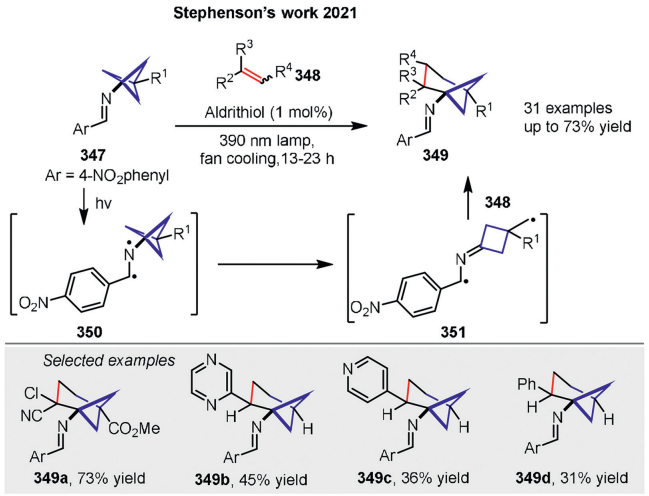


Scheme 42. Ir-catalyzed [4+2] cycloaddition of cyclobutylaniline with alkyne.

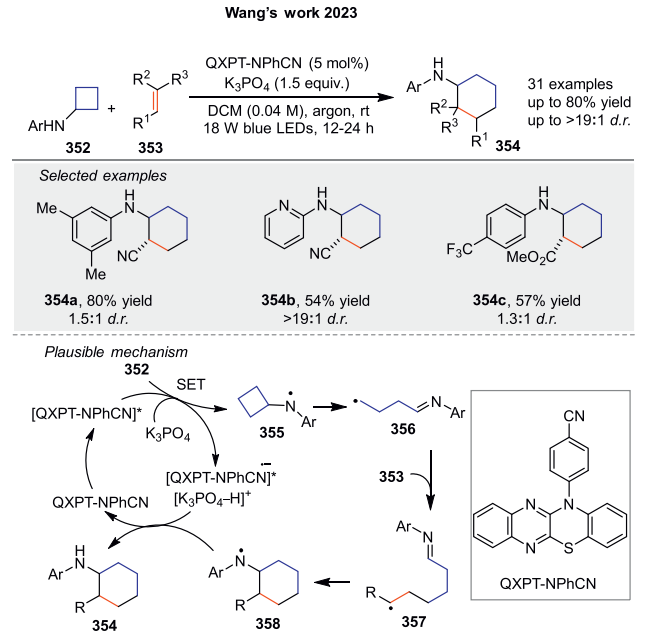


Scheme 43. Visible-light-mediated dearomative [4+2] cycloaddition of azaarenes with alkenes.

using QXPT-NPhCN as an organic photoredox catalyst (Scheme 45) [122]. First, the single-electron oxidation of **352** is accompanied by the deprotonation under the action of K_3PO_4 and photoexcited [QXPT-NPhCN]*, generating the nitrogen radical intermediate **355** and the radical anion [QXPT-NPhCN]$^{\bullet-}$. The ring tension leads to the ring-opening of cyclobutane to form the alkyl radical **356**. Intermolecular addition of the carbon radical in **356** to the olefins



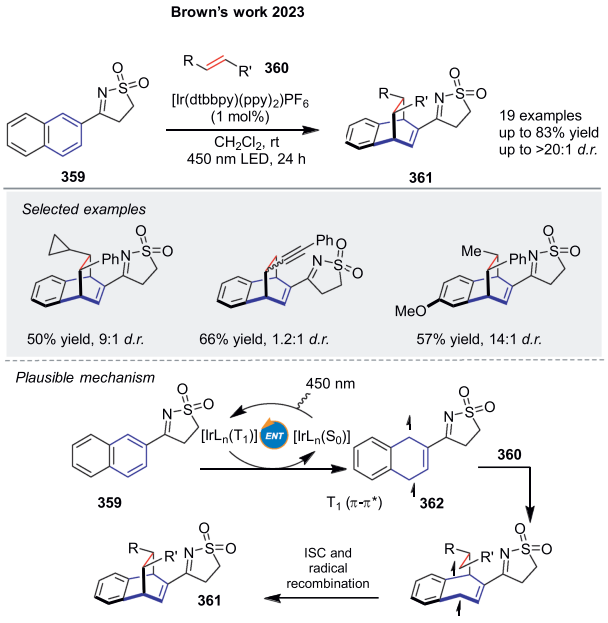
Scheme 44. N-Centered radical induced photocycloadditions of imine-substituted bicyclo[1.1.1]pentanes and alkenes.



Scheme 45. Visible-light organophotoredox-mediated intermolecular formal [4+2] cycloadditions of arylcyclobutylamines with olefins.

353 affords **357**. Intramolecular addition of the newly generated carbon radical to the iminium affords the nitrogen radical intermediate **358**. The free radical anion QXPT-NPhCN$^{\bullet-}$ performs single-electron reduction of **358**, which is accompanied by protonation to give **354** and the ground state QXPT-NPhCN is regenerated to complete the catalytic cycle.

Photosensitized [4+2] cycloaddition reactions of *N*-sulfonylimines **359** was presented by Brown's group in 2023, a method for the stereoselective construction of 3D bicyclic scaffolds **361**. This [4+2] cycloaddition involves the use of a rigid sulfonyl imine **359**, which provides high diastereoselectivity and yield when reacted with various alkenylarenes **360**. Mechanistic studies suggested that the reactions proceed *via* Dexter energy transfer, where the excited triplet state of the photosensitizer transfers energy to the substrate, leading to the formation of a diradical intermediate **362** that subsequently reacts with alkene **360** to form the cycloaddition products **361** (Scheme 46) [77].



Scheme 46. Ir-catalyzed [4+2] photocycloadditions of imine-substituted bicyclo[1.1.1]pentanes and alkenes.

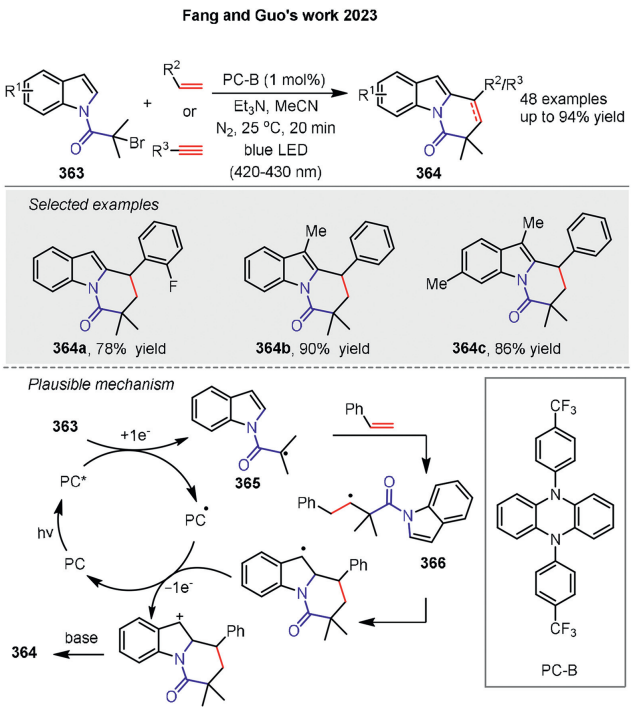
Fang and Guo group recently introduced a novel method for synthesizing pyrido[1,2-*a*]indol-6(7*H*)-ones **364** *via* a visible light-photocatalyzed formal [4+2] cycloaddition reaction involving indole-derived bromides **363** and alkenes or alkynes [123]. The reaction mechanism commences with the photoexcitation of the organic photocatalyst (PC-B) under visible light, generating an excited state with sufficient reducing power to induce the formation of a free radical **365** from the indole-derived bromide **363**. This radical subsequently reacts with the alkene or alkyne substrate to form a second radical intermediate **366**, which then undergoes radical cyclization by attacking the 2-position of the indole ring to yield the final product **364**. Control experiments confirmed that both the photocatalyst and visible light are essential for the reaction, and the addition of a radical scavenger significantly inhibits the reaction, thereby validating its radical nature (Scheme 47).

Shortly, Brown group presented a novel strategy for photosensitized dearomative [4+2] cycloaddition of naphthalenes **368** using a boron-enabled temporary tethering strategy (Scheme 48) [80]. The success of the reaction hinges on the use of dihaloboranes **367**, which provide increased Lewis acidity necessary for amine coordination. This dienophile [4+2] cycloaddition yields complex 3D borylated bicyclic motifs **369** with high selectivity through energy transfer to the naphthalene **368**, followed by stepwise radical cycloaddition.

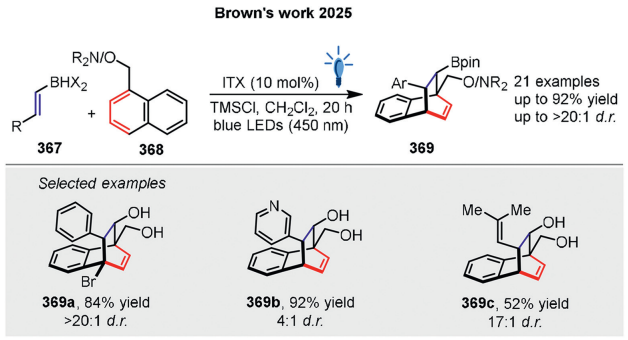
3. Transition metal catalyzed RCRs

3.1. [2+2] cycloaddition

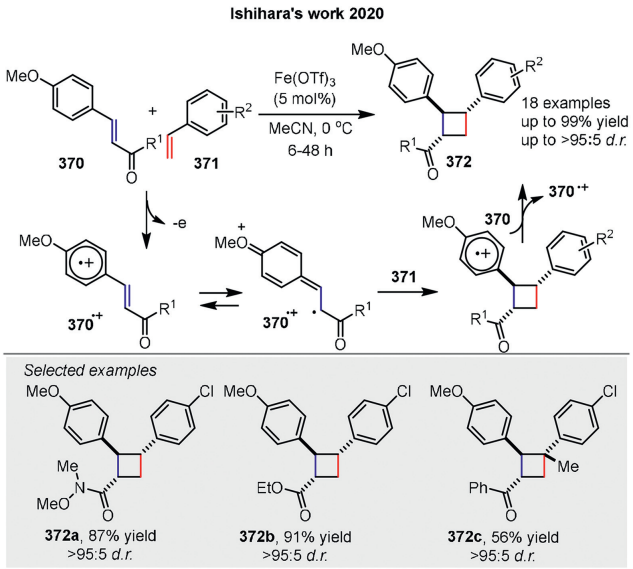
A radical-cation-induced crossed [2+2] cycloaddition of electron-deficient anetholes initiated by Iron^{III} salt, described by Ishihara and coworkers. The use of $Fe(OTf)_3$ to initiate the crossed [2+2] cycloaddition of electron-deficient anetholes **370** with styrenes **371**, producing 1,2-diarylcyclobutanes **372**. The mechanism involves the formation of a radical cation intermediate from the anethole (**370**$^{\bullet+}$), which reacts with styrene to form the cyclobutane product. This study highlights the utility of radical intermediates in constructing complex cyclic structures with broad substrate scopes and high yields (Scheme 49) [124].



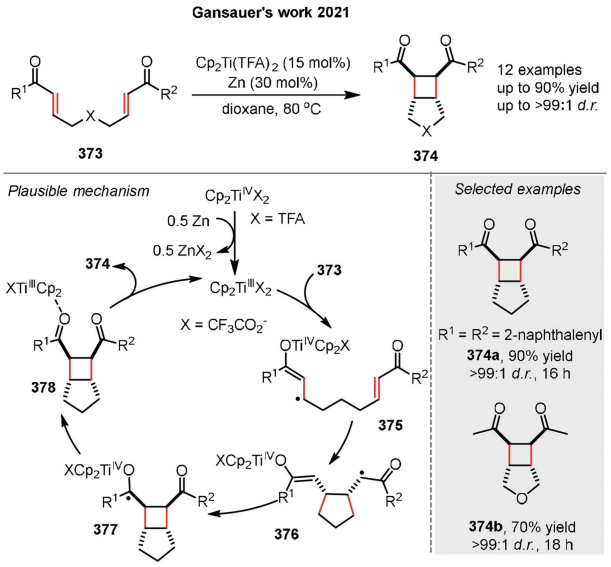
Scheme 47. Visible-light photocatalyzed formal [4+2] cycloaddition of indole-derived bromides and alkenes or alkynes.



Scheme 48. Dearomative [4+2] photocycloaddition of naphthalenes using a boron-enabled temporary tethering strategy.



Scheme 49. Fe-catalyzed [2+2] cycloaddition of electron-deficient anetholes.



Scheme 50. Ti-catalyzed [2+2] cycloaddition of bisenones.

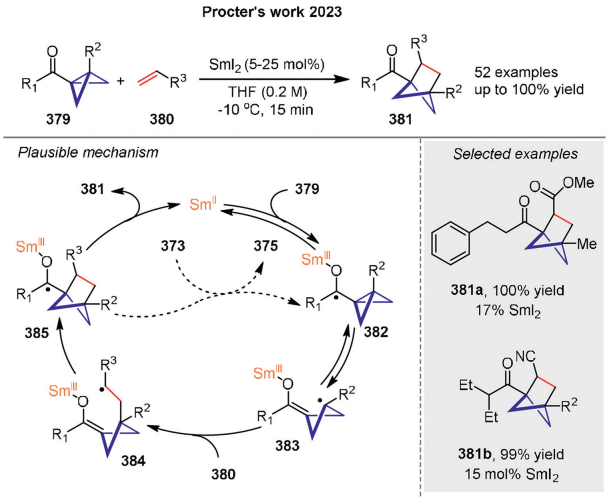
In 2021, Gansauer and co-workers reported a titanocene-catalyzed [2+2] cycloaddition reaction of bisenones **373** (Scheme 50) [125]. Both experimental evidence and theoretical results support the proposed radical pathway. The reaction begins with an inner-sphere electron transfer to the enone complexed to Ti^{III}, generating the stabilized radical **375**, which constitutes the oxidative addition step. This is followed by a 5-exo cyclization of the stabilized radical anion **375** to yield intermediate **376**. Radical **377** is then formed by a 4-exo cyclization of the enoyl radical in **376** to the titanocene enolate. Finally, product **374** is released, and the catalyst is regenerated by back electron transfer from the ketyl radical to Ti^{IV} and dissociation of **378**$^*Cp_2Ti^{III}TFA$.

Recently, Procter and coworkers disclosed a broadly applicable catalytic approach that delivers substituted bicyclo[2.1.1]hexanes **381** by intermolecular coupling between olefins **380** and bicyclo[1.1.0]butyl ketones **379**. The product bicyclo[2.1.1]hexane ketones have been shown to be versatile synthetic intermediates through selective downstream manipulation. The proposed mechanism involves reversible SET from SmI_2 to ketones **380**, generating ketyl radicals **382**, which fragment to give enolate radicals **383**. Intermolecular coupling with electron-deficient alkenes **380** generates radicals **384**, which rebound by addition to the Sm^{III}-enolate moiety, generating new ketyl radicals **385**. Back electron transfer to Sm^{III} regenerates the SmI_2 catalyst and liberates product **381** (Scheme 51) [126]. It is also possible that ketyl radical **385** directly reduces the starting ketone **379**, although computational calculations favor a radical relay process.

3.2. [3+2] cycloaddition

Since William A. Nugen's pioneering work in 1988 on Ti^{III}-induced cyclization of epoxyolefins [127], Ti^{III}-based reductive SET reagents have become widely used for mediating cyclizations. In 2012, Robert A. Flowers II's group introduced a novel approach to catalytic reactions employing oxidative additions and reductive eliminations in single-electron steps [128]. The success of radical aromatic substitution relies critically on a mechanism-based approach for tuning the stability and electronic properties of the catalyst.

In 2017, Lin and co-workers reported a Ti-catalyzed radical formal [3+2] cycloaddition of *N*-acylaziridines **386** with alkenes **387** The process begins with the coordination of the Ti catalyst to **376**,

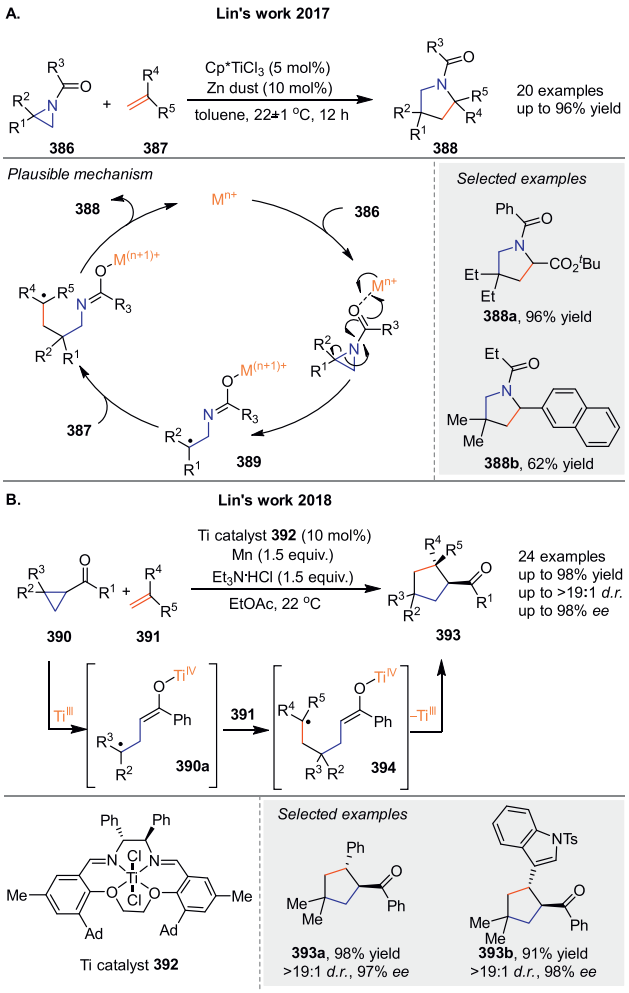


Scheme 51. SmI_2-catalyzed insertion of electron-deficient alkenes into bicyclo[1.1.0]butyl ketones.

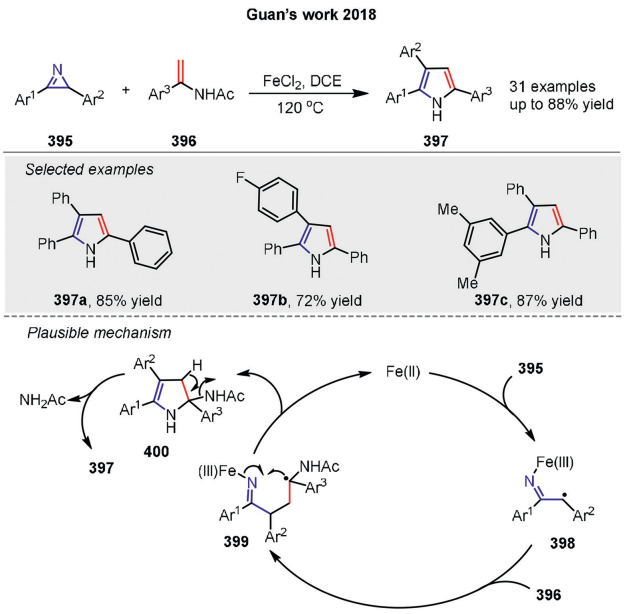
inducing homolytic cleavage of the C-N bond and subsequent SET from the metal center to the substrate. This generates the radical intermediate **389**, which adds to alkene **387** to form radical adduct. Cyclization of this adduct yields the final product **388**, completing the cycloaddition. Meanwhile, the metal complex is reduced and released from the pyrrolidine product, regenerating the active catalyst (Scheme 52A) [129]. Shortly thereafter, employing the same radical redox relay strategy, the same group reported a diastereo- and enantioselective formal [3 + 2] cycloaddition of cyclopropyl ketones **390** with alkenes **391** [130]. Utilizing **392** as the Ti catalyst, a wide range of alkenes were found to be excellent coupling partners, affording the corresponding products with high diastereoselectivity (*d.r.*) and enantioselectivity (*ee*). In 2020, the group conducted mechanistic studies of this asymmetric [3 + 2] cycloaddition [131]. The reaction commences with the generation of an active Ti^{III} catalyst through single-electron reduction by Mn. Subsequently, the cyclopropyl substrate **390** undergoes regioselective reductive ring opening by the Ti^{III} catalyst, yielding a tertiary carbon-centered radical **390a**. This radical adds to alkene **391** to form intermediate **394**, which then cyclizes to produce the final product **393** (Scheme 52B).

A Fe-catalyzed radical cycloaddition of 2*H*-azirines **395** and enamides **396** for the synthesis of substituted pyrroles **397** has been developed by Guan's group in 2018 (Scheme 53) [132]. The reaction uses readily available starting materials, tolerates various functional groups, and proceeds through a conceptually new homolytic C-N bond cleavage and radical coupling with enamides under mild conditions, allowing the rapid synthesis of valuable triaryl-substituted pyrroles in high yields. A tentative mechanism is proposed in Scheme 53. First, the reductive radical ring-opening of 2*H*-azirine **395** occurs in the presence of Fe^{II} to give a secondary radical intermediate **398**. Next, radical coupling of intermediate **398** with enamide **396** affords the tertiary radical intermediate **399**. Then, oxidative radical ring closure of intermediate **399** gives intermediate **400**. Simultaneously, the active Fe^{II} catalyst is released to facilitate the next catalytic cycle. Finally, elimination of a molecule of amide (NH_2Ac), followed by tautomerization, produces the pyrrole **397**.

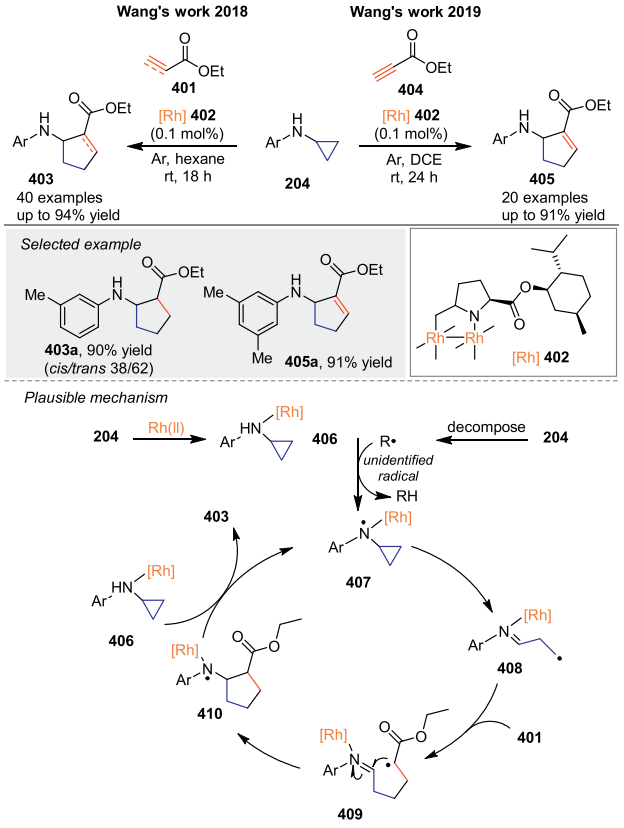
In 2018, Wang and co-workers detailed the development of [3 + 2] cycloaddition reactions catalyzed by dirhodium(II) complexes **402** between *N*-arylaminocyclopropanes **204** and alkene derivatives **401** [133]. Soon after, they reported a similar reaction between *N*-arylaminocyclopropanes **204** and alkyne derivatives **404**, which broadens the scope of this method to include



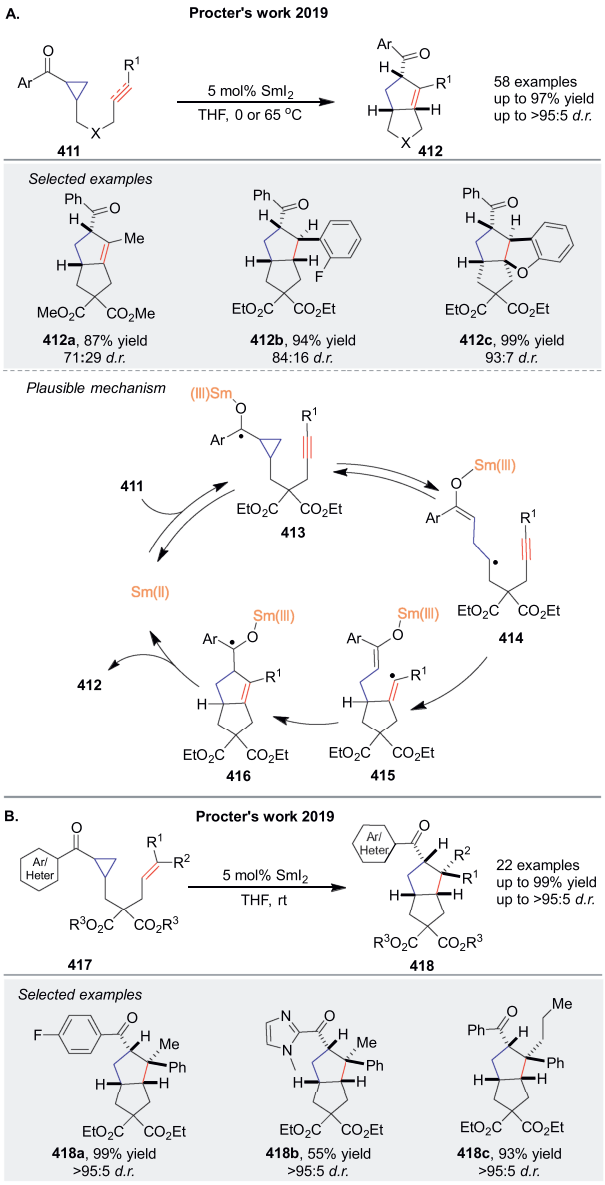
Scheme 52. Ti-catalyzed radical formal [3 + 2] cycloadditions of *N*-acylaziridines and cyclopropyl ketones with alkenes.



Scheme 53. Fe-catalyzed radical cycloaddition of 2*H*-azirines and enamides.



Scheme 54. Rh(II)-catalyzed [3 + 2] cycloaddition of the *N*-arylaminocyclopropane with alkene and alkyne derivatives.



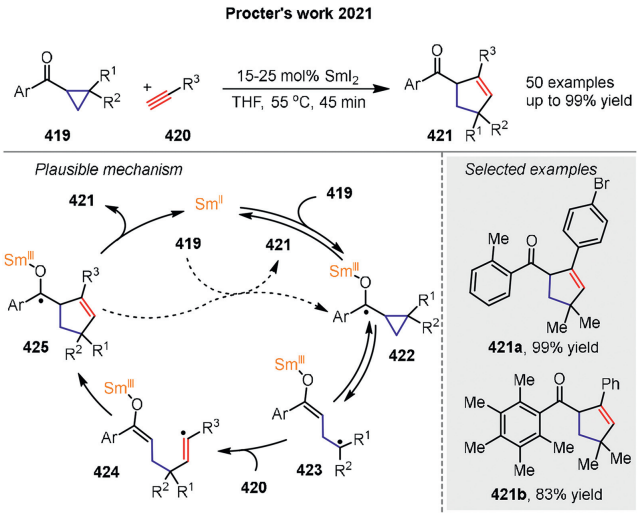
Scheme 55. SmI_2-catalyzed intramolecular [3 + 2] cycloaddition by radical relay.

alkynyl groups (Scheme 54) [134]. Preliminary mechanistic studies suggest that dirhodium(II) complexes **402** may facilitate the formation of *N*-centered radicals **407** by the loss of a hydrogen atom. This is followed by cyclopropane ring-opening to generate radical **408**, which is trapped by alkene **401** to form intermediate **409**. Subsequently, intramolecular free radical addition occurs to yield **410**. After HAT from complex **406**, the desired product **403** is obtained, and the N-centered radical **407** is regenerated.

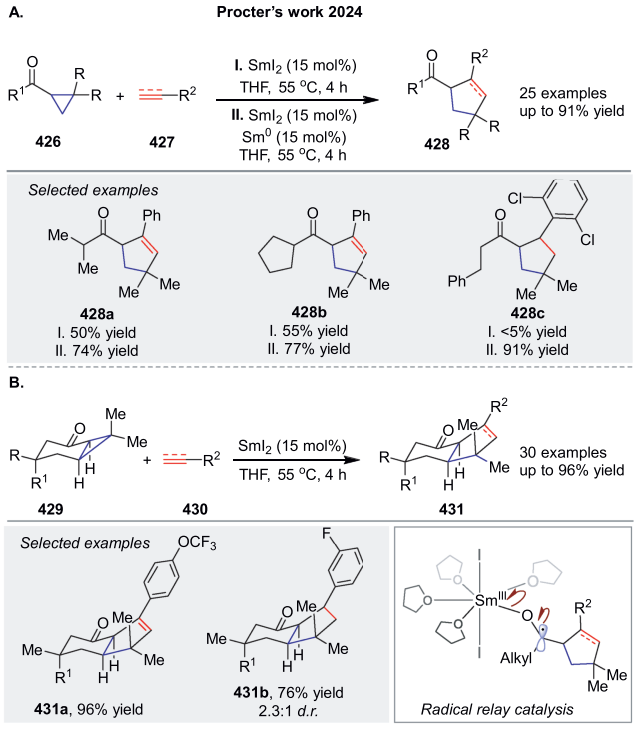
Since its first use 40 years ago, SmI_2 (Kagan's reagent) has remained one of the most versatile and selective SET reagents. Procter and co-workers have extensively explored the use of SmI_2 to catalyze various intramolecular and intermolecular cycloaddition reactions, making significant contributions to the field. In 2019, they reported an intramolecular radical cyclization cascade catalyzed by SmI_2 (Scheme 55A) [135]. Using as little as 5 mol% SmI_2, they achieved the synthesis of complex three-dimensional polycyclic products **412** containing up to four stereocenters, typically with high yields and good diastereocontrol. Mechanistic studies support a radical relay mechanism. The key step involves the formation of ketyl radical **413** *via* reversible SET from SmI_2 to substrate **411**. Ketyl radical **413** fragments to form distal radical **414**, which then cyclizes to generate radical **415**. This radical rebounds by adding to the Sm^{III}-enolate moiety, forming new ketyl radical **416**. Back electron transfer to Sm^{III} regenerates the SmI_2 catalyst and releases product **412**. In the same year, they also reported a similar SmI_2-catalyzed radical cascade cyclization of **417** that constructs quaternary stereocenters **418** (Scheme 55B) [136], with a reaction mechanism consistent with their previously proposed catalytic cycle.

In 2021, based on their previous work, they described a SmI_2-catalyzed intermolecular radical coupling of aryl cyclopropyl ketones **419** and alkynes **420** [137]. The process shows a broad substrate scope and delivers a library of decorated cyclopentenes **421** with SmI_2 loadings as low as 15 mol% (Scheme 56). The proposed mechanism involves reversible SET from SmI_2 to ketone **419**, generating ketyl radical **422**, which fragments to give enolate/radical **423**. Intermolecular coupling with alkynes **420** generates radical **424**, which rebounds by addition to the Sm^{III}-enolate moiety, generating new ketyl radical **425**. Back electron transfer to Sm^{III} regenerates the SmI_2 catalyst and liberates product **421**. It is also possible that ketyl radical **425** directly reduces the starting ketone **419**, feeding an electron-transfer-chain mechanism.

In 2024, Procter's group reported an approach to catalytic formal [3 + 2] cycloadditions using alkyl cyclopropyl ketones **426** as substrates, including more complex bicyclic alkyl cyclopropyl ketone **429**. This method efficiently delivers complex, sp^3-rich products **428** and **431** through cycloadditions with alkenes, alkynes, and enynes (Scheme 57) [138]. The key to engaging these relatively unreactive substrates lies in using SmI_2 as a catalyst, combined with sub stoichiometric amounts of Sm^0 to prevent catalyst deactivation. The mechanism involves a SET from SmI_2 to the carbonyl group, generating a ketyl radical intermediate that undergoes



Scheme 56. SmI_2-catalyzed intermolecular radical coupling of aryl cyclopropyl ketones and alkynes.

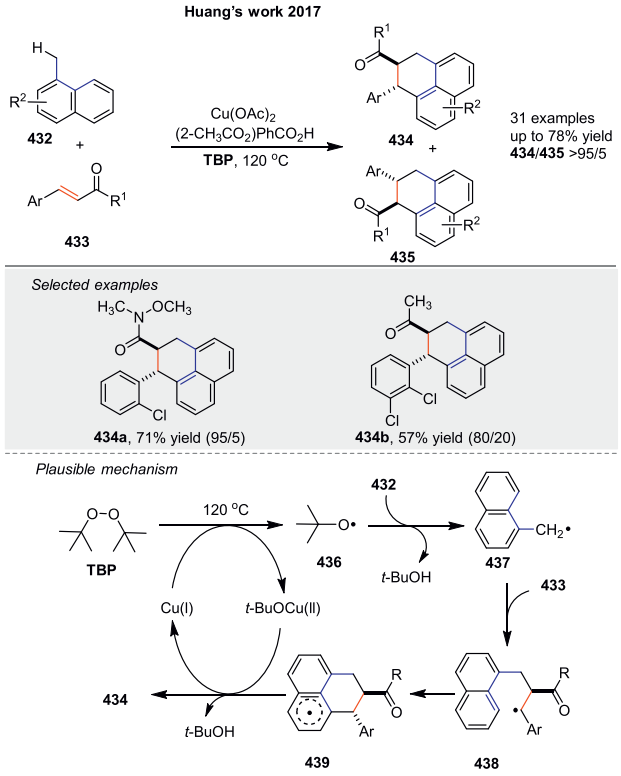


Scheme 57. SmI_2-catalyzed [3 + 2] cycloaddition of alkyl cyclopropyl ketones.

ring-opening and subsequent coupling with the alkene or alkyne partner. Computational studies reveal that reactivity is influenced by both electronic and steric factors, with bicyclic substrates showing lower activation barriers. This work expands the scope of substrates for catalytic [3 + 2] cycloadditions and offers practical approaches for SmI_2 catalysis.

3.3. [4 + 2] cycloaddition

In 2017, Huang group developed a novel Cu-catalyzed highly diastereoselective and regioselective formal [4 + 2] cycloadditions between simple methylnaphthalenes **432** and electron-deficient alkenes **433** (Scheme 58) [139]. A plausible reaction pathway is depicted in Scheme 58. Initially, homolytic fission of TBP by Cu^{I} affords the *tert*-butoxyl radical **436** and a Cu^{II} species, assisted by



Scheme 58. Copper-catalyzed dehydrogenative formal [4 + 2] cycloadditions of methylnaphthalenes and electron-deficient alkenes.

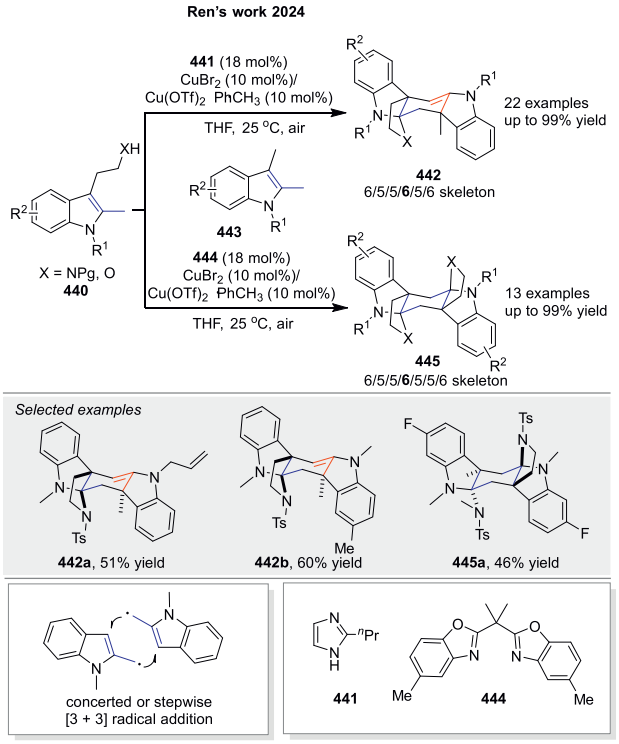
the carboxylic acid. Hydrogen abstraction from methylnaphthalene **432** by **436** generates *t*-BuOH and **437**, which then adds to the alkene **433**, giving the radical intermediate **438**. The radical in **438** site-selectively adds to the α-position of the naphthalene, affording intermediate **439**. Finally, direct hydrogen-atom transfer from **439** to **432** forms the product **434**, or single-electron oxidation of **439** by Cu^{II} generates a cation that is then deprotonated by *t*-BuO^{-} to deliver the desired product **434** and *t*-BuOH. Meanwhile, Cu^{I} is regenerated to enter the next catalytic cycle.

3.4. [3+3] cycloaddition

In 2024, Ren group presented a copper-catalyzed [3+3] radical cycloaddition reaction for the synthesis of six-membered cyclohexane-type rings using benzylic C(sp^3)-H bond functionalization. The reaction involves selective activation of the 2-benzylic C-H bond of an indole (**440**), which serves as a C3 synthon (Scheme 59) [140]. The mechanism begins with SET oxidation of the indole by a copper catalyst, forming a radical cation intermediate. This intermediate undergoes deprotonation of the benzylic C-H bond, generating a benzylic radical. This radical then participates in an intermolecular [3 + 3] cycloaddition, leading to the formation of a cycloadduct. Further SET oxidation and intramolecular nucleophilic attack complete the cyclization to yield the final product.

3.5. Miscellaneous

In 2020, Wei and co-workers rationally designed a new class of alkyne-tethered oximes **446** and applied them in an unprecedented iron-catalyzed radical relay protocol for the rapid assembly of a wide array of structurally novel and interesting fused pyridines **449**, **450** (Scheme 60) [141]. As shown in Scheme 60, oxime **446** can undergo a radical reduction by $Fe^{II}(acac)_2$, yielding an iminyl



Scheme 59. Copper-catalyzed [3 + 3] radical cycloaddition through benzylic C-H bond functionalization.

radical **451** and releasing $Fe^{III}(acac)_2OBz$. Subsequently, a HAT occurs, providing a tertiary alkyl radical **452**. Then, an intramolecular radical addition occurs, forming a vinyl radical **453**. At this point, there are two competitive pathways leading to the formation of either the target product **454** or the side product **456**. In the major pathway, a radical addition of the vinyl radical **453** to **447** takes place, yielding **454**. Then, a rapid ring-closing process generates radical **455**, which undergoes oxidation to finally yield the product **449**.

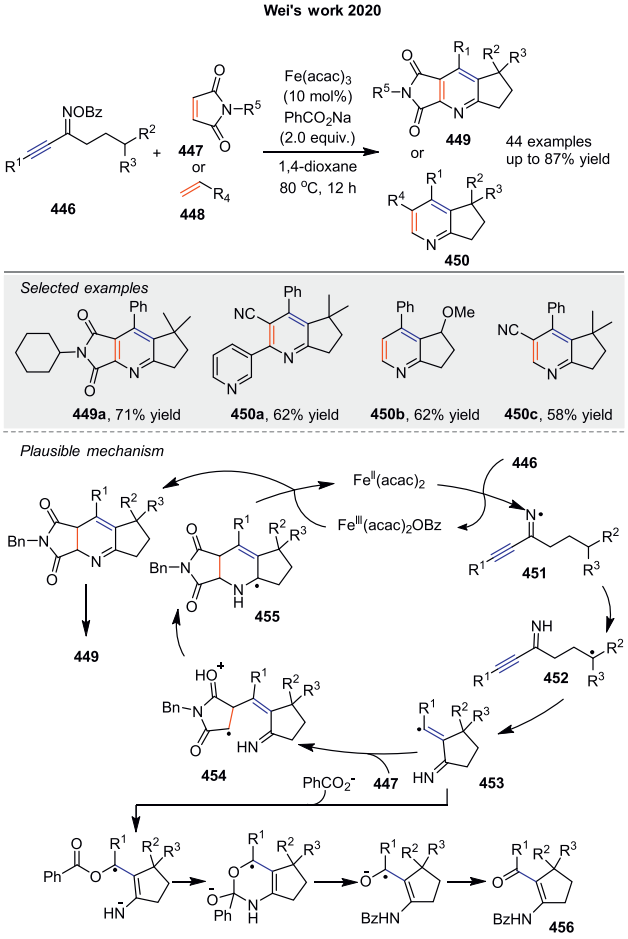
Soon after, the same group successfully prepared a series of structurally novel and interesting azepine **460** and spirotetrahydropyridine derivatives **461** in moderate to good yields by integrating iminyl radical-triggered HAT and [5 + 2] or [5 + 1] annulation processes (Scheme 61) [142]. SET from Fe^{II} to the oxime **457** results in N-O bond cleavage to generate Fe^{III} and an iminyl radical (**462**). **462** undergoes 1,5-HAT to form an alkyl carbon radical **465**. Through the addition of **463** to the alkene **458**, a new carbon radical **464** is produced. The carbon radical of **464** adds to the intramolecular imine group to form an intermediate **465**, which can be oxidized by Fe^{III} to form an iminium ion **466**, with concurrent regeneration of the Fe^{II} catalyst. After deprotonation, the azepine derivative **460** is generated.

4. Small molecule catalyzed RCRs

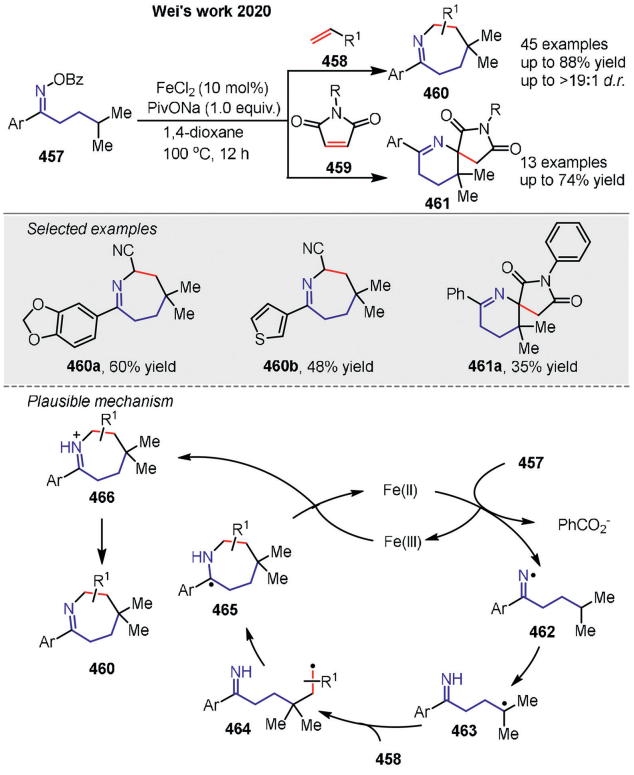
4.1. [3 + 2] cycloaddition

Organic thiyl radicals are uniquely capable of catalyzing radical reactions. In nature, thiyl-radical-mediated catalytic reactions are essential for the biosynthesis of various compounds, such as the conversion of ribonucleotides to deoxyribonucleotides. This catalytic ability has also been harnessed in organic chemistry, significantly advancing synthetic methodologies.

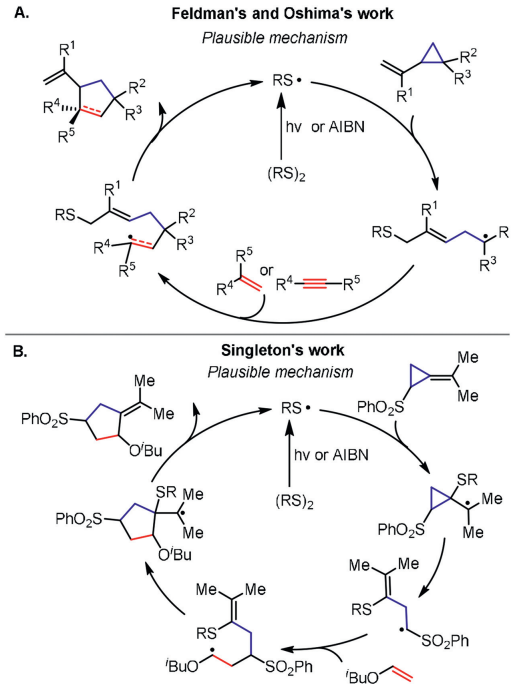
Since 1988, researchers including Feldman [143–145], Oshima (Scheme 62A) [146], and Singleton (Scheme 62B) [147–149] have



Scheme 60. Fe-catalyzed radical relay enabling the modular synthesis of fused pyridine.



Scheme 61. Fe-catalyzed, iminyl radical-triggered cycloaddition.



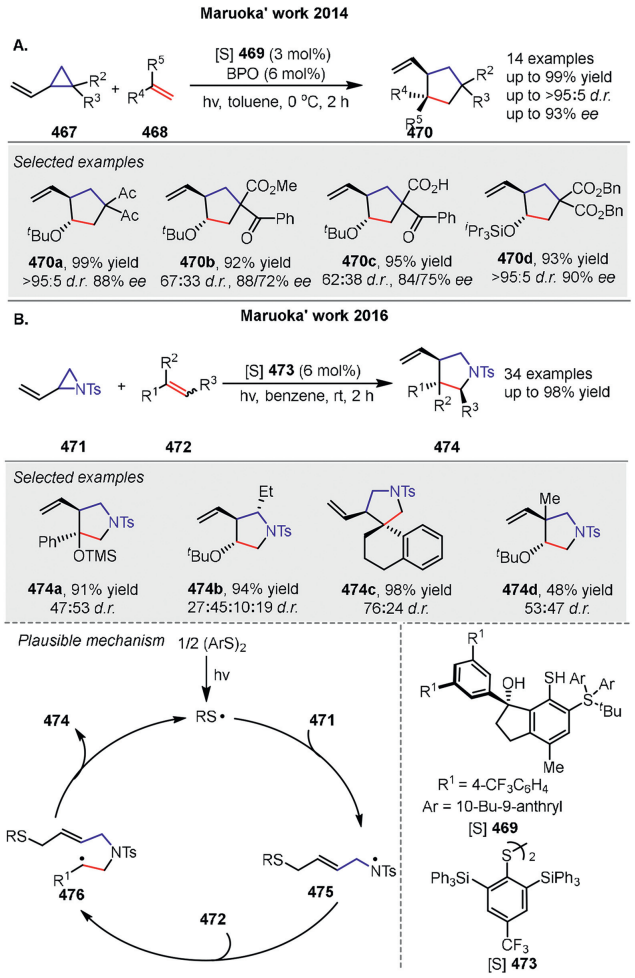
Scheme 62. Some early cycloaddition reactions catalyzed by organic thiyl radicals.

reported on the use of organic thiyl-radical catalysis to synthesize substituted cyclopentanes through cycloaddition strategies. Mechanistically, a thiyl radical is generated photolytically from a chiral disulfide. This radical then adds to vinylcyclopropane, forming radical species. Subsequent radical addition to an alkene yields an intermediate, which undergoes a ring-closure reaction to produce the final cyclopentane product and regenerate the thiyl radical, thus completing the catalytic cycle.

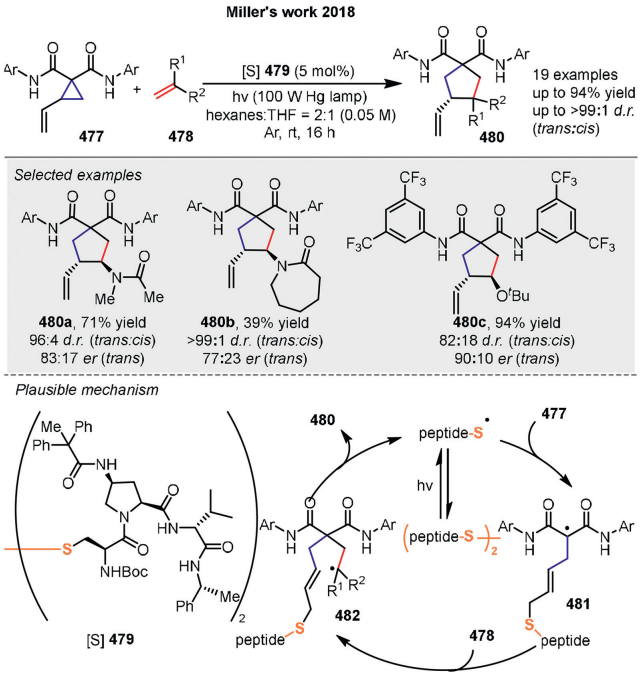
In 2014, Maruoka group reported the design of an organic thiyl radical catalyst featuring a carefully designed chiral pocket around a chiral thiol precatalyst **469**, which enables highly diastereo- and enantioselective radical cyclization of electron-deficient vinylcyclopropanes **467** achieving rigorous stereocontrol in radical C-C bond formation **470** (Scheme 63A) [150]. In 2016, the same group extended this thiyl-radical catalysis to the [3+2] cyclization of N-tosyl vinylaziridines **471** with various alkenes **472** (Scheme 63B) [151]. The reaction begins with a thiyl radical attacking vinylaziridine **471** to form aminyl radical **475**. Within the productive catalytic cycle, this radical species reacts with alkene **472** to produce carbon radical **476**, which then cyclizes to yield the final product **474** while regenerating the thiyl radical.

In 2018, Miller and co-workers reported an enantioselective vinylcyclopropane ring-opening/cycloaddition cascade catalyzed by thiyl radicals [152]. The proposed catalytic cycle is depicted in Scheme 64. Active thiyl radical catalysts are generated *in situ* through UV light-promoted homolysis of cystine-based dimers **479**. These radicals add to the vinylcyclopropane substrate **477**, forming the stabilized radical intermediate **481**. Subsequent addition of an olefin to **478** yields intermediate **482**, which cyclizes to produce the final product **480** while regenerating the active thiyl radical catalyst (Scheme 64). In 2021, reaction progress kinetic analysis revealed that the ring-opening of the vinylcyclopropane is both rate- and enantio-determining [153].

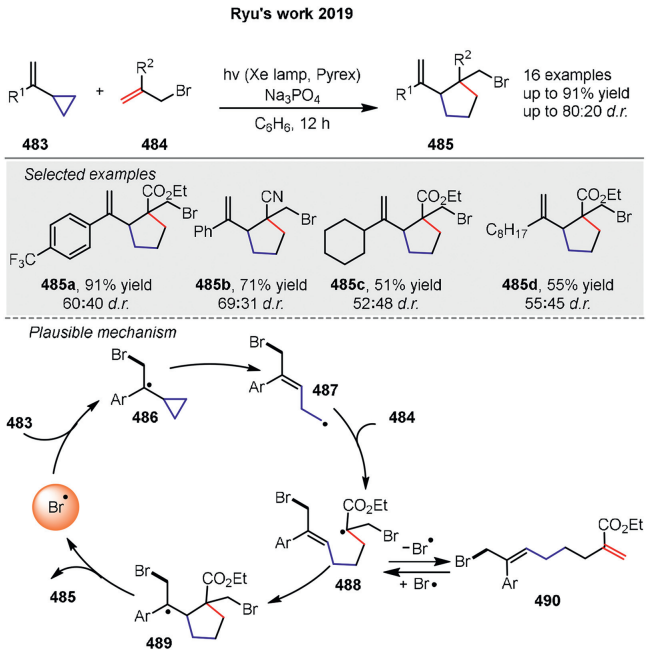
In 2019, Ryu and co-workers reported the first bromine-radical-mediated [3+2] cycloaddition reaction, yielding 2-bromomethyl-substituted alkenylcyclopentanes in good yields (Scheme 65) [154]. The process begins with the generation of a bromine radical through C-Br bond homolysis in allyl bromide **484** under photoir-



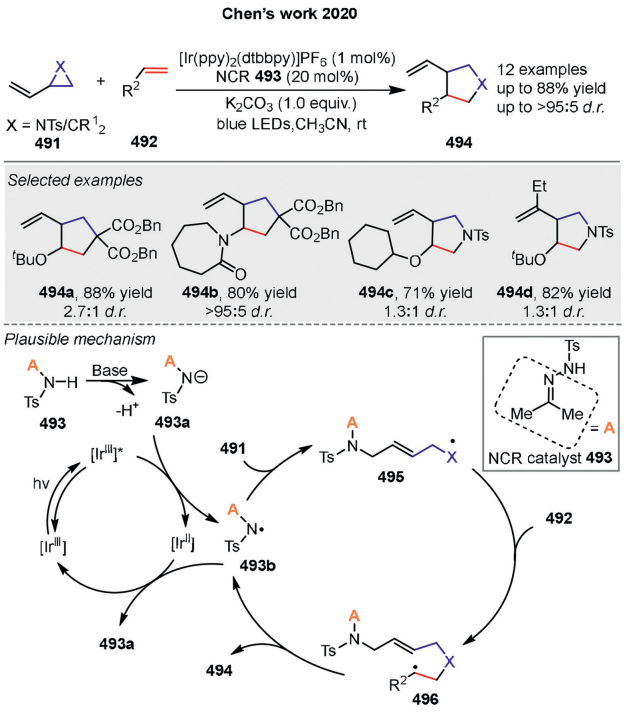
Scheme 63. Thiyl-radical-catalyzed [3+2] cyclization reactions of vinylcyclopropanes/*N*-tosyl vinylaziridines and alkenes.



Scheme 64. Vinylcyclopropane ring-opening/cycloaddition reaction through thiyl radical catalysis.



Scheme 65. Bromine-radical-mediated [3 + 2] cycloaddition reaction of vinylcyclopropanes and allyl bromides.

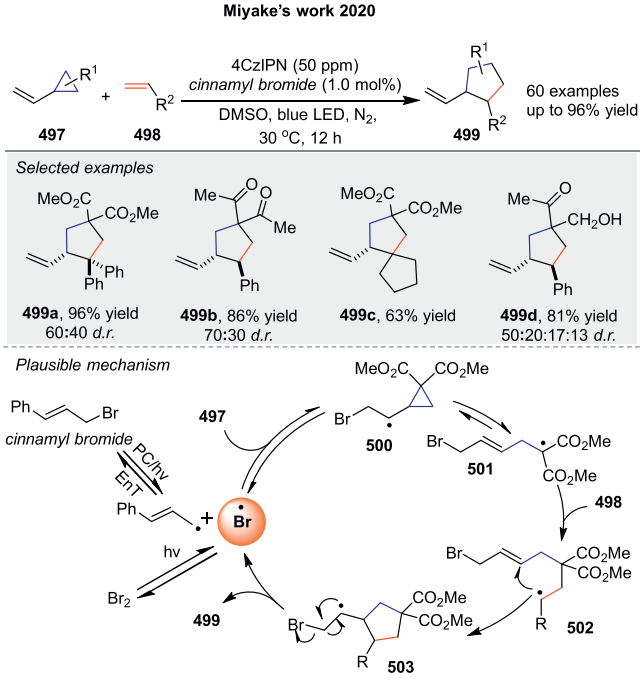


Scheme 66. Visible-light-driven nitrogen radical-catalyzed [3 + 2] cyclization of vinylcyclopropanes and *N*-tosyl vinylaziridines with alkenes.

radiation conditions. This bromine radical adds to substrate **483**, forming cyclopropylcarbinyl radical **486**, which readily undergoes ring-opening to give homoallyl radical **487**. The addition of **484** to allyl bromide **487** then produces 5-alkenyl radical **488**. This radical may undergo β-scission to give bromo-1,6-diene **490**. However, a bromine radical can add to **492** again, reforming linear radical **488**, which eventually leads to the cyclized product **485** *via* 5-exo cyclization followed by β-scission.

In 2020, Chen group introduced a visible light photoredox-promoted and nitrogen-centered radical (NCR) covalent catalysis for the radical [3 + 2] cyclization of vinylcyclopropanes and *N*-tosyl vinylaziridines **491** with alkenes **492** (Scheme 66) [155]. This innovative catalytic strategy employs $[Ir(ppy)_2(dtbbpy)]PF_6$ as a photoinitiator to generate the NCR catalyst **493**, potentially expanding the scope of nitrogen radical catalysis. The proposed mechanism begins with the *in-situ* generation of hydrazone anion **493a** from **493** in the presence of K_2CO_3. This anion undergoes SET oxidation by the photoexcited Ir^{III*} catalyst, yielding hydrazonyl radical **493b** and the reduced form of the photocatalyst Ir^{II}. Subsequently, **493b** performs a ring-opening radical addition to vinylcyclopropane **491**, forming intermediate **495**. This intermediate reacts with alkene **492** to produce another radical species **496**. Finally, **496** cyclizes to form product **494**, regenerating hydrazonyl radical **493b** and completing the nitrogen radical catalysis cycle.

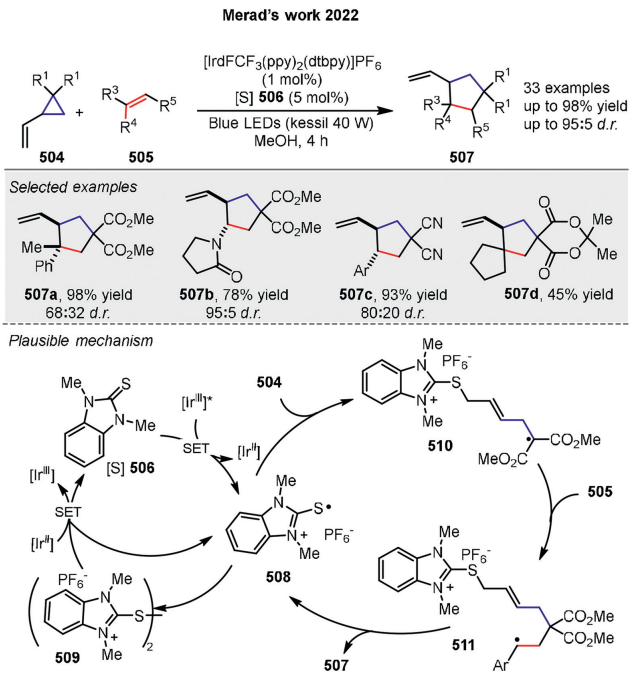
In 2020, Miyake group introduced a mild, safe, and user-friendly bromine radical catalysis system that enables efficient [3 + 2] cycloaddition reactions of diversely substituted vinyl- and ethynylcyclopropanes **497** with a broad range of alkenes **498** (Scheme 67) [156]. The key to this success is the visible light-induced generation of bromine radicals from cinnamyl bromide. In the proposed catalytic cycle, upon visible light irradiation, the photocatalyst 4CzIPN sensitizes the triplet-state fragmentation of cinnamyl bromide to release a bromine radical. This bromine radical adds to the vinyl group of **497**, forming radical species **500**, which then undergoes a fast but reversible ring-opening process to yield intermediate **501**. Subsequent radical addition of **501** to alkenes **498** produces radical **502**, which then undergoes a ring-closure reaction to form intermediate **503**. In this step, the spin center shifts to the



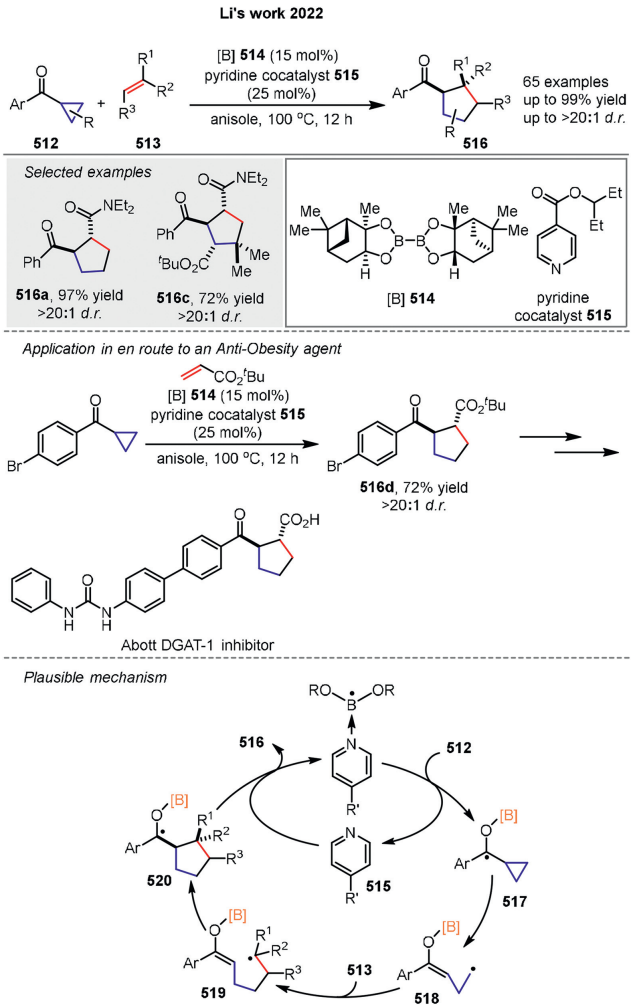
Scheme 67. Visible light-gated bromine radical-catalyzed [3 + 2] cycloaddition of vinylcyclopropanes and alkenes.

position for β-elimination, yielding the final product **499** and regenerating the bromine radical to continue the catalytic cycle.

More recently, Merad group reported the pioneering use of cationic sulfur-centered radicals **508** in covalent radical catalysis, demonstrating their synthetic potential and versatility in a [3 + 2] radical cascade between vinylcyclopropanes **504** and olefins **505** (Scheme 68) [157]. The proposed mechanism begins with the single-electron oxidation of **506** to generate the thiyl radical **508**,



Scheme 68. Cationic sulfur-centered radicals catalyzed [3 + 2] radical cascade between vinylcyclopropanes and olefins.

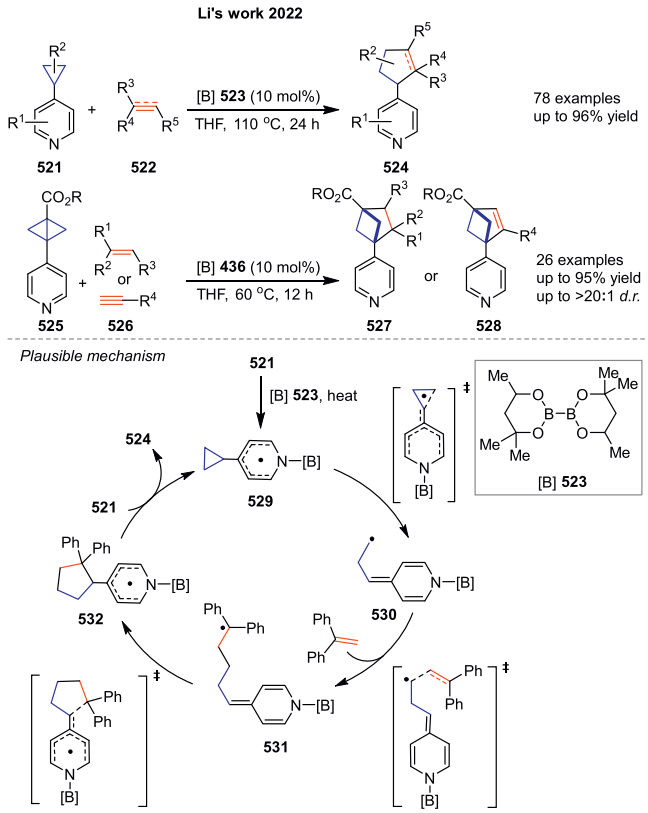


Scheme 69. Pyridine-assisted boronyl radical catalyzed [3 + 2] cycloaddition reactions of cyclopropanes and alkenes.

which is rapidly captured by vinylcyclopropane **504** to form intermediate **510**. This intermediate then undergoes intermolecular radical addition to an alkene **505**, yielding intermediate **511**. The final 5-*exo*-*trig* cyclization releases product **507** in a favored trans configuration and regenerates the thiyl radical **508**. In the last step, the dicationic dimer **509** is reduced by Ir^{II}, facilitating the regeneration of **506** and completing the catalytic cycle.

Pyridine-assisted boronyl radical-catalyzed radical cycloaddition reactions represent an innovative approach in organic synthesis, leveraging the unique reactivity of boronyl radicals to facilitate the formation of complex cyclic structures. Boronyl radicals, generated from boronate esters, have garnered significant attention due to their ability to participate in a wide range of radical processes. The use of pyridine as a co-catalyst or ligand in these reactions has been shown to enhance the stability and reactivity of boronyl radicals, thereby improving the efficiency and selectivity of the cycloaddition process [158,159].

The pioneering work in this area was reported by the Li group in 2022, who disclosed an elegant mechanism for pyridine-assisted boronyl radical-catalyzed radical cycloaddition reactions and presented the first example of an atom-economical [3 + 2] cycloaddition reaction between cyclopropanes **512** and alkenes **513** [160]. This innovative approach utilizes commercial diboron **514** as the catalyst and pyridine **515** as the co-catalyst. This work not only demonstrates the first application of a pyridine-assisted boronyl radical catalyst but also highlights the potential for developing new, green, and efficient boron-catalyzed organic reactions. The utility of this boronyl radical-catalyzed cycloaddition reaction was demonstrated by a concise synthetic route of the key intermediate (**516d**) for a glycerolacyltransferase (DGAT-1) inhibitor which had been developed as a potent and selective anti-obesity agent by Abbott (Scheme 69). The proposed mechanism for this reaction



Scheme 70. Pyridine-assisted boronyl radical catalyzed [3 + 2] cycloaddition reactions of 4-pyridinyl cyclopropanes and alkenes or alkynes.

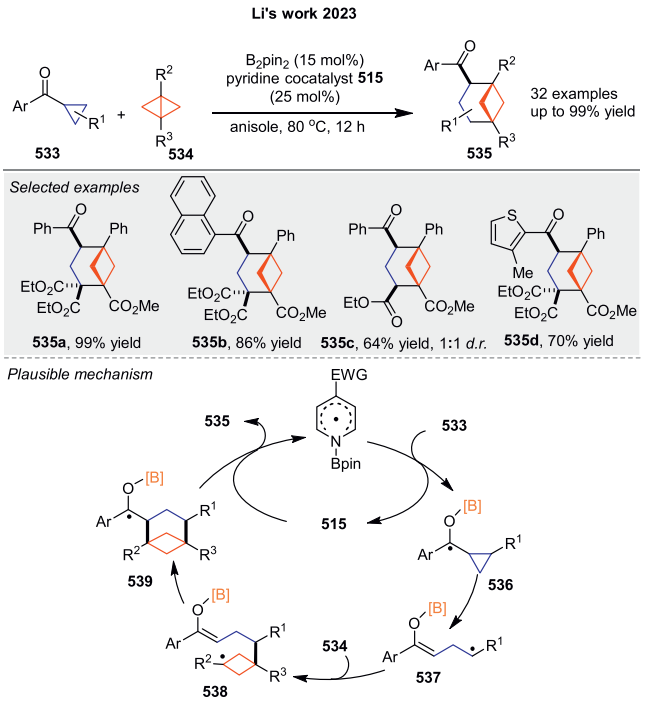
is outlined in Scheme 69. Initially, the interaction of tetraalkoxydiboron **514** with **515** forms the pyridine-assisted boronyl radical under heating conditions. This radical adds to the cyclopropyl ketone **512** to form carbon radical intermediate **517**. Subsequent β-scission delivers radical intermediate **518**. The addition of radical **518** to alkene **513** then generates radical **519**. The final steps involve intramolecular radical cyclization and a pyridine-mediated stepwise boronyl transfer process, ultimately forging the final product **516**

In the same year, expanding on their previous work, Li group developed another [3+2] cycloaddition involving 4-pyridinyl cyclopropanes **521** or pyridinyl bicyclo[1.1.0]butanes **525** with alkenes or alkynes, enabling the modular synthesis of pyridine-substituted cyclopentanes or cyclopentenes **524**, and bicyclo[2.1.1]hexanes **527** or **528**, which are challenging to access using conventional methods (Scheme 70) [161]. This study introduced a novel through-(hetero)arene radical transmission concept for the selective activation of a remote bond. The proposed mechanism is depicted in Scheme 70. Under heating conditions, the pyridine-stabilized boronyl radical is homolytically formed from 2 equiv. of **521** and the boron catalyst **523**, serving as the active catalyst in the cycloaddition. The boron-originated single electron is effectively transmitted to the 4-position *via* the pyridine ring due to the conjugative effect. This leads to ring-opening of the cyclopropane and dearomatization, forming an alkylidene dihydropyridine radical intermediate **530** *via* a transition state. The subsequent radical addition of **530** to styrene yields the tertiary radical **531**. This is followed by a 5-*exo-trig* rearomative ring-closing step, resulting in another pyridine-stabilized boronyl radical **532**. Through ligand exchange, the desired product **524** is released, and the boronyl radical is transferred to the next substrate to regenerate **529**, thus completing the catalytic cycle.

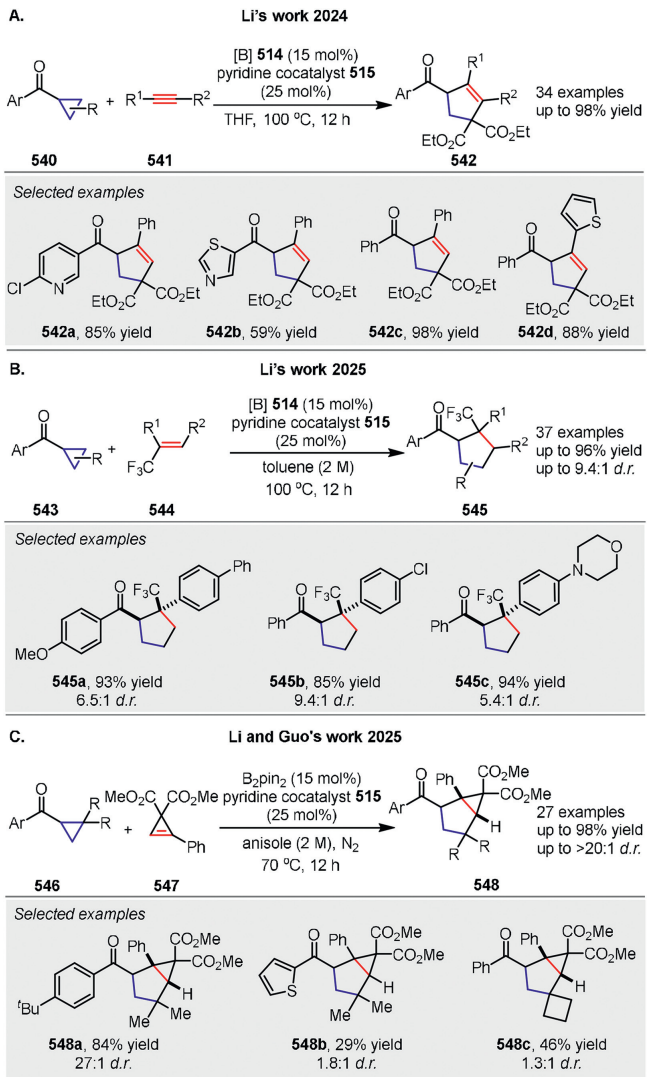
Subsequently, Li group extended the same catalytic strategy to the [2σ+2σ] or [3+2] radical cycloaddition between bicyclo[1.1.0]butanes **533** and cyclopropyl ketones **534**. This reaction offers a chemoselective and regioselective σ-bond metathesis transformation, which has been highly challenging *via* other pathways, and provides a synthetic route to the medicinally attractive but synthetically challenging highly functionalized BCH compounds **535** (Scheme 71) [162]. The formation of the reactive radical intermediate **536** follows the mechanism described in Scheme 71. Subsequently, radical **537** attacks the bridgehead carbon in **534**, yielding a flat cyclobutyl radical **538**. The following 6-*exo-trig* ring-closing step is highly exergonic, leading to a new benzylic ketyl radical **539**. Finally, a facile pyridine-mediated stepwise boronyl transfer process releases the [2σ+2σ] cycloaddition product **535** and regenerates the pyridine-assisted boronyl radical, thus completing the catalytic cycle.

Very recently, Li group and Guo group have reported three sophisticated examples of pyridine-assisted boronyl radical-catalyzed [3+2] cycloaddition reactions. These intermolecular [3+2] cycloaddition reactions involve cyclopropanes **540** with alkynes **541** [163], cyclopropanes **543** with trifluoromethyl-substituted alkenes **544** [164], and cyclopropanes **546** with cyclopropenes **547** [165], achieving high yields and broad substrate scopes (Scheme 72). The mechanisms of these [3+2] cycloaddition reactions are similar to the one described in Scheme 69.

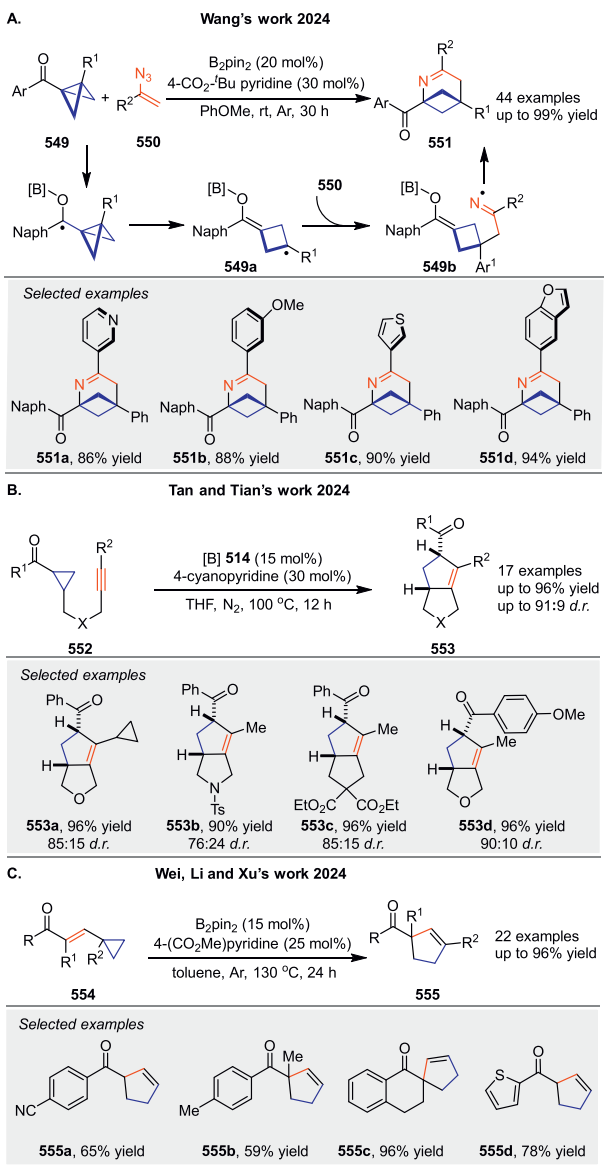
Followed the same mechanism, Wang group reported a pyridine-boryl radical-catalyzed [3π+2σ] cycloaddition reaction between vinyl azides **550** and bicyclo[1.1.0]butanes (BCBs) **549**,



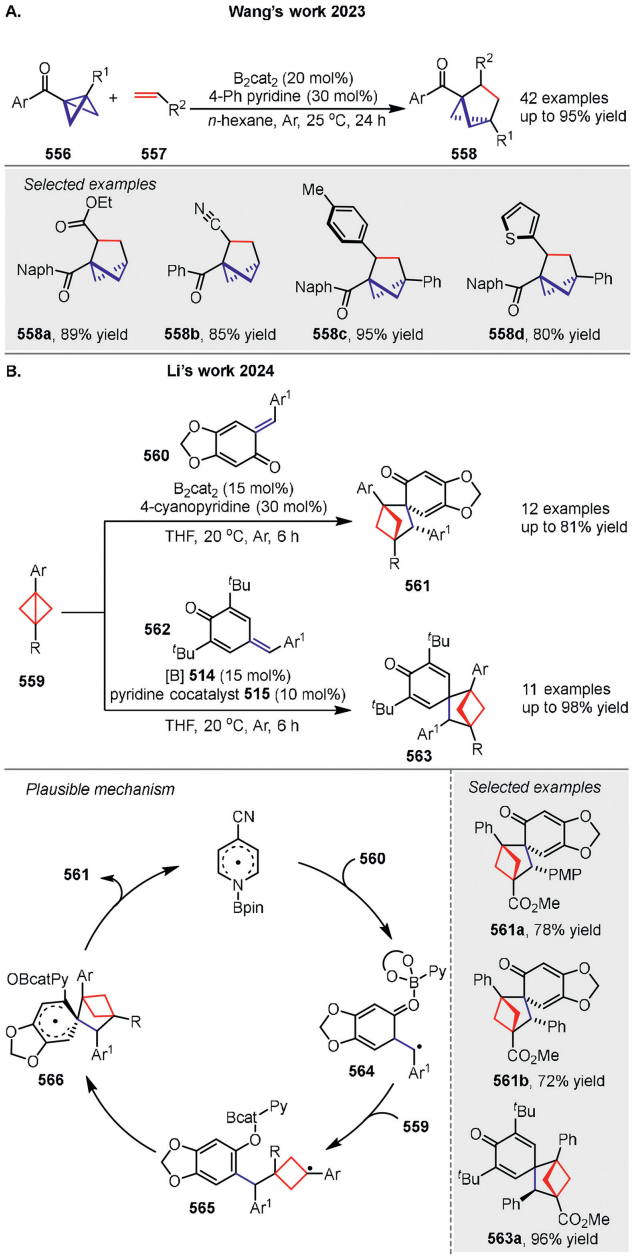
Scheme 71. Pyridine-assisted boronyl radical catalyzed [3+2] cycloaddition between bicyclo[1.1.0]butanes and cyclopropyl ketones.



Scheme 72. Pyridine-assisted boronyl radical catalyzed [3+2] cycloaddition of cyclopropane with alkene and alkyne.



Scheme 73. Pyridine-assisted boronyl radical catalyzed [3 + 2] cycloadditions of BCB, alkyne-tethered cyclopropyl ketones and vinylcyclopropanes.

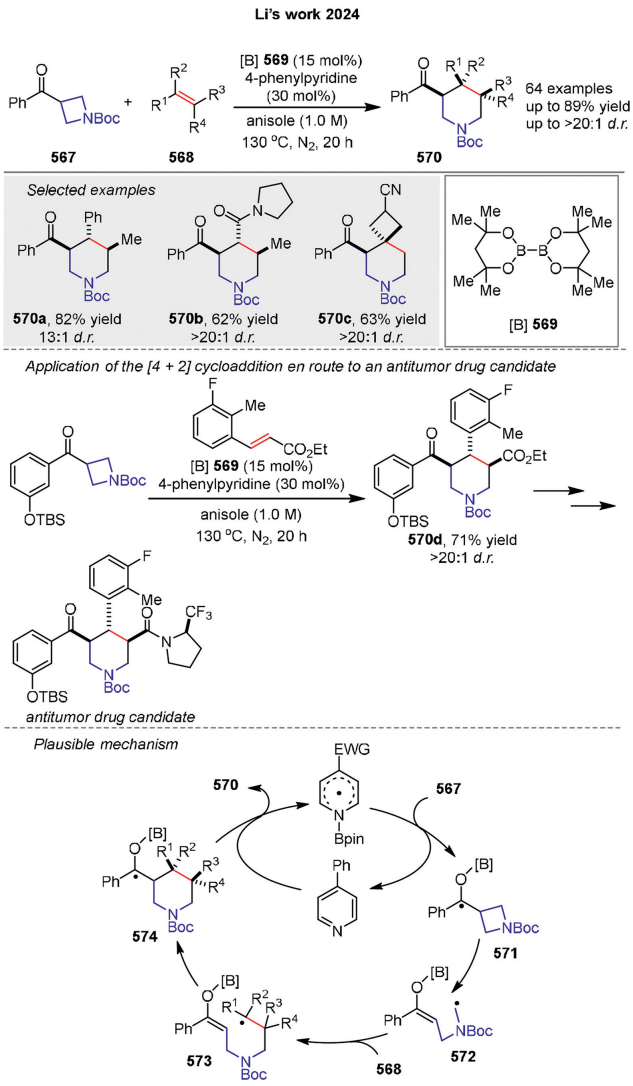


Scheme 74. Pyridine-assisted boronyl radical catalyzed [2 + 2] cycloaddition of bicyclo[1.1.0]butanes.

leading to the synthesis of 2-azabicyclo[3.1.1]heptenes **551**, which serve as potential bioisosteres of pyridine (Scheme 73A) [166]. The reaction is efficient, atom-economical, and tolerant of various functional groups. The mechanism involves the generation of a cyclobutyl radical **549a** *via* boryl-mediated ring opening of BCB, which adds to the vinyl azide to form an iminyl radical **549b**, followed by a 6-*exo*-*trig* radical cyclization to yield the bicyclic product **551**. In the same year, Tan and tian group described the same pyridine-boryl radical-catalyzed [3 + 2] cycloaddition of alkyne-tethered cyclopropyl ketones **552** to produce bicyclo[3.3.0]octanes **553** (Scheme 73B). The reaction involves ketyl radical formation and a radical cascade process, achieving high yields and good diastereoselectivity. The mechanisms of these [3 + 2] cycloaddition reactions are similar to the one described in Scheme 69 [167]. Another pyridine assisted boronyl radical catalyzed intramolecular radical cycloaddition of vinylcyclopropane **554** was reported by Wei, Li and Xu group. Same mechanistic pathway provided an array of cyclopentene derivatives **555** chemoselectively under relatively mild conditions (Scheme 73C) [168].

4.2. [2 + 2] cycloaddition

Recently, Wang group reported a facile synthesis of BCHs **558** *via* a strain-release-driven [2π + 2σ] cycloaddition of bicyclo[1.1.0]butanes **556** with alkenes **557** facilitated by a pyridine-boronyl radical catalyst (Scheme 74A) [169]. Shortly ago, a novel synthetic approach for constructing diverse arene-fused [n.1.1]-bridged molecules **561**, **563** through a boronyl radical-catalyzed [2σ + 2π] cycloaddition between *ortho*-quinone methides (*o*-QMs) **560** or *para*-quinone methides (*p*-QMs) **562** and bicyclo[1.1.0]butanes **559** was reported by Li's group. These spirocyclic compounds serve as intermediates for further Lewis acid-catalyzed rearrangements to produce a variety of 2D/3D polycyclic scaffolds (Scheme 74B) [170]. The mechanism begins with the generation of a boronyl radical from a diboron compound and pyridine, which then forms a benzylic radical intermediate **564** by



Scheme 75. Pyridine-assisted boronyl radical catalyzed [4+2] cycloaddition between 3-aroyl azetidines and alkenes.

transferring to the quinone methide **560**. This intermediate undergoes radical addition to the bicyclo[1.1.0]butane **559**, followed by an intramolecular dearomatizing radical cyclization to form the spirocyclic product **559**. This method offers a modular, atom-economical, and efficient route to synthesize complex 2D/3D scaffolds with potential applications in drug discovery.

4.3. [4+2] cycloaddition

Very recently, a boronyl radical-catalyzed [4+2] cycloaddition reaction for the synthesis of polysubstituted piperidines **570** was also reported by Li and coworkers. The reaction uses commercially available diboron compounds **569** and 4-phenylpyridine as catalyst precursors to facilitate the cycloaddition between 3-aroyl azetidines **567** and various alkenes **568**, including previously unreactive 1,2-di-, tri-, and tetrasubstituted alkenes, yielding polysubstituted piperidines **568** with high diastereoselectivity and atom economy under metal-free conditions. The proposed mechanism involves the formation of a benzylic ketyl radical intermediate **571** *via* a boronyl radical transfer process. This intermediate undergoes α,β-scission of the azetidine ring, overcoming a rate-determining step with an energy barrier of 30.3 kcal/mol. The resulting radical species **572** then attacks the alkene **568**, leading to a chair-like 6-*exo* ring closure to form the piperidine product **570**. The boronyl radical catalyst is regenerated through a pyridine-assisted transfer process, completing the catalytic cycle. This method provides a modular and efficient route to complex piperidine derivatives that are challenging to access using traditional synthetic methods. Potential utility of this boronyl radical-catalyzed [4+2] cycloaddition reaction was demonstrated by the synthesis of a biological molecule, a known antitumor drug candidate (Scheme 75) [171].

The development of small molecule-catalyzed radical cycloaddition reactions, such as those involving thiyl radicals and boronyl radicals, has significantly improved the efficiency and selectivity of the cycloaddition reactions. By using readily accessible starting materials, atom-economical and metal-free reaction generated products with broad functional group tolerance and various degrees of substitution including quaternary carbons, heteroatoms, spirocyclic or bridged rings. The simple operation, low costs were additional benefits. The products are rich in medicinally attractive rings, sp^3 centers and diverse 3D structures.

5. Conclusions and perspectives

Over the past decades, the development of radical cycloaddition reactions has significantly advanced the field of organic synthesis, offering powerful tools for constructing complex carbo- and heterocycles that are commonly found in natural products with intriguing biological properties and potential applications in medicinal chemistry. These reactions have gained considerable attention due to their ability to tolerate a wide range of functional groups, operate under mild conditions, and proceed through non-charged intermediates, which simplify reaction pathways and reduce byproduct formation. Three main types of catalytic mechanisms have been developed and applied to build these significant complex structures: visible light-driven radical photocycloaddition, transition metal-catalyzed radical cycloaddition, and organic small molecule-catalyzed radical cycloaddition. Each approach brings unique advantages and challenges. Visible light-driven photocycloaddition leverages the energy of light to initiate reactions, often using photosensitizers to generate reactive radicals. Transition metal-catalyzed reactions rely on the unique properties of transition metals to facilitate radical formation and transfer, while organic small molecule-catalyzed reactions utilize the specific interactions of small organic molecules to guide the reaction pathway. Despite substantial progress, there remains considerable scope for further development in this area. Future efforts should focus on developing alternative catalytic methods, such as electrocatalysis, to enhance reaction controllability and expand the range of substrates that can be used. There is also a need for more efficient catalysts to replace traditional transition metal catalysts and photosensitizers, thereby reducing catalyst loading and making reactions greener, more efficient, and cost-effective. Additionally, exploring asymmetric radical cycloaddition reactions to improve enantioselectivity is crucial for the synthesis of chiral compounds, which are essential in the development of new pharmaceuticals. These advancements will continue to drive innovation and expand the application of radical cycloaddition reactions in the synthesis of complex and bioactive molecules. By addressing these challenges, researchers can further harness the potential of radical cycloaddition reactions to create new and valuable chemical entities, contributing to the ongoing evolution of organic synthesis.

Declaration of competing interest

The authors declare that they have no known competing financial interests or personal relationships that could have appeared to influence the work reported in this paper.

CRediT authorship contribution statement

Saima Perveen: Writing – review & editing, Writing – original draft, Validation, Supervision. **Lulu Qin:** Formal analysis. **Min Zhao:** Formal analysis. **Zhengwei Ding:** Supervision. **Yingying Wang:** Formal analysis. **Zaicheng Nie:** Data curation. **Pengfei Li:** Supervision, Conceptualization.

Acknowledgments

The financial support from the National Natural Science Foundation of China (Nos. 22150410339, W2432012, 22301237 and 22171218), the Ministry of Science and Technology China (No. wgxz2022188) is greatly acknowledged.

References

[1] J. Liao, X. Yang, L. Ouyang, et al., Org. Chem. Front. 8 (2021) 1345–1363.
[2] L. Chen, H. Huang, B. Luo, et al., New J. Chem. 47 (2023) 41–45.
[3] X. Zhang, J. Xu, Org. Chem. Front. 9 (2022) 6708–6716.
[4] A.R. Katritzky, Chem. Rev. 104 (2004) 2125–21261.
[5] M. Gomberg, Ber. Dtsch. Chem. Ges. 33 (1900) 3150–3163.
[6] M. Gomberg, J. Am. Chem. Soc. 22 (1900) 757–771.
[7] W. Zhou, X. Chen, L. Lu, et al., Chin. Chem. Lett. 35 (2024) 108902.
[8] T. Zou, Y. He, R. Liu, et al., Chin. Chem. Lett. 34 (2023) 107822.
[9] N. Zhang, S.R. Samanta, B.M. Rosen, V. Percec, Chem. Rev. 114 (2014) 5848–5958.
[10] M. Yan, J.C. Lo, J.T. Edwards, P.S. Baran, J. Am. Chem. Soc. 138 (2016) 12692–12714.
[11] J. Jiang, K.L. Wang, X. Li, et al., Chin. Chem. Lett. 34 (2023) 108699.
[12] X. Wang, J. Meng, D. Zhao, S. Tang, K. Sun, Chin. Chem. Lett. 34 (2023) 107736.
[13] A. Studer, D.P. Curran, Angew. Chem. Int. Ed. 55 (2016) 58–102.
[14] S.Z. Zard, Org. Lett. 19 (2017) 1257–1269.
[15] A. Deepthi, V. Sathi, V. Nair, Tetrahedron Lett. 59 (2018) 2767–2777.
[16] J. Liao, X. Yang, L. Ouyang, et al., Org. Chem. Front. 8 (2021) 1345–1363.
[17] J. Panda, S. Mohapatra, M. Ansar Ahemad, S. Nayak, S. Mohapatra, Chemistry-Select 9 (2024) e202303643.
[18] A.J. McCarroll, J.C. Walton, Angew. Chem. Int. Ed. 40 (2001) 2224–2248.
[19] A. Gansäuer, Adv. Synth. Catal. 344 (2002) 564 -564.
[20] E. Oueis, M. Elkadi, R. Rios, Adv. Synth. Catal. 366 (2024) 635–697.
[21] Y. Yin, M. You, X. Lia, Z. Jiang, Chem. Soc. Rev. 54 (2025) 2246–2274.
[22] S. Li, J. Dong, Curr. Org. Chem. 27 (2023) 1020–1035.
[23] M. Lautens, W. Klute, W. Tam, Chem. Rev. 96 (1996) 49–92.
[24] M. Wu, K. Ren, C. Zou, et al., Chin. Chem. Lett. 36 (2025) 110213.
[25] M. Song, J. Zhao, E.Q. Li, et al., Chin. Chem. Lett. 33 (2022) 2372–2382.
[26] H. Huang, M.H. Garduno-Castro, C. Morrill, D.J. Procter, Chem. Soc. Rev. 48 (2019) 4626–4638.
[27] J. Du, Y.F. Li, E.Q. Li, et al., Chin. Chem. Lett. 34 (2023) 108401.
[28] M. Wang, Y. Zhang, S. Liu, et al., Chin. Chem. Lett. 36 (2025) 110758.
[29] Z.Q. Wang, L.W. Wei, Z.Q. Wang, et al., Chin. Chem. Lett. (2025), doi:10.1016/j.cclet.2025.111377.
[30] Y. Du, L. Yao, X. Li, et al., Chin. Chem. Lett. 34 (2023) 107512.
[31] A.S. Harmata, B.J. Roldan, C.R.J. Stephenson, Angew. Chem. Int. Ed. 62 (2023) e202213003.
[32] X. Wang, F. Liu, T. Xu, Chin. Chem. Lett. 34 (2023) 107624.
[33] J. Wang, Z. Li, S. Bai, et al., Chin. Chem. Lett. 34 (2023) 107823.
[34] B.G. Cai, G.Y. Xu, J. Xuan, Chin. Chem. Lett. 34 (2023) 108335.
[35] X.E. Cai, Z.Y. Wang, W.C. Tian, et al., Org. Biomol. Chem. 21 (2023) 6068–6082.
[36] M. Ramaiah, Tetrahedron Lett. 43 (1987) 3541–3676.
[37] B. Giese, Angew. Chem. Int. Ed. 22 (1983) 753–764.
[38] M.P. Sibi, J. Ji, Angew. Chem. Int. Ed. 36 (1997) 274–276.
[39] M.A. Ischay, M.E. Anzovino, J. Du, T.P. Yoon, J. Am. Chem. Soc. 130 (2008) 12886–12887.
[40] J. Du, T.P. Yoon, J. Am. Chem. Soc. 131 (2009) 14604–14605.
[41] M.A. Ischay, Z. Lu, T.P. Yoon, J. Am. Chem. Soc. 132 (2010) 8572–8574.
[42] Z. Lu, T.P. Yoon, Angew. Chem. Int. Ed. 51 (2012) 10329–10332.
[43] S.O. Scholz, J.B. Kidd, L. Capaldo, et al., Org. Lett. 23 (2021) 3496–3501.
[44] M.A. Ischay, M.S. Ament, T.P. Yoon, Chem. Sci. 3 (2012) 2807–2811.
[45] E.L. Tyson, E.P. Farney, T.P. Yoon, Org. Lett. 14 (2012) 1110–1113.
[46] E.M. Sherbrook, H. Jung, D. Cho, M.H. Baik, T.P. Yoon, Chem. Sci. 11 (2020) 856–861.
[47] E. Hurtley, Z. Lu, T.P. Yoon, Angew. Chem. Int. Ed. 53 (2014) 8991–8994.
[48] J. Du, K.L. Skubi, D.M. Schultz, T.P. Yoon, Science 344 (2014) 392–396.
[49] Z.D. Miller, B.J. Lee, T.P. Yoon, Angew. Chem. Int. Ed. 56 (2017) 11891–11895.
[50] Z.C. Girvin, L.F. Cotter, H. Yoon, et al., J. Am. Chem. Soc. 144 (2022) 20109–20117.
[51] S.J. Chapman, W.B. Swords, C.M. Le, et al., J. Am. Chem. Soc. 144 (2022) 4206–4213.
[52] E.F. Plachinski, R.Z. Qian, R. Villanueva, et al., J. Am. Chem. Soc. 146 (2024) 31400–31404.
[53] N. Hu, H. Jung, Y. Zheng, et al., Angew. Chem. Int. Ed. 57 (2018) 6242–6246.
[54] S.C. Coote, A. Pçthig, T. Bach, Chem. Eur. J. 21 (2015) 6906–6912.
[55] A. Troster, R. Alonso, A. Bauer, T. Bach, J. Am. Chem. Soc. 138 (2016) 7808–7811.
[56] M. de Robichon, T. Kratz, F. Beyer, et al., J. Am. Chem. Soc. 145 (2023) 24466–24470.
[57] L.M. Mohr, T. Bach, Synlett 28 (2017) A–E.
[58] L.M. Mohr, A. Bauer, C. Jandl, T. Bach, Org. Biomol. Chem. 17 (2019) 7192–7203.
[59] N. Jeremias, L.M. Mohr, T. Bach, Org. Lett. 23 (2021) 5674–5678.
[60] C. Brenninger, A. Pçthig, T. Bach, Angew. Chem. Int. Ed. 56 (2017) 4337–4341.
[61] S. Poplata, T. Bach, J. Am. Chem. Soc. 140 (2018) 3228–3231.
[62] S. Poplata, A. Bauer, G. Storch, T. Bach, Chem. Eur. J. 25 (2019) 8135–8148.
[63] F.M. Hçrmann, C. Kerzig, T.S. Chung, A. Bauer, O.S. Wenger, T. Bach, Angew. Chem. Int. Ed. 59 (2020) 9659–9668.
[64] T. Rigotti, T. Bach, Org. Lett. 24 (2022) 8821–8825.
[65] T. Rigotti, D.P. Schwinger, R. Graßl, C. Jandl, T. Bach, Chem. Sci. 13 (2022) 2378–2384.
[66] M. Golfmann, L. Glagow, A. Giakoumidakis, C. Golz, J.C.L. Walker, Chem. Eur. J. 29 (2023) e202202373.
[67] M. Reinhold, J. Steinebach, C. Golz, J.C.L. Walker, Chem. Sci. 14 (2023) 9885–9891.
[68] M. Golfmann, M. Reinhold, J.D. Steen, et al., ACS Catal. 14 (2024) 13987–13998.
[69] R. Kleinmans, T. Pinkert, S. Dutta, et al., Nature 605 (2022) 477–482.
[70] Y. Liang, R. Kleinmans, C.G. Daniliuc, F. Glorius, J. Am. Chem. Soc. 144 (2022) 20207–20213.
[71] R. Kleinmans, S. Dutta, K. Ozols, et al., J. Am. Chem. Soc. 145 (2023) 12324–12332.
[72] J.L. Tyler, F. Schäfer, H. Shao, et al., J. Am. Chem. Soc. 146 (2024) 16237–16247.
[73] S. Dutta, D. Lee, K. Ozols, et al., J. Am. Chem. Soc. 146 (2024) 2789–2797.
[74] S. Dutta, Y.L. Lu, J.E. Erchinger, et al., J. Am. Chem. Soc. 146 (2024) 5232–5241.
[75] Y. Liu, D. Ni, M.K. Brown, J. Am. Chem. Soc. 144 (2022) 18790–18796.
[76] Y. Liu, M.K. Brown, J. Am. Chem. Soc. 145 (2023) 25061–25067.
[77] W. Wang, M.K. Brown, Angew. Chem. Int. Ed. 62 (2023) e202305622.
[78] R. Guo, Y.C. Chang, L. Herter, et al., J. Am. Chem. Soc. 144 (2022) 7988–7994.
[79] Y.C. Chang, C. Salome, T. Fessard, M.K. Brown, Angew. Chem. Int. Ed. 62 (2023) e202314700.
[80] S. Adak, P.S. Hazra, C.B. Fox, M.K. Brown, Angew. Chem. Int. Ed. 64 (2025) e202416215.
[81] Q. Fu, S. Cao, J. Wang, et al., J. Am. Chem. Soc. 146 (2024) 8372–8380.
[82] J. Jeong, S. Cao, H.J. Kang, et al., J. Am. Chem. Soc. 146 (2024) 27830–27842.
[83] S. Tian, R. Liu, K. Zhang, et al., Org. Lett. 27 (2025) 3818–3824.
[84] W.J. Shen, X.X. Zou, M. Li, Y.Z. Cheng, S.L. You, J. Am. Chem. Soc. 147 (2025) 11667–11674.
[85] B. Keen, C. Cong, A. Castanedo, et al., Org. Lett. 27 (2025) 1673–1678.
[86] D. Suárez-García, M.A. Rodríguez, I. Barbolla, R. Vicente, Org. Lett. 27 (2025) 3825–3830.
[87] Z. Lu, M. Shen, T.P. Yoon, J. Am. Chem. Soc. 133 (2011) 1162–1164.
[88] A.G. Amador, E.M. Sherbrook, T.P. Yoon, J. Am. Chem. Soc. 138 (2016) 4722–4725.
[89] A.G. Amador, E.M. Sherbrook, Z. Lu, T.P. Yoon, Synthesis 50 (2018) 539–547.
[90] A.G. Amador, E.M. Sherbrook, T.P. Yoon, Asian J. Org. Chem. 8 (2019) 978–985.
[91] R. Blum, Y. Zhu, S.A. Nordeen, T.P. Yoon, Angew. Chem. Int. Ed. 53 (2014) 11056–11059.
[92] S. Maity, M. Zhu, R.S. Shinabery, N. Zheng, Angew. Chem. Int. Ed. 51 (2012) 222–226.
[93] T.H. Nguyen, S. Maity, N. Zheng, Beilstein J. Org. Chem. 10 (2014) 975–980.
[94] T.H. Nguyen, S.A. Morris, N. Zheng, Adv. Synth. Catal. 356 (2014) 2831–2837.
[95] Y. Cai, J. Wang, Y. Zhang, et al., J. Am. Chem. Soc. 139 (2017) 12259–12266.
[96] C. Wang, X. Ren, H. Xie, Z. Lu, Chem. Eur. J. 21 (2015) 9676–9680.
[97] X. Huang, J. Lin, T. Shen, et al., Angew. Chem. Int. Ed. 57 (2018) 5454–5458.
[98] D. Staveness, T.M. Sodano, K. Li, et al., Chem 5 (2019) 215–226.
[99] D. Staveness, J.L. Collins III, R.C. McAtee, C.R.J. Stephenson, Angew. Chem. Int. Ed. 58 (2019) 19000–19006.
[100] J.L. Collins III, D. Staveness, M.J. Sowden, C.R.J. Stephenson, Org. Lett. 24 (2022) 4344–4348.
[101] A.R. Allen, A.E. Tharp, C.R.J. Stephenson, ChemRxiv (2022), doi:10.26434/chemrxiv-2022-42h36.
[102] A.S. Harmata, E. Tatunashvili, A. Chang, T. Wang, C.R.J. Stephenson, Angew. Chem. Int. Ed. 64 (2025) e202413695.
[103] D. Uraguchi, Y. Kimura, F. Ueoka, T. Ooi, J. Am. Chem. Soc. 142 (2020) 19462–19467.
[104] Y. Yin, Y. Li, T.P. Goncalves, et al., J. Am. Chem. Soc. 142 (2020) 19451–19456.
[105] Y. Dai, S. Liang, G. Zeng, et al., Chem. Sci. 13 (2022) 3787–3795.
[106] N. Tang, Y. Xu, T. Niu, et al., Org. Chem. Front. 8 (2021) 3118.
[107] J. Paternoga, J. Kuhlborn, N.O. Rossdam, T. Opatz, J. Org. Chem. 86 (2021) 3232.
[108] Y. Zheng, W. Huang, R.K. Dhungana, et al., J. Am. Chem. Soc. 144 (2022) 23685.
[109] L. Mollari, M.A. Valle-Amores, A.M. Martıńez-Gualda, et al., Chem. Commun. 58 (2022) 1334–1337.
[110] S. Le, J. Li, G. Feng, et al., Nat. Commun. 13 (2022) 4734.
[111] P. Bellotti, T. Rogge, F. Paulus, et al., J. Am. Chem. Soc. 144 (2022) 15662–15671.
[112] W. Lee, Y. Koo, H. Jung, S. Chang, S. Hong, Nat. Chem. 15 (2023) 1091–1099.
[113] T.V.T. Nguyen, A. Bossonnet, M.D. Wodrich, J. Waser, J. Am. Chem. Soc. 145 (2023) 25411–25421.

[114] A. Petti, M.J. Karrasch, P. Chahar, et al., J. Am. Chem. Soc. 147 (2025) 13276–13285.
[115] S. Lin, M.A. Ischay, C.G. Fry, T.P. Yoon, J. Am. Chem. Soc. 133 (2011) 19350–19353.
[116] S. Lin, S.D. Lies, C.S. Gravatt, T.P. Yoon, Org. Lett. 19 (2017) 368–371.
[117] S.P. Pitre, J.C. Scaiano, T.P. Yoon, ACS Catal. 7 (2017) 6440–6444.
[118] J. Wang, N. Zheng, Angew. Chem. Int. Ed. 54 (2015) 11424–11427.
[119] J. Ma, S. Chen, P. Bellotti, et al., Science 371 (2021) 1338–1345.
[120] R. Guo, S. Adak, P. Bellotti, et al., J. Am. Chem. Soc. 144 (2022) 17680–17691.
[121] A.S. Harmata, T.E. Spiller, M.J. Sowden, C.R.J. Stephenson, J. Am. Chem. Soc. 143 (2021) 21223–21228.
[122] Z. Luo, Z. Xing, R. Gao, et al., Org. Biomol. Chem. 21 (2023) 4637–4642.
[123] M. Wei, C. Liu, C.S. Wang, et al., Green Chem. 25 (2023) 2453–2457.
[124] T. Horibe, K. Katagiri, K. Ishihara, Adv. Synth. Catal. 362 (2020) 960–963.
[125] Z. Zhang, J.B. Stöckrath, S. Grimme, A. Gansäuer, Angew. Chem. Int. Ed. 60 (2021) 14339–14344.
[126] S. Agasti, F. Beltran, E. Pye, et al., Nat. Chem. 15 (2023) 535–541.
[127] A. Gansäuer, M. Behlendorf, D. von Laufenberg, et al., Angew. Chem. Int. Ed. 51 (2012) 4739–4742.
[128] W.A. Nugent, T.V. RajanBabu, J. Am. Chem. Soc. 110 (1988) 8561–8562.
[129] W. Hao, X. Wu, J.Z. Sun, et al., J. Am. Chem. Soc. 139 (2017) 12141–12144.
[130] W. Hao, J.H. Harenberg, X. Wu, S.N. MacMillan, S. Lin, J. Am. Chem. Soc. 140 (2018) 3514–3517.
[131] S.G. Robinson, X. Wu, B. Jiang, M.S. Sigman, S. Lin, J. Am. Chem. Soc. 142 (2020) 18471–18482.
[132] M.N. Zhao, Z.H. Ren, D.S. Yang, Z.H. Guan, Org. Lett. 20 (2018) 1287–1290.
[133] Y. Kuang, Y. Ning, J. Zhu, Y. Wang, Org. Lett. 20 (2018) 2693–2697.
[134] W. Liu, Y. Kuang, Z. Wang, J. Zhu, Y. Wang, Beilstein J. Org. Chem. 15 (2019) 542–550.
[135] H.M. Huang, J.J.W. McDouall, D.J. Procter, Nat. Catal. 2 (2019) 211–218.
[136] H.M. Huang, Q. He, D.J. Procter, Synlett 31 (2020) 45–50.
[137] S. Agasti, N.A. Beattie, J.J.W. McDouall, D.J. Procter, J. Am. Chem. Soc. 143 (2021) 3655–3661.
[138] J.I. Mansell, S. Yu, M. Li, et al., J. Am. Chem. Soc. 146 (2024) 12799–12807.
[139] G. Qin, Y. Wang, H. Huang, Org. Lett. 19 (2017) 6352–6355.
[140] J. Shi, X.J. Li, S.Y. Jiang, W. Wu, H. Ren, ACS Catal. 14 (2024) 5605–5611.
[141] W. Liang, K. Jiang, F. Du, et al., Angew. Chem. Int. Ed. 59 (2020) 19222–19228.
[142] F. Du, S.J. Li, K. Jiang, et al., Angew. Chem. Int. Ed. 59 (2020) 23755–23762.
[143] K.S. Feldman, A.L. Romanelli, R.E. Ruckle Jr., R.F. Miller, J. Am. Chem. Soc. 110 (1988) 3300–3302.
[144] K.S. Feldman, R.E. Ruckle Jr., A.L. Romanelli, Tetrahedron Lett. 30 (1989) 5845–5848.
[145] K.S. Feldman, A.L. Romanelli, R.E. Ruckle Jr., G. Jean, J. Org. Chem. 57 (1992) 100–110.
[146] K. Miura, K. Fugami, K. Oshima, K. Utimoto, Tetrahedron Lett. 29 (1988) 5135–5138.
[147] C.C. Huval, D.A. Singleton, J. Org. Chem. 59 (1994) 2020–2024.
[148] C.C. Huval, D.A. Singleton, Tetrahedron Lett. 35 (1994) 689–690.
[149] D.A. Singleton, K.M. Church, J. Org. Chem. 55 (1990) 4780–4782.
[150] T. Hashimoto, Y. Kawamata, K. Maruoka, Nat. Chem. 6 (2014) 702–706.
[151] T. Hashimoto, K. Takino, K. Hato, K. Maruoka, Angew. Chem. Int. Ed. 55 (2016) 8081–8085.
[152] J.M. Ryss, A.K. Turek, S.J. Miller, Org. Lett. 20 (2018) 1621–1625.
[153] A.K. Turek, M.H. Sak, S.J. Miller, J. Am. Chem. Soc. 143 (2021) 16173–16183.
[154] T. Fukuyama, T. Kippo, K. Hamaoka, I. Ryu, Sci. China Chem. 62 (2019) 1525–1528.
[155] Q.Q. Zhao, X.S. Zhou, S.H. Xu, et al., Org. Lett. 22 (2020) 2470–2475.
[156] D.F. Chen, C.H. Chrisman, G.M. Miyake, ACS Catal. 10 (2020) 2609–2614.
[157] G. Archer, P. Cavalère, M. Médebielle, J. Merad, Angew. Chem. Int. Ed. 61 (2022) e202205596.
[158] J. Doe, Radical reactions in organic chemistry, in: J. Smith (Ed.), Advances in Organic Chemistry, Wiley, 2023, pp. 123–145.
[159] J. Wang, Y.L. Phang, Y.J. Yu, et al., Angew. Chem. Int. Ed. 63 (2024) e202405863.
[160] Z. Ding, Z. Liu, Z. Wang, et al., J. Am. Chem. Soc. 144 (2022) 8870–8882.
[161] M. Xu, Z. Wang, Z. Sun, et al., Angew. Chem. Int. Ed. 61 (2022) e202214507.
[162] T. Yu, J. Yang, Z. Wang, et al., J. Am. Chem. Soc. 145 (2023) 4304–4310.
[163] J. Wen, Z. Ding, P. Li, Org. Lett. 26 (2024) 7021–7025.
[164] L. Qin, T. Yu, Z. Ding, M. Zhao, P. Li, Synthesis 57 (2025) 2633–2649.
[165] K. Zhang, Y. Xia, S. Tian, et al., ChemCatChem (2025) e202401909.
[166] Y. Liu, S. Lin, Z. Ding, et al., Chem 10 (2024) 3699–3708.
[167] H. Huang, X.D. An, Y.F. Wang, Y.X. Tan, P. Tian, Adv. Synth. Catal. 367 (2025) e202401015.
[168] T. Li, L. Wei, Z. Wang, et al., Org. Lett. 26 (2024) 5341–5346.
[169] Y. Liu, S. Lin, Y. Li, et al., ACS Catal. 13 (2023) 5096–5103.
[170] T. Yu, X. Zhao, Z. Nie, et al., Angew. Chem. Int. Ed. 64 (2025) e202420831.
[171] Z. Ding, Z. Wang, Y. Wang, et al., Angew. Chem. Int. Ed. 63 (2024) e202406612.